

**Triggering the Ventilator during
Non-Invasive Ventilation in Infants using
Transcutaneous Electromyography
of the Diaphragm**

- A proof of principle study -



Amber van Elburg

Triggering the Ventilator during Non-Invasive Ventilation in Infants using Transcutaneous Electromyography of the Diaphragm

A proof of principle study

Master thesis
Technical Medicine – Medical Sensing and Stimulation

by
Amber N. van Elburg
31 oktober 2022

GRADUATION COMMITTEE

Chairman	Dr.ir. R. Hagmeijer
Medical supervisor	Dr. G.J. Hutten
Technical supervisor	Dr.ir. F.H.C. de Jongh
Process supervisor	Drs. A.G. Lovink
External member	Dr. E. Mos – Oppersma
Extra member	Dr. R.W. van Leuteren

Voorwoord

Na iets meer dan een jaar lang mijn afstudeerstage gelopen te hebben op de Neonatale Intensive Care Unit, is nu dan eindelijk het moment gekomen voor mij om mijn werk te presenteren en af te studeren. Dit markeert voor mij het einde van zeven mooie studiejaren en het begin van een nieuwe levensfase. Ondanks dat ik met veel plezier terugkijk op de afgelopen jaren en ik persoonlijk ontzettend veel gegroeid ben, kijk ik erg uit naar deze nieuwe periode en ben ik benieuwd wat de toekomst mij zal gaan brengen.

Het onderzoek waarop ik afstudeer gaat over de mogelijkheid van het aansturen van een ventilator bij neonaten aan de niet-invasieve beademing door middel van transcutaan gemeten diafragma elektromyografie. Dit onderzoek is tot stand gekomen wegens de behoefte vanuit de kliniek om deze patiëntengroep op geheel niet-invasieve wijze zo goed mogelijk te kunnen ondersteunen in hun ademhaling. Het uitvoeren van dit onderzoek was niet mogelijk geweest zonder de hulp van mijn begeleiders.

Ik wil daarom graag beginnen met het bedanken van mijn begeleiders, die mij allen dit afgelopen jaar zo goed geholpen en ondersteund hebben. Jeroen, bedankt voor alle klinische inzichten die je mij gegeven hebt en voor mij er regelmatig op wijzen dat ik soms wel wat positiever en trotser mocht zijn op mijzelf en op mijn werk. Frans, jou wil ik graag bedanken voor je scherpe opmerkingen die mij er toe gezet hebben om altijd kritisch naar mijn eigen werk te blijven kijken. Ook in het algemeen bedankt voor je inzet en de ruime tijd die je altijd genomen hebt om mij verder te helpen. Ruud, jij bent natuurlijk het meeste betrokken geweest bij mijn onderzoek, en ik heb ontzettend veel aan jou gehad het afgelopen jaar. Bedankt dat je altijd voor mij klaar stond, erg fijn met mij meedacht en mij altijd gesteund hebt. Ik heb ook een erg mooie tijd in Italië gehad, waarbij ik het leuk vond dat we elkaar toen wat beter hebben leren kennen. Ook jou, Anouk, wil ik erg graag bedanken. Tijdens de wekelijkse TG-meetings kwam jij vaak met goede adviezen en andere invalshoeken die zeker terug te vinden zijn in mijn eindresultaat. Ook wist ik dat ik altijd op jouw hulp kon rekenen. Annelies, ik ben ontzettend blij geweest met jou als mijn procesbegeleider. Ik kan soms een wat nuchter persoon zijn, wat niet altijd een goede combinatie is met procesbegeleiding, maar jij hebt mij daarin altijd in mijn waarde gelaten. Toch heb je mij de juiste vragen weten te stellen, waardoor ik onder jouw begeleiding erg veel over mijzelf geleerd heb.

Ten slotte wil ik graag mijn familie en vrienden bedanken. In het bijzonder mijn ouders, huisgenoten en iedereen bij wie ik mijn ei kwijt kon: dank jullie wel voor het aanhoren van al mijn verhalen, successen en frustraties van het afgelopen jaar. Ik kon hiervoor altijd bij jullie terecht, en dat heeft mij zonder meer erg goed gedaan.

Amber van Elburg

Leiden, oktober 2022

Abstract

Introduction. Delivering respiratory support to preterm infants is often life-saving due to a premature respiratory system. Non-invasive respiratory support is preferred, as invasive mechanical ventilation is associated with long-term detrimental outcome. The most advanced form of non-invasive support is nasal intermittent positive pressure ventilation (nIPPV). However, the inflations from nIPPV are often not synchronized with the infants own inspiration, because a technique which is both non-invasive and reliable is unavailable. Recently, transcutaneous diaphragm electromyography (tc-dEMG) has been suggested as a novel method to establish reliable and non-invasive inspiratory triggering, which was further investigated in this study.

Method. A triggering algorithm based on tc-dEMG was developed in Simulink. The algorithm was designed to reduce noise and detect inspiratory efforts in real-time. After simulation testing, the algorithm was integrated into a hardware prototype, which was used in a bench set-up that converted the triggers into inflations by a custom-made ventilator. To determine the algorithm performance, the results were compared with a reference study using non-synchronized nIPPV. The amount of matching and extra triggers, and the amount of unsupported inspirations were compared between the two settings. Lastly, the quality of the matched triggers was assessed by determining the amount of synchronous, early and late triggers and calculating the trigger delay.

Results. The algorithm was tested using 2-minute epochs from pre-recorded tc-dEMG measurements of 15 (preterm) subjects. The percentage of matching and extra triggers, and unsupported inspirations was respectively 93.4% (IQR 71.2 – 96.7), 6.6% (IQR 3.3 – 28.8) and 7.1% (IQR 2.1 – 9.7). All performance indicators were better compared to the reference study, which was only significant for the percentage of unsupported inspirations (7.1 % vs. 22%, $p < 0.05$). For all subjects, most matching triggers were categorized as late, 84.9% (IQR 70.5 – 92.8). The trigger delay was estimated at ~404 ms, which mostly consisted of the delay introduced by the time needed to detect an inspiratory effort based on the tc-dEMG signal, which was 341 ms (IQR 315 – 374). Once the inspiration was detected, the prototype was able to successfully trigger the ventilator in the bench set-up.

Conclusion. This study showed for the first time that a dEMG-based triggering algorithm is capable of real-time extraction of inspiratory triggers and subsequent triggering of the ventilator. However, the inspiratory triggers were given relatively late. Future research should focus on further reduction of the trigger delay and testing of the algorithm in various bench and clinical settings.

Table of contents

Voorwoord.....	i
Abstract.....	iii
Table of contents.....	1
List of abbreviations and symbols.....	3
1. Introduction.....	5
1.1 Rationale.....	7
1.2 Research questions.....	8
1.3 Outline of thesis.....	8
2. Background.....	9
2.1 Clinical Background.....	9
2.1.1 Fetal respiratory development and physiology.....	9
2.1.2 Impairment of neonatal breathing.....	11
2.1.3 Respiratory support.....	11
2.2 Technical background.....	13
2.2.1 Introduction to DSP system design.....	13
2.2.2 Project definition.....	14
2.2.3 Detailed design.....	15
2.2.4 Project testing and integration.....	20
3. Methods.....	23
3.1 Phase I: Software.....	23
3.1.1 Description of dataset.....	23
3.1.2 Development of algorithm.....	24
3.1.3 Data acquisition: Simulink simulations.....	27
3.1.4 Statistical analysis.....	28
3.2 Phase II: Hardware prototype.....	29
3.2.1 Description of dataset.....	29
3.2.2 Development of hardware prototype.....	29
3.2.3 Data acquisition: Bench set-up.....	29
3.2.4 Statistical analysis.....	31
4. Results.....	33
4.1 Description of the datasets.....	33
4.2 Development of the algorithm and hardware prototype.....	33
4.3 Data acquisition: Simulink simulations.....	36
4.4 Data acquisition: Bench set-up.....	39
5. Discussion.....	43

5.1 Interpretation of results.....	43
5.1.1 Primary outcome: extraction of inspiratory triggers	43
5.1.2 Secondary outcome: quality of triggering.....	44
5.2 Previous studies	45
5.3 Study strengths and limitations.....	45
6. Recommendations and future perspectives.....	47
6.1 Reduction of the trigger delay	47
6.2 Further enhancement of the algorithm	47
6.3 Optimization of system parameters.....	48
6.4 Future perspectives	48
7. Conclusion.....	51
References.....	53
Appendix.....	61
A. Flowchart pre-existing offline dEMG processing algorithm	61
B. DSP design applied to tc-dEMG based triggering algorithm	62
C. System parameter values.....	63
D. Detailed description of Simulink algorithm.....	64
E. Description of dataset per subject.....	73
F. Steps to follow for future research into tc-dEMG based triggering.....	74

List of abbreviations and symbols

Abbreviations

AI	Asynchrony index
AOP	Apnea of prematurity
BPD	Bronchopulmonary dysplasia
C	Compliance
CMRR	Common-mode-rejection-ratio
CMV	Conventional mechanical ventilation
dEMG	Diaphragm electromyography
im-	intramuscular-
tc-	transcutaneous-
te-	transesophageal-
DSP	Digital signal processing
EMG	Electromyography
ETT	Endotracheal tube
FiO ₂	Fraction of inspired oxygen
FIR	Finite impulse response
FRC	Functional residual capacity
GA	Gestational age
GC	Graseby capsule
HFNC	High flow nasal cannula
HFOV	High frequency oscillatory ventilation
HPF	High-pass filter
HR	Heart rate
IIR	Infinite impulse response
I/O	Input/output
IQR	Interquartile range
LFNC	Low flow nasal cannula
MA	Moving average
ML	Machine learning
MV	Mechanical ventilation
NAVA	Neurally adjusted ventilatory assist
nCPAP	Nasal continuous positive airway pressure
NICU	Neonatal intensive care unit
nIPPV	Nasal intermittent positive pressure ventilation
s-	synchronized-
P	Pressure
PCV	Pressure controlled ventilation
PEEP	Positive end-expiratory pressure
PICU	Paediatric intensive care unit
PIP	Peak inflation pressure
PVA	Patient-ventilator asynchrony
R	Resistance
RAM	Random access memory
iRDS	Infant respiratory distress syndrome
RR	Respiratory rate
SAFER	Safe and effective respiratory support
SpO ₂	Peripheral oxygen saturation
TV	Tidal volume
VCV	Volume controlled ventilation
VIDD	Ventilator-induced diaphragm dysfunction
WOB	Work of breathing

Symbols

f_{\max}	Maximum frequency
f_r	Frequency resolution
f_s	Sample frequency
k	Timing factor for trigger-block
L_{gate}	Length of QRS-gate
N_{ins}	Number of inspirations
r	Radius
T_s	Sampling period
T_{block}	Trigger-block period
T_{cycle}	Time of respiratory cycle
T_i	Inspiratory time
t_o	Duration of I/O operations
t_p	Processing time
T_{seg}	Time of past data segment
Th_{EMG}	Threshold for dEMG
X_{gate}	dEMG samples within QRS-gates
γ	Surface tension
τ_{align}	Delay to align QRS-gates
τ_{HF}	Delay of high-pass filter

1. Introduction

The Neonatal Intensive Care Unit (NICU) is the primary care center for critically ill newborns that require specialized treatment. The patients are admitted for a variety of clinical indications, such as extreme (<28 weeks gestational age (GA)) or very premature (≥ 28 and < 32 weeks GA) birth, congenital or genetic disorders, complications during birth or a combination of factors. Delivering respiratory support to patients admitted to the NICU is often crucial for their survival. This mainly applies to premature infants, but also to term infants with other morbidities. The primary goal of providing respiratory support in the NICU is to compensate for impaired lung function and deficient control of breathing. In successfully doing so, a sufficient level of gas exchange is maintained and the work of breathing (WOB) is reduced [1]. Respiratory support can be divided into invasive mechanical ventilation (MV) and non-invasive respiratory support. Invasive MV is defined as respiratory support for which inflations are administered with an endotracheal tube (ETT) that passes the vocal cords. Non-invasive respiratory support is preferred, since invasive MV is a risk factor for developing the chronic lung disease bronchopulmonary dysplasia (BPD), which is associated with impaired neurological outcome [1]. Therefore, invasive MV is predominantly reserved for infants who failed with non-invasive forms of respiratory support, which is the case if the gas exchange and WOB are not improved sufficiently [2]. Three common modalities of non-invasive respiratory support are high flow nasal cannula (HFNC), nasal continuous positive airway pressure (nCPAP) and nasal intermittent positive pressure ventilation (nIPPV). HFNC transmits an air flow to the patient, typically at a higher flow than the patient is able to generate. nCPAP transmits continuous airway pressure to the infant which prevents airway collapse during expiration. nIPPV is the most supportive mode of non-invasive respiratory support, as it provides superimposed inflations on top of a positive end-expiratory pressure (PEEP) with a set peak inflation pressure (PIP) and rate [3]. nIPPV is indicated when nCPAP provides insufficient support, e.g. due to a low inspiratory drive of the infant, resulting in periods of apnea and subsequently desaturations and possibly bradycardia [4].

Over the past decades, improving non-invasive respiratory support has been a major topic of investigation. Part of this research is focused on providing synchronized nIPPV (s-nIPPV), i.e. delivering PIP based on the own inspiratory effort of the infant. Currently the pressure inflations during nIPPV are not synchronized with the infants own breathing effort, which results in a certain level of patient-ventilator asynchrony (PVA). The PIP and rate is set by the treating physician, which indirectly determines the degree of PVA. A recent study by de Waal et al. investigated PVA, by calculating the asynchrony index (AI) during nIPPV: a percentage of asynchronous inflations with respect to the total amount of inflations. With an acceptable margin of 33% timing difference to distinct synchronous from asynchronous inflations, they found an inspiratory AI of 0.68 ± 0.05 and an expiratory AI (start cycling off) of 0.67 ± 0.07 . Additionally, a substantial amount of inspiratory efforts were not supported at all, and also extra inflations were given [5].

Synchronization non-invasive respiratory support

It is hypothesized that synchronization leads to more effective respiratory support, partly because the infants inspiratory effort will improve the upper airway patency prior to an inflation [3]. A number of studies have investigated the short-term effects of s-nIPPV compared to nIPPV in infants. In these studies it was found that for s-nIPPV the WOB and spontaneous RR decreased, the gas exchange improved and there was a reduction in PIP, fraction of inspired oxygen (F_{iO_2}) and frequency and length of apnea episodes (along with a reduced amount of bradycardia and desaturations) [6]–[10]. Furthermore, from studies on adults and children on invasive MV it was found that non-synchronized invasive MV can lead to rapid weakness of respiratory muscles and in extension to ventilator-induced diaphragm dysfunction (VIDD) [11]–[13]. For children (median age 3 months) the observed VIDD (measured through diaphragm atrophy) was even more extensive compared to adults, possibly because young children (≤ 1

year) have less resistance to diaphragmatic fatigue due to a different composition of muscle fiber types [13], [14]. Using synchronized invasive MV and therefore utilizing spontaneous inspiratory efforts, was able to reduce VIDD in adults [15]. Therefore, if s-nIPPV is also beneficial for diaphragm function for infants, it might lead to a lower incidence of invasive MV, potentially reducing the development of BPD and therefore improving the long term outcome of infants who require respiratory support.

Synchronization in (premature) infants is more challenging compared to delivering synchronized respiratory support to older children and adults. Infants have a higher and more variable respiratory rate (RR), and in case of premature born infants, frequent periods of apnea [16]–[18]. As a result, in order to provide synchronization breath cycling must continuously be adapted to the current state of neonatal breathing. Also, due to short inspiratory times (T_i), there is only a small window available in which to detect an inspiratory effort and to subsequently administer a supporting inflation. Furthermore, infants have small tidal volumes (TV), causing these to be more difficult to detect [19]. Finally, masks to deliver non-invasive ventilation to infants typically have flow leaks. For adults and children these leaks can be limited (e.g. by use of a tight-fitting oronasal mask), but for infants the masks often have a suboptimal fit, as they can not be secured as tightly due to the accompanied risk of nasal trauma [20]. Also, infants have a more heterogenous facial anatomy which can cause air leaks when using generic masks [21], [22]. In case of a flow-based triggering modality, this limits the accuracy of spontaneous breath detection [23], [24].

So far three methods have been applied to accomplish s-nIPPV on infants: based on (1) abdominal wall pressure, (2) flow and (3) the electrical activity of the diaphragm. For abdominal wall pressure-based s-nIPPV a Graseby capsule (GC) is used, which is a pneumatic sensor attached to the abdominal wall of the infant. By detecting expansion of the abdomen through pressure differences, the GC is able to detect spontaneous inspirations of the infant. This signal can be used as a trigger for a ventilator inflation [6], [7], [25]. Studies have indicated that the accuracy of the GC is arguable, since not all initiated breaths are detected. Also, GC-based triggering is relatively late since the inspiration is detected only after chest expansion [26], [27]. Finally, using the GC only inspirations and not expirations can be synchronized with the respiratory support [5]. The second method, flow-based s-nIPPV, is achieved with a pneumotachograph or flow sensor. When the infant initiates a breath, an inspiratory flow is generated which is detected by the sensor. At a set threshold of inspiratory flow, an inspiratory trigger is placed which can activate a supportive ventilator inflation. The primary disadvantage of this type of s-nIPPV is the flow leaks that occur regularly during nIPPV. Furthermore, like pressure-based s-nIPPV, the detection of inspirations is relatively late using flow-based triggering. The third and currently last available technique is based on diaphragm electromyography (dEMG) [10], [28]. The basic concept behind using dEMG for synchronizing relies on the role the diaphragm plays as the primary respiratory muscle for inspiration and active expiration in infants [29]. dEMG can be measured transesophageal (te-dEMG), intramuscular (im-dEMG) and transcutaneous (tc-dEMG). However, for synchronization purposes, only te-dEMG has been applied so far. For this method a specific nasogastric tube is inserted into the stomach to measure the te-dEMG, which is used to synchronize the breathing effort with the inflations [30], [31]. The trigger mechanism differs from the forementioned pressure- and flow-based synchronization mechanisms. An inflation is activated directly and linearly proportional to the dEMG, attempting to create PIP that correspond to the neural respiratory drive of the infant. The mechanical inflation is terminated at a 30% decrease of the dEMG peak activity. To prevent overinflation of the lungs, the administered PIP is limited in case of disproportionate large dEMG values. This trigger mechanism establishes that the infant is in control of the RR, inspiratory and expiratory time, and the magnitude of the mechanical inflations [19], [32]–[35]. A downside of using te-dEMG, is that the technique is invasive, expensive and not available with all ventilator distributors [27]. Also, the dEMG signal typically contains a large amount of noise and therefore requires processing. Specifically for the neonatal

population, due to high and irregular heart rates (HR) and RR's, obtaining interpretable data in a real-time setting can thus be challenging. However, the detection of inspirations using dEMG is relatively early compared to the two prior methods, as physiologically the diaphragm contraction precedes inspiratory flow and thorax expansion [36]. Also, loss of efficacy due to flow leaks during flow-based synchronization will not be a factor using dEMG.

Although dEMG-based synchronization has multiple advantages over the other existing modalities, it is not preferred in its current form, using te-dEMG. As it is also possible to measure the diaphragm activity through tc-dEMG, this can be considered as a potential new method for synchronization. Unlike te-dEMG, tc-dEMG is non-invasive, relatively cheap and easily available. Tc-dEMG is measured by placing surface electrodes on the skin. The obtained signal requires several processing steps, after which inspiratory efforts can be detected. However, whether it is possible to use tc-dEMG to reliably detect inspiratory efforts in infants in a real-time setting is yet unknown.

1.1 Rationale

The hypothesized benefits of s-nIPPV over nIPPV for infants advocate further investigation into providing s-nIPPV. However, the clinical potential of current methods available for synchronization are limited, either in accuracy or in availability. Therefore, it is relevant to investigate the potential of tc-dEMG to be used to synchronize non-invasive respiratory support.

The main challenge that can be expected when considering tc-dEMG as a modality for synchronization, is to obtain an interpretable inspiratory signal within an as short as possible timeframe. The raw tc-dEMG signal contains a large amount of noise, especially for the neonatal population due to cardiac interference (with high and irregular HR's) and possible movement artifacts (due to nursing, discomfort, etc.). In order to obtain an interpretable signal, multiple processing steps are indicated. However, when doing so in a real-time setting, the processing options are limited as processing induces a relevant time delay. Delay in processing the signal will inevitably result into a delayed detection of inspiratory efforts, and thus slower triggering. As infants have high RR's and therefore short T_i 's, it is crucial to minimize this trigger delay in order to aim for administration of inflations during inspirations. In order to promote the swift placement of triggers after the start of an inspiratory effort, the aim was to maximally reduce the amount and complexity of processing operations, and therefore diminishing the delay as much as possible. In this phase of the study, the goal is not yet to attain a delay under a set value, but rather to obtain insight in the different processing operations and the delay they induce, and to provide guidance for future studies to further improve processing and reduce the delay to a level that is acceptable for clinical use.

In this thesis, the possibilities of tc-dEMG as a synchronization modality will be explored by developing a triggering algorithm using digital signal processing. In this algorithm it is attempted to perform a series of processing steps to the tc-dEMG input signal with the primary aim to extract inspiratory triggers from this signal in real-time, which can subsequently be used to activate a ventilator to administer inflations to the patient. In order to evaluate whether the algorithm is capable of this, it will be assessed how many inspiratory triggers correspond to an inspiratory effort (matching triggers), how many extra triggers are given and how many triggers are missing (i.e. unsupported inspiratory efforts). Another focus point is how the matched triggers are placed with respect to the inspiratory efforts. This can be analysed by categorizing the placement of each matched trigger as synchronous, early or late. Ultimately, from these results the trigger delay can be evaluated, which is defined as: the time between the raw dEMG signal being acquired and the start of a mechanical inflation.

1.2 Research questions

The primary aim of this thesis is to develop an algorithm that is capable of real-time extraction of inspiratory triggers from a tc-dEMG signal, and for it to be tested in a bench set-up in which the algorithm can activate a ventilator. The performance of this algorithm is evaluated by analysing the amount of matching and extra triggers, and the unsupported inspiratory efforts. As a secondary outcome, the quality of the inspiratory triggers is assessed, by further categorizing all matching triggers into synchronous, early and late placement, and by calculating the trigger delay.

Therefore, the primary research question is:

- Is it possible to trigger the ventilator during non-invasive ventilation, using a triggering algorithm based on transcutaneous electromyography of the diaphragm in (preterm) infants?

The secondary research question is:

- What is the quality of triggering based on transcutaneous electromyography of the diaphragm, i.e. of the matching triggers how many are synchronous, early and late and what is the median trigger delay?

1.3 Outline of thesis

The research questions described above are answered in this thesis report. In the next chapter a clinical and a technical background will be given. The clinical background will provide insight into respiratory challenges for the neonatal population, and current respiratory support modalities that are available. In the technical background the basics of designing a (real-time) algorithm are discussed and how this applies to a triggering application. Chapter 3 contains the methods, divided into two parts. In the first phase of the methods the software algorithm will be developed and tested through simulations. In the second phase of the methods the software will be integrated into a hardware prototype, which will be tested in a bench set-up. In chapter 4 the results are described, which will be discussed in chapter 5. Chapter 6 consists of the recommendations and future perspectives of this study. And finally, the conclusion is given in chapter 7.

2. Background

To ensure understanding of the aims, approach and challenges of this thesis, a clinical and technical background is provided.

2.1 Clinical Background

2.1.1 Fetal respiratory development and physiology

The differentiation of the respiratory system commences as early as day twenty-two of gestation and continues into early childhood. During this timeframe the lungs and respiratory tree undergo different stages of development, in chronological order: the embryonic, pseudoglandular, canalicular, saccular and alveolar stage. Each stage is characterized by the next phase in the differentiation process that begins with the respiratory diverticulum and ends with mature alveoli [37]. In the embryonic stage (day 22 – week 6 GA) the trachea and three generations of bronchi are formed, already distinctly marking the individual lung lobes. This process continues into the pseudoglandular stage (week 6 – week 16 GA) in which the respiratory tree is branched further, resulting in the formation of terminal bronchioles. In the canalicular stage (week 16 – week 28 GA) the terminal bronchioles divide into multiple respiratory bronchioles. Also, respiratory vasculature starts developing and the mesenchyme is thinning, which both mark the first critical steps towards enabling gas exchange, although still very limited [38], [39]. The increased vascularization also stimulates the differentiation of lung epithelium into specialized cells, such as type I and II pneumocytes. The next phase is the saccular stage (week 28 – week 36 GA), in which the respiratory bronchioles are subdividing into terminal sacs and the lung epithelium is thinning further. The alveolar stage (week 36 GA – 8 years of life) is the last phase of lung development, in which the terminal sacs differentiate into mature alveoli [37]. Further growth of the lungs after early childhood is only established by increasing alveolar size [39].

Simultaneously with lung formation during the pseudoglandular stage, the pleuroperitoneal cavity is closed. This marks the formation of the diaphragm (i.e. the primary respiratory muscle), as myoblasts within the pleuroperitoneal fold later differentiate into diaphragm myofibers. At the same time, phrenic nerve cells migrate towards the diaphragm-precursor myoblasts to establish innervation of the muscle [40]. During further development of the diaphragm, it starts performing regular contractions, known to be fetal breathing movements. Although the mechanism and reason behind fetal breathing is not yet quite understood, it is assumed to serve as a preparation for breathing in later extrauterine life [18]. After birth, the composition of the diaphragmatic muscle fibers is altered. Whereas the infants respiratory muscles mainly contain type 2 muscle fibers, during later life (≥ 1 year) this shifts to a majority of type 1 muscle fibers. Type 1 muscle fibers have higher endurance compared to type 2 fibers, and are therefore more resistant to fatigue [14], [41].

The main purpose of the respiratory system is establishing gas exchange and to regulate the pH, through inhalation and exhalation [42]. Through diffusion O_2 and CO_2 are exchanged across the alveolocapillary membrane [43]. The alveolocapillary surface is lined with type I and II pneumocytes. Type I pneumocytes cover approximately 95% of the alveolar surface and are characterized as extremely thin, stretched out cells, resulting in a very thin barrier fit for diffusion-based gas exchange [44]–[46]. Type II pneumocytes, accounting for the remaining 5% of alveolar surface coverage, have a vital role in the synthesis and secretion of pulmonary surfactant. Surfactant is a mixture of proteins and lipids that reduces the surface tension, to prevent respiratory airways from collapsing and therefore reduces the airway resistance [47], [48]. According to Laplace's Law for spheres (often used to describe the alveolar mechanism, see Eq. 2.1), increasing surface tension (γ) results into an increased pressure across the spherical barrier (ΔP), which means that an increased pressure is required to open the spherical structure and for it to be kept open. It also states that spheres with a small radius (r) are more prone to collapse (i.e. even further increases the necessary ΔP) [49]. The surfactant synthesis and

secretion begins at approximately 22 weeks of gestation, and further develops with GA, until approximately 35 weeks.

$$\Delta P = \frac{2\gamma}{r} \quad \text{Eq. 2.1}$$

The regulation of breathing is executed by the central nervous system through chemoreceptors and mechanoreceptors. Central and peripheral chemoreceptors constantly provide information to the brainstem regarding blood homeostasis, in order to adapt breathing to the metabolic condition. Furthermore, the mechanoreceptors in the lungs and airways play an important part in detecting pulmonary mechanics, such as stretch of the lungs, and thereby prevent overinflation [50]. Breathing regulation is accomplished through control of the respiratory muscles. The respiratory muscles are divided into three categories: inspiratory muscles, expiratory muscles and accessory respiration muscles. The most important inspiratory muscle is the diaphragm, as it accounts for approximately 70-80% of the inspiration effort in normal tidal breathing [29], [51]. During inspiration, the diaphragm contracts and flattens into the abdominal cavity. As a result of the increased thoracic cavity, the intra-thoracic pressure decreases which causes air to flow into the lungs. This process is reversed for expiration [29]. Furthermore, it has been described that the diaphragm also plays a part during expiration in healthy premature and term infants. During expiration the diaphragm upholds post-inspiratory activity, possibly to maintain/elevate end-expiratory lung volume [52], [53]. The external intercostal muscles help expanding the ribcage during inspiration, whereas the internal intercostal muscles decrease the ribcage size during expiration. The abdominal muscles mainly function to assist expiration, but can also assist inspiration during cycles of active expiration through storing elastic recoil energy in the chest wall during expiration, which assists chest wall expansion at the next inspiration. Finally, the accessory respiration muscles are those which help expand the rib cage during increased ventilatory demands, by assisting inspiration. The muscles surrounding the upper airways are also considered as accessory respiration muscles, as they manage air flow patency within the airways [51].

The respiratory muscles and supporting structures differ for infants compared to adults, which can complicate neonatal breathing. One of these differences is the anatomy of the respiratory tract including the relatively large head size of infants, which results into an anatomic dead space approximately 50% greater per unit body weight compared to older children and adults. It is suggested that the relatively large dead space limits the respiratory reserve capacity of infants, as TV's must sufficiently exceed dead space volume to enable gas exchange [54]. Furthermore, the (upper) airway structures in infants have higher compliance and smaller diameters compared to older children and adults, which results in higher airway resistance and in higher susceptibility for collapse during forceful inspiration. The lung compliance of especially preterm infants is typically low due to surfactant deficiency, whereas the thorax still has high compliance as it consists mainly from cartilage tissue [55]. Due to the high thoracic compliance, it is less capable of counteracting collapse of the low compliant lung [56]. As a result, preterm infants tend to have a lower functional residual capacity (FRC). Techniques to increase FRC are post-inspiratory activity of the inspiratory muscles, increasing RR with short expiratory times and expiratory laryngeal breaking [57]. Expiratory breaking is an interruption of expiratory flow, mainly accomplished through closure of the glottis, which is often realized by crying [18], [58]. Furthermore, the infant thorax has horizontal orientated ribs, which makes it more difficult for infants to increase thoracic size using the intercostal muscles. Therefore, infant inspiratory efforts are less efficient and mostly reliant on the use of the diaphragmatic muscle [55]. Finally, infants are more prone to fatigue of the inspiratory muscles, as these muscles consist of mostly type 2 muscle fibers [14], [41].

2.1.2 Impairment of neonatal breathing

In addition to physiological difficulties of neonatal breathing, there are a variety of factors that can lead to impairment of neonatal breathing, e.g. in case of premature birth. One of the factors that can obstruct normal breathing, is insufficient surfactant production. This is the case for premature born infants, due to immature type II pneumocytes [59]. In addition, the development of their respiratory system is still in either the canalicular or saccular phase, which means that the alveoli have not yet been developed or are only beginning to develop. As a result, the respiratory tissue that is fit for gas exchange is limited. Therefore, preterm infants are at risk of developing infant respiratory distress syndrome (iRDS), a risk that is inversely proportional to the GA. Infants suffering from iRDS can be treated with exogenous surfactant therapy and with various forms of respiratory support, primarily intended to reduce the infants' WOB and increase oxygenation [59], [60]. iRDS is a risk factor for BPD, especially in combination with clinical factors as lung inflammation, treatment-induced oxygen injury, and prolonged use of (invasive) respiratory support [61].

A common condition among preterm infants is apnea of prematurity (AOP). AOP is defined as a cessation of breathing in infants < 37 weeks of gestation for ≥ 20 seconds, or ≥ 10 seconds if accompanied with a period of desaturation ($SpO_2 < 80\%$) and bradycardia ($< 80/\text{min}$) [62]. Frequent hypoxic events are associated with retinopathy of prematurity, impaired growth, cardiorespiratory instability and poor neurological outcome in later life [63], [64]. There are three types of AOP: central, obstructive and mixed apnea, from which the latter is most prevalent. Central apnea in preterm infants can be caused due to an immature chemoreceptor response to arterial blood gas values and/or an insufficient respiratory drive [65]–[68]. Also, both term and preterm infants have an elevated apnoeic threshold, the level of PCO_2 under which breathing ceases, which can result in frequent episodes of apnea [16], [69], [70]. Obstructive breathing can be caused by occlusion of the (upper) airways, e.g. due to immaturity of pharyngeal and laryngeal muscles [67]. AOP can be treated with respiratory support, pharmaceuticals and/or prone positioning.

2.1.3 Respiratory support

Understanding neonatal lung development and physiology, it is not surprising that infants admitted to the NICU are often in need of respiratory assistance. There are several forms of respiratory support available, which are foremost divided into invasive MV and non-invasive support.

Non-invasive respiratory support

Non-invasive ventilation is administered to the patient through either a nasal mask or nasal prongs. Inflation can also be delivered through a facemask, but this is mostly reserved for acute settings, e.g. directly after birth. In general, there are four types of non-invasive ventilation: HFNC, low flow nasal cannula (LFNC), nCPAP and nIPPV.

With HFNC therapy an adjustable, heated and humidified air flow with supplemented oxygen (FiO_2 0.21-1 at 2-12 L/min) is administered to the patient. HFNC can lead to reduced nasal resistance and dead space, washout of the upper airways, recruitment of collapsed alveolar regions and an increase of the FRC [71]. Furthermore, due to the heating and humidity of the airflow, mucosal injury can be prevented, the clearance of mucus secretions is aided, and bronchoconstriction is reduced [71]. LFNC administers an air flow up to 2 L/min, which is standard not heated and humidified [71], [72]. nCPAP is the most frequent used non-invasive modality in respiratory care at the NICU. It submits a continuous distending pressure to the airways, thereby setting a certain level of PEEP. Due to the PEEP, CPAP aids in increasing the FRC, stenting of the airways, preventing alveolar collapse, and lowering the WOB. Finally, nIPPV is the most supportive non-invasive respiratory support modality. nIPPV combines nCPAP with a set of superimposed inflations at a fixed PIP and rate.

Invasive respiratory support

Invasive MV is a form of respiratory support where mechanical inflations are administered to the patient through an ETT [73]. Invasive MV is only applied to infants who fail with non-invasive forms of respiratory support, as invasive MV is associated with increased risk of VILI, and by extension BPD. When intubation is deemed necessary, treatment strategies will be in large part focused on extubation as quickly as possible. The most common indications for invasive MV are increased WOB, persistent AOP, sepsis, necrotizing enterocolitis or surgery for which general anaesthesia is required [73], [74].

A common type of invasive MV is conventional mechanical ventilation (CMV) [73]. CMV is divided into pressure controlled ventilation (PCV) and volume controlled ventilation (VCV). During PCV a mechanical inflation is administered to the patient through a fixed PIP on top of a pre-set PEEP. As a result, the TV that is given using PCV is variable and depends on the pulmonary dynamics of the infant. VCV, on the other hand, regulates the TV, allowing the administered pressure to vary [1]. Another common type of invasive MV at the NICU is high frequency oscillatory ventilation (HFOV). During HFOV small TV's are delivered at a high frequency (typically between 6-15 Hz for infants), superimposed on a continuous distending pressure. Due to the small TV's, HFOV is a lung-protective form of invasive MV [75].

Synchronization of respiratory support

In case of non-invasive respiratory support, only nIPPV can potentially be synchronized with the patients breathing, as it is the only modality that operates with inflations. However, in current clinical practice nIPPV is not yet synchronized [5], [76].

For CMV and HFOV, only CMV is eligible for synchronization. Both types of CMV can be synchronized with the patient's own breathing effort. Several studies have reported that synchronization of CMV leads to improved oxygenation, lower administered levels of PIP and shorter duration of mechanical ventilation [77]–[81]. The most common method to provide synchronization is detecting the inspiratory effort of the patient through measuring the flow at the airway opening. If a certain threshold level, set by the clinician, is reached, an inspiratory effort will be supported with a mechanical inflation, either through PCV or VCV. Disadvantages of flow-based triggering on invasive MV is that the flow sensor adds to dead space volume. Also, the accuracy might be impacted through ETT leak, or accumulation of condensation resulting in auto triggering. Another method to synchronize is through detection of airway pressure. As the PEEP decreases to a certain threshold, an inspiration is detected and subsequently supported. For this method, no flow sensor is required and therefore no additional dead space volume is needed. However, in order for the infant to decrease PEEP below a reliable threshold, an increased WOB is required. Another synchronization modality for CMV in infants is neurally adjusted ventilatory assist (NAVA), which uses te-dEMG to synchronize [1].

2.2 Technical background

To our knowledge, this is the first study to investigate synchronization based on tc-dEMG. Therefore, in this thesis a triggering algorithm was created using digital signal processing (DSP). As a guideline for the development, a pre-existing offline tc-dEMG processing algorithm was used, which was developed earlier within this department [4]. A flowchart of the basic processing steps from this algorithm can be found in Appendix A. In this section a background is given in basic DSP system design and how this applies to designing a tc-dEMG based triggering algorithm and prototype.

2.2.1 Introduction to DSP system design

DSP is performing a series of analyses and/or modifications to digital data, which can be stored, transmitted and extracted. This can be done offline or in real-time. Offline DSP is performed with pre-recorded data stored in digital form, whereas real-time DSP systems run on either live recorded data or on pre-recorded data transmitted in a real-time fashion (e.g. in a simulation setting) [82].

Designing a DSP system is a step-by-step process in which software and hardware can be integrated into a hardware prototype, see Figure 2.1. The first step is to define the project by considering the aimed application to be build and specifying the type of input data and desired output data (i.e. based on the operational needs of the user). This determines the kind of processing that needs to be performed and is therefore essential for the next step: detailed (software) design. The type of software language to be used highly depends on the kind of processing operations and the system requirements (e.g. whether or not the system is meant to run in real-time). In general, for DSP system design the high-level language tool C/C++ is often used, as it is easy-to-handle and good transferrable to most hardware DSP processors using a C-

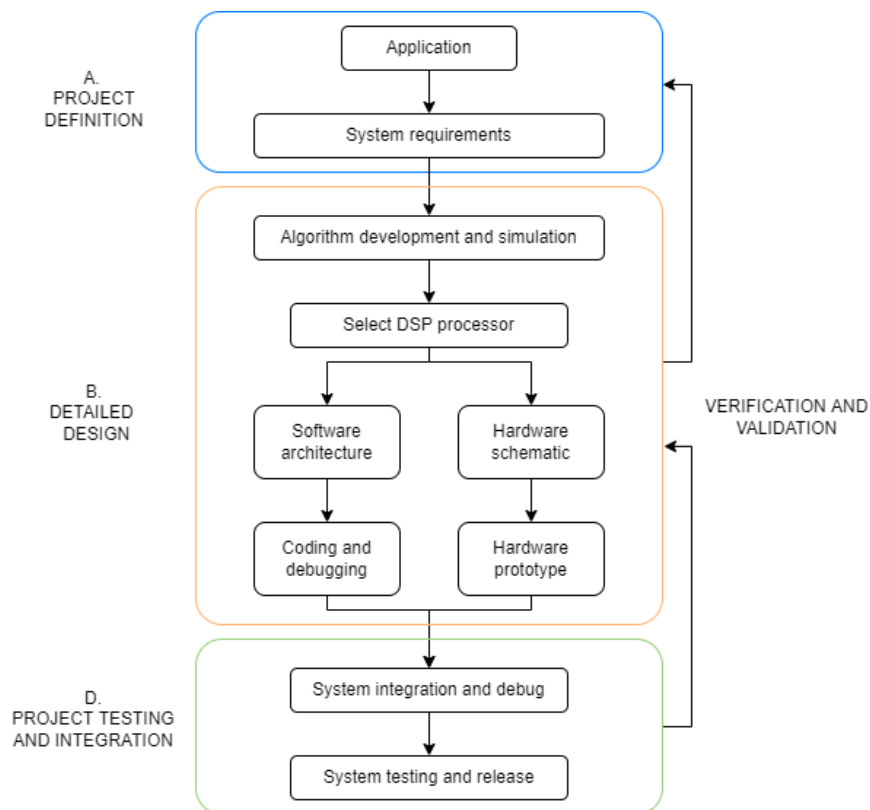


Figure 2.1: Simplified DSP design flow, divided into three phases: (A) project definition, (B) detailed design and (C) project testing and integration. Image adapted from Real-Time Digital Signal Processing: Fundamentals, Implementations and Applications [82].

code compiler. The developed algorithm can be tested using a simulator which generates and saves the simulation output, from which the system behaviour can be analysed. If the model performance is deemed adequate, the algorithm can be implemented through conversion in a hardware prototype. For hardware prototyping, nucleo circuit boards (a type of microcontrollers) are a useful tool. The software algorithm can be uploaded on this dedicated hardware, which contains the necessary components (e.g. memory) fit for the application to be run. Requirements for the nucleo board and its integrated DSP processor can include: sufficient processing speed and efficiency of data flow (especially for real-time applications), sufficient random-access memory (RAM), power consumption (in case of portable devices), connectivity (e.g. Bluetooth, LAN, etc.) and ease of software-hardware integration. After the appropriate hardware is chosen, the software algorithm is integrated with the hardware into a prototype which can be subsequently tested, e.g. using a bench set-up. During this process, verification and validation of the system should be repeatedly carried out, i.e. ensuring that the system requirements and operational needs of the user are still conformed. After finalizing this process (i.e. the desired output data is obtained from the hardware prototype), the model can be integrated with its target hardware. [82]

In the following paragraphs (2.2.2-2.2.4) the global steps from Figure 2.1 to develop a DSP system will be evaluated for the application of a tc-dEMG based triggering algorithm.

2.2.2 Project definition

In order to evaluate the possibility of using tc-dEMG recorded data to trigger a ventilator, a DSP application must be designed that is able to do so. The goal is to obtain inspiratory triggers from the input signal.

The first choice to consider is the operating mechanism of the application to be build. For an inspiratory triggering application it is possible to aim for real-time triggering (i.e. a trigger is placed to support the current inspiratory effort) or for prediction-based triggering (i.e. a trigger is predicted and placed to support the next inspiratory effort(s)). Infants typically have high and irregular RR's, which makes it difficult to select the most suitable mechanism. The high RR's advocate for a prediction-based triggering model, as the accompanying short T_i's provide a challenge to real-time triggering, since there is little time available for extracting inspiratory triggers. However, as infants also have an irregular RR, a prediction-based model is likely to be less accurate compared to a real-time triggering modality. Another factor to be taken into consideration when selecting a method of triggering, are the characteristics of the input signal (tc-dEMG). Tc-dEMG is known to be a noisy signal that needs a considerable amount of processing in order to be interpretable for breath detection, thus potentially favouring prediction-based triggering. On the other hand, a valuable advantage of diaphragm-activity based triggering compared to methods as flow- or pressure-based triggering, is that it potentially enables earlier breath detection. This factor makes it highly relevant to look into the real-time triggering potential of tc-dEMG, as this could potentially set tc-dEMG based triggering apart from the other available neonatal triggering modalities.

The system requirements of a real-time tc-dEMG based triggering algorithm can be determined by evaluating the input data and deciding on the desired output. In this first phase of developing the algorithm, the input data will be originating from pre-recorded measurements in the neonatal population. In clinical practice, tc-dEMG is commonly measured by placing two electrodes bilaterally on the costo-abdominal margin on the midclavicular line and one reference electrode at the sternum, see Figure 2.2 [83]. Using this electrode configuration, the output of the dEMG device are two unipolar raw tc-dEMG signals. Therefore, these traces should be considered as the input to the DSP system. The output of the system should be defined based on its purpose. In this particular case of a triggering algorithm, the output signal must be capable of activating a ventilator (or simulator) to administer inflations. This can be accomplished

through a binary output signal, in which the start of inspiratory efforts (i.e. inspiratory triggers) are defined.

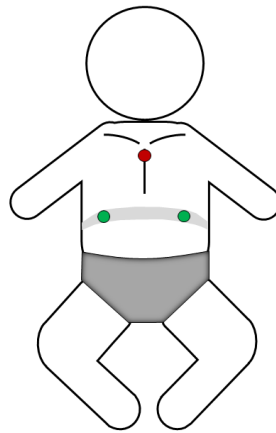


Figure 2.2: Positioning of dEMG electrodes. The upper (red) reference electrode is placed on the sternum. The lower (green) electrodes are placed bilaterally on the costo-abdominal margin on the midclavicular line. Adapted from van Leuteren et al. (2021) [4].

2.2.3 Detailed design

When choosing the appropriate software tools to develop the algorithm, the specific requirements for the triggering algorithm should be taken into account, as well as consideration of the developmental phase of the project. Inherent to the chosen applications operating mechanism, the triggering system must be able to operate in real-time. Therefore, a computationally efficient software language is indicated to limit time delay. With regard to the developmental phase, it is preferred to use a high-level software language, as they are relatively easy to write, test (e.g. through simulation) and improve/adapt. Also, the ease of software-hardware integration should be taken into account, for later hardware prototyping. The high-level language C/C++ complies with these conditions. However, the C-compiled code can be inefficient in both processing speed and memory usage. The alternative is to use assembly language (a symbolic programming language that closely resembles binary machine language), which is highly complicated and time consuming and therefore not recommended during first phase DSP system design. Therefore, although potentially inefficient, C is generally deemed most suitable.

The selected software will be the primary tool to develop the tc-dEMG based triggering algorithm. There are several steps within the algorithm: (1) obtaining the input data, (2) data processing, and (3) obtaining the output data. An additional factor to consider for this specific algorithm, is incorporating adaptivity of the system (i.e. a system that can cope with the variable respiratory conditions that are characteristic to the neonatal population).

1. Obtaining the input data

The first challenge to face when real-time processing tc-dEMG data, is how to obtain the input data as tc-dEMG data typically contains a considerable amount of (environmental/cardiac) noise. Apart from reducing the noise through processing, it is key to reduce the different sources of noise as much as possible during recording of the data. The sources of noise can be divided into four categories: (1) power supply interference, (2) subject related, (3) use of electrodes and (4) amplifier settings. The noise originating from power supply interference is often easily dealt with, either by changing the experimental set-up to protect the measurement equipment from electrical interference (e.g. shielding the cables and/or using high common-mode-rejection-ratio

(CMRR) for the amplifier) or by using an appropriate filter during pre-processing of the signal. Subject related noise cannot always be prevented, neither can it be reduced using plain filtering techniques. Forms of subject related noise are the skin-electrode interface, signal strength reduction due to patient anatomy (e.g. subcutaneous tissue), electrode placement, motion artifacts and cross-talk (i.e. picking up activity from adjacent muscles to the muscle of interest). Especially the two latter types of subject related noise are a challenge for tc-dEMG recordings of infants. Motion artifacts occur during infant movements and kangaroo care. Not only do these motions potentially cause an unusable signal, they also might affect the skin-electrode interface. The most prominent example of cross-talk while conducting tc-dEMG is cardiac interference. Since the cardiac signal is considerably larger in amplitude compared to the diaphragm activity, elimination of the cardiac interference is essential [84]. Particularly when studying (premature) infants, this is challenging in a real-time setting, due to an often high and variable HR. Furthermore, the type of electrode used can affect the amount of recorded noise. Not only the choice of electrodes is important (type, material, size), also the electrode configuration has an impact. A bipolar derivation (two unipolar electrodes subtracted from each other) is preferred over a unipolar derivation, since noise is often present in both leads and is therefore chiefly eliminated in the subtraction. Motion artifacts and cross-talk can be further reduced by using a double differential tc-dEMG instead of single differential. However this method is challenging on infants since the space for additional electrodes is limited [85]. Finally, noise can be originating from the amplifier. The amplifier noise can be reduced by setting the appropriate gain, CMRR and sample frequency (f_s) (to prevent aliasing). Also, each amplifier has inherent noise which presents itself as stochastic noise [86].

2. Data processing

After obtaining the input signal, certain processing steps must be performed to obtain a signal from which respiratory information can be extracted. In case of designing a real-time DSP system, controlling the processing time becomes considerably more important compared to its offline counterpart. A real-time DSP system receives data at a certain sampling frequency (f_s), from which follows the sampling period (T_s), see Eq. 2.2. To ensure that each sample is processed prior to receiving the next sample, the system is restricted to a processing time within T_s at which the input data is sent. This is defined in Eq. 2.3, in which t_p is processing time and t_o is the duration of input/output (I/O) operations of the hardware device (time it takes to receive input data and transmit the resultant output data).

$$T_s = \frac{1}{f_s} \quad \text{Eq. 2.2}$$

$$T_s > t_p + t_o \quad \text{Eq. 2.3}$$

To illustrate, an input signal at 500 Hz has a sampling period of 2 ms, and therefore the system requires a maximal t_p of $2 - t_o$ ms in order to permit real-time operations. Increasing the f_s will only further reduce T_s and therefore the amount of time available for processing. As the t_p can only be reduced to a certain extent, the bandwidth of the input signal (i.e. the maximum frequency component in the signal, f_{max}) is also limited. The f_{max} is already bounded to the Nyquist-Shannon sampling theorem in order to prevent signal aliasing, see Eq. 2.4. For real-time applications this results in an additional restriction, taking into account the minimal t_p and t_o , see Eq. 2.5 [82].

$$f_{max} \leq \frac{f_s}{2} \quad \text{Eq. 2.4}$$

$$f_{max} \leq \frac{f_s}{2} < \frac{1}{2(t_p + t_o)} \quad \text{Eq. 2.5}$$

Depending on the type of input signal, the minimal bandwidth at which no information is lost should be evaluated, so the maximum time for processing can be determined. An additional option to increase time for processing is to relatively reduce the t_o by implementing a block-by-block processing approach, instead of sample-by-sample. Using block processing, input samples are first placed in memory buffers, which are processed after the block is full. In this case, processing of a block must be completed prior to the arrival of the next block of samples. Block processing does pose an additional time delay between the input and output, proportional to the block size.

Processing time must not be confused with processing delay. Whereas, processing time refers to the time needed to make a mathematical computation, processing delay is the delay induced by the nature of the computation (e.g. signal time shifting due to filtering). The main processing operations that need to be performed on a raw tc-dEMG signal for triggering purposes, include baseline correction and removing of cardiac interference [4]. For these processing operations, a trade-off must be made between the quality of processing and an acceptable level of both processing time and processing delay, which is further evaluated below.

Baseline correction

The tc-dEMG signal contains a baseline offset, which is a continuously present low frequency noise that causes the baseline to deviate from zero. The baseline offset can be corrected through high-pass filtering. However, as filtering requires a certain amount of processing time and additionally induces a processing delay, it is important to choose the correct filter and its settings accordingly. Filters can be categorized into causal and non-causal filters. A filter is causal if the output is only dependent on present and past inputs, whereas a non-causal filter also takes into account future inputs. In real-time applications, only causal filters can be used. The amount of passed inputs used in the filter is determined by the order of the filter, P . A P^{th} order filter has $P + 1$ coefficients, as the present input is also taken into account. The higher the order of the filter, the sharper the magnitude response transition. However, increasing the order of the filter also increases the processing delay that is induced on the output signal with respect to the input, as the filter response is affected by a higher amount of past inputs. Furthermore, filters are also divided into finite impulse response (FIR) filters and infinite impulse response (IIR) filters. Generally, IIR filters need fewer coefficients to achieve a similar magnitude response transition as FIR filters, and therefore can be computationally more efficient and result in smaller processing delays. This makes IIR filtering useful for real-time applications. The filter impulse response using an IIR filter, $z(n)$, is a function of the $P+1$ current and passed inputs ($x(n - j), j = 0 \dots P$) and the Q passed outputs ($z(n - i), i = 1 \dots Q$), in which b_j and a_j are the filter coefficients, see Eq. 2.6. [87]

$$z(n) = \frac{1}{a_0} (\sum_{j=0}^P b_j x(n - j) - \sum_{i=1}^Q a_i z(n - i)) \quad \text{Eq. 2.6}$$

Removing cardiac interference

The cardiac interference highly distorts the tc-dEMG signal and therefore must be removed to allow interpretation of the signal. In a review by van Leuteren et al. (2019) multiple methods to reduce cardiac interference are described, being: frequency domain filtering, adaptive filtering, QRS-gating, template subtraction, independent component analysis and wavelet analysis. The methods are compared by analysing the characteristics processing time, processing delay, adaptivity to changing signal characteristics and real-time feasibility, the latter being fundamental for triggering purposes. In this review, only the methods frequency domain filtering, QRS-gating and template subtraction were described to be feasible in real-time processing, as no future input is required for processing, nor are these techniques depending on larger amounts of (past) data [86].

- *Frequency domain filtering*: a traditional method for cardiac interference removal is applying high-pass filtering (HPF). The cardiac interference is located in the frequency components up to 100 Hz, which overlaps with the EMG signal's frequency band. HPF is often applied with a cut-off frequency between 20-60 Hz, which can therefore result into EMG signal attenuation of the lower frequency components. This leads to loss of EMG information, whilst higher ECG frequency components remain [88]. Another factor to consider is that HPF is not an adaptable algorithm, i.e. not suitable for signals with a (highly) variable HR. On the other hand, HPF is a low computational technique [86], [89]. HPF can be applied to real-time signal processing provided a causal filter is used.
- *QRS-gating*: the gating method is focused on eliminating the QRS-complexes from the dEMG signal. The R-peaks are detected and a gate is placed around it, e.g. with a width of 100 ms [90]. As the QRS-complex commences prior to detection of the R-peak, the input signal must be delayed in order for the gate to align with the complex. All EMG data within the gates is deleted, as to remove the QRS-complexes. The gates are filled afterwards. There are multiple ways to do so, two of them being: replacing all data within the gates with a constant value (either zeros or the mean of a previous segment), or filling the gates with a copy of the previous segment [86]. In contrast to frequency domain filtering, QRS-gating is an adaptive algorithm, as the detection of R-peaks is unrelated to the HR. However, this method does induce a considerable processing delay (due to alignment of the gates) and has a higher computational cost compared to HPF [86], [90].
- *Template subtraction*: the concept of template subtraction is to detect multiple QRS-peaks, place a gate around them, and average the gates to create a template of a QRS-complex. Subsequently, if a R-peak is detected, the accompanying QRS-complex is eliminated by subtraction of the QRS-template [91]. The QRS-template can either be standardized or continuously updated based on a number of past QRS-complexes, in order to make the method more adaptive. The computation time of template subtraction method is higher compared to the previous methods, and also the induced processing delay is at least equal or higher compared to the gating technique [86]. Moreover, this technique requires some start-up time before actual QRS removal can be performed.

When comparing the different methods of removing cardiac interference for the neonatal population, it is particularly important to take into account the loss of information and the processing time and delay that the method will inflict upon the input signal. Infants typically have a very high (and irregular) HR compared to adults and older children, which makes the process of detecting and removing cardiac interference using QRS-gating more challenging as a higher proportion of the signal is discarded. In theory, template subtraction should result in less data loss. However, QRS-gating is executed under the assumption that the removed EMG data is redundant due to the cardiac interference [92]. HPF is generally a debatable method as much information of interest is lost due to the overlap in the removed frequencies and the dEMG signal. Furthermore, in the context of a triggering algorithm, it is imported that the processing time and delay is minimized as much as possible, especially considering the high RR of infants. In this regard, QRS-gating is superior to template subtraction as it induces less processing time and possibly also less processing delay. For HPF the induced processing delay increases with the filter order, which must be set high in order to sufficiently reduce the cardiac interference [93]. Therefore, considering above characteristics QRS-gating is currently considered most useful for real-time cardiac interference removal in the neonatal population

3. Obtaining the output data

In the pre-existing offline tc-dEMG processing algorithm, the respiratory information is extracted from the respiratory waveform, see Figure 2.3 (lower graph). The respiratory waveform can be constructed by rectification of the so-far processed signal, followed by

computation of the moving average (MA) with a window length around 0.25-0.5 seconds. From this waveform, the start of inspiratory efforts can be detected. As the processing delay of a MA is $\frac{1}{2}$ times the window length, implementing the moving average in a real-time application will introduce an unacceptable long processing delay, especially considering the relatively short T_i of infants. Therefore, in the development of a tc-dEMG based triggering algorithm, ideally the signal is processed such to avoid the necessity of performing a MA. As (most) inspiratory efforts can be visually located from the signal prior to computing the MA, see Figure 2.3 (upper graph), the possibility of extracting inspiratory triggers from the pre-MA signal were explored in this thesis.

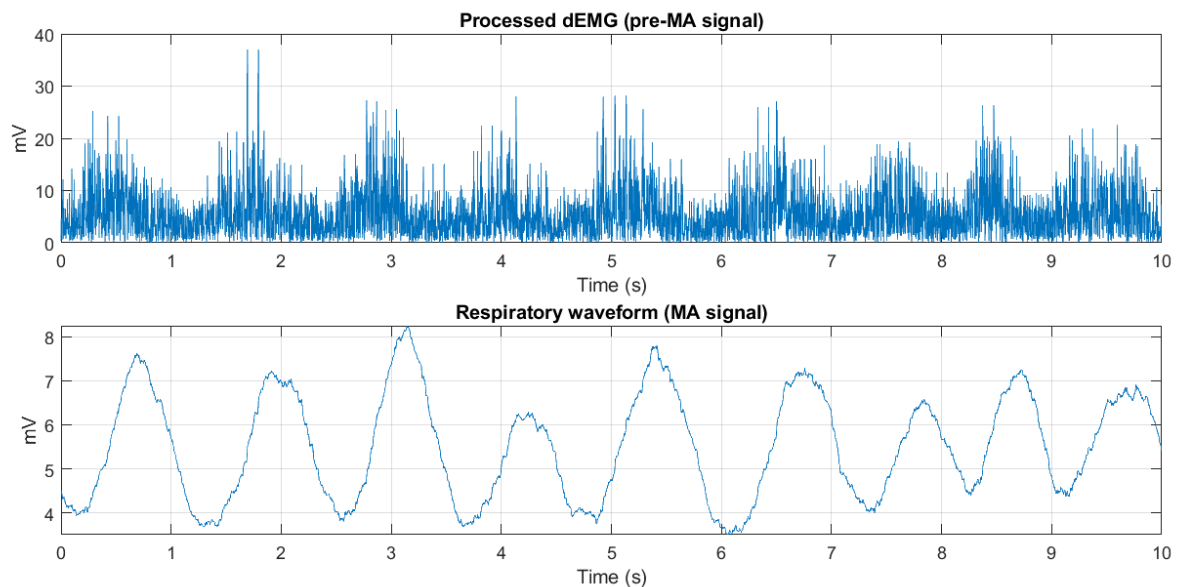


Figure 2.3: Upper graph: an example of a processed dEMG (pre-MA signal). Lower graph: an example of the corresponding respiratory waveform (MA signal).

Adaptivity of the algorithm

Both the clinical and environmental conditions of infants are known to be variable, which highly advocates for an adaptive triggering algorithm. During these variable conditions, it is important to maintain proper placement of inspiratory triggers. A way to accomplish this, is to make the algorithm adaptive by allowing system parameters that are affected by changing conditions to be variable over time. In order to do so, input data should be continuously saved for a certain past extent of time, upon which the adaptive system parameters can be continuously updated.

Selecting DPS processor

After the development of the algorithm, the appropriate hardware is selected. The choice of the hardware DSP processor can be based on its processing speed, efficiency of data flow, RAM capacity and characteristics of its I/O operations. The RAM capacity is particular important for realizing the adaptivity of the algorithm. During the stage of prototype testing, past data that must be saved in order to create an adaptive algorithm, will be saved on the hardware device. Therefore, implementation of this technique will rely on the RAM capacity of the chosen hardware processor, i.e. the amount of available computer memory. As a result, there is an upper bound to the amount of past data that can be continuously saved, coupled to the RAM capacity. On the other hand, there is also a lower bound to the amount of past data needed to obtain useful system parameters. Therefore, to make the algorithm adaptive, it is important to consider the amount of past data needed and choose the hardware accordingly. Furthermore, the duration of I/O operations is specific to the hardware device, and preferably as short as possible for real-time DSP systems. Generally, STM32 nucleo development boards are accessible and

easy-to-use devices with a large variety in specifications to fit the requirements of a specific DSP system and are therefore deemed suitable for first phase prototype development.

2.2.4 Project testing and integration

The resultant prototype can be tested, e.g. by using a bench set-up. From the bench set-up the output data can be recorded and saved, in order to evaluate whether it coincides with the previously determined desired output format. Next, the performance of the system can be determined by further analysis of the obtained output. In order to do so, performance measures must be formulated, that are specific to the developed application. For a newly developed triggering algorithm, it is relevant to evaluate whether it is capable of placing the triggers based on the inspiratory efforts and to further evaluate the quality of the placed triggers.

Ability of triggering

In order to demonstrate that the algorithm is capable of placing inspiratory triggers, it can be defined that it must perform better compared to random placement of triggering. The performance can be indicated by the amount of matching and extra triggers, and the amount of unsupported inspirations. In a previous study executed in this department, the PVA in preterm infants on nIPPV was analysed (and therefore the administered inflations were random). This study will be considered as the reference study for random placement of triggering. It can be stated that the triggering algorithm is capable of extracting inspiratory triggers if its performance is better compared to the nIPPV performance from the reference study. This is the case if ≥ 1 of these performance indicators is significantly better, as long as none of these factors perform significantly worse.

Quality of triggering

In addition to determining whether the triggering algorithm is capable of extracting inspiratory triggers, it can be assessed how these triggers are placed with respect to the inspiratory efforts. It is only relevant to evaluate this for the triggers that were categorized as matching, as algorithm enhancement will be focused on improving the placement of only these triggers. To this end, the NeuroSync Index can be used, which was established by Sinderby et al. (2013) to classify PVA during CMV [94]. This index defines a negative inspiratory window (-100% at the end of the previous inspiration till 0% at the start of the current inspiration) and a positive inspiratory window (0% at start current inspiration till +100% at end current inspiration), see Figure 2.4. Sinderby defined the start of an inspiration at the onset of the dEMG and the end of an inspiration at 30% decrease in peak dEMG. The latter definition is slightly modified to fit the neonatal population, as they tend to have dEMG baseline activity above 0 mV. Therefore, the end of an inspiration was defined at 30% decrease in dEMG amplitude instead (measured from start inspiration till peak activity). Using these inspiratory windows, it can be determined for all matching triggers whether it is synchronous (placed within $\pm 33\%$) or dyssynchronous (placed in -100% till -33% of the negative window, or placed in +33% till +100% of the positive window).

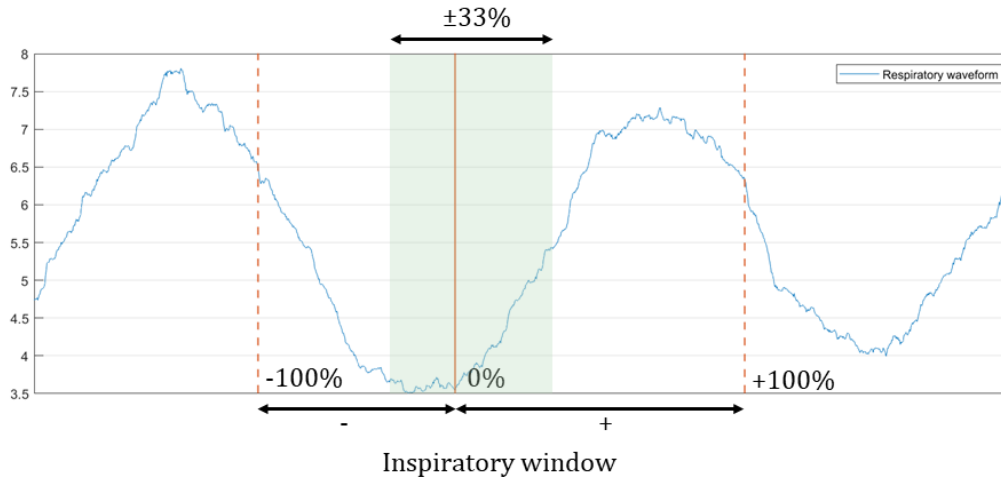


Figure 2.4: Definition of the negative and positive inspiratory window, in which the start of an inspiration is defined at the onset of dEMG activity, and the end of an inspiration at 30% decrease of dEMG amplitude (from onset till peak activity). A trigger is considered matching when placed within the green plane ($\pm 33\%$ of inspiratory window). Derived from Sinderby et al. (2013) [94].

The quality of the triggers can be further evaluated by obtaining the trigger delay. The trigger delay is defined from the start of an inspiratory effort to the administration of an inflation, and can be divided into five different components:

- Transmission
- Computation
- Detection
- Ventilation
- Mechanical delay

The transmission delay is the duration between obtaining real-time data from a dedicated dEMG device till the moment the recording is received by the algorithm. This type of delay is dependent on the communication protocol between the dEMG device and the selected hardware for the prototype. The computation delay is the amount of time it takes to convert the raw input signal into the processed dEMG. Next, the detection delay is defined as the duration to detect the start of an inspiratory effort, and is fully dependent on the developed software. The ventilation delay is the time it takes for the output signal of the algorithm to activate the ventilator, and the subsequent mechanical delay is the amount of time it takes for the inflation pressure to start building, measured at the airway opening.

3. Methods

The primary aim of this thesis was to evaluate whether inspiratory triggers can be extracted from tc-dEMG data, for which an algorithm was developed using DSP. An overview of the algorithm development is given in Appendix B, though the implementation of Figure 2.1. Second, we evaluated the performance of the algorithm by assessing the quality of the inspiratory triggers.

The methods section is divided into two phases. In phase I the development of the tc-dEMG based triggering algorithm is described. The algorithm was tested through simulations, in which the ability of the algorithm to place inspiratory triggers was assessed, along with the quality of triggering. After the developmental phase, the algorithm was integrated into a hardware prototype and a bench set-up was created, which will be outlined in phase II of the methods. From the bench set-up the algorithm was further tested, by assessing the hardware-dependent components of trigger delay.

3.1 Phase I: Software

The tc-dEMG based triggering algorithm was developed using Simulink as primary software tool, supported by MATLAB (version R2021b, The Mathworks Inc, Natick, MA), as it is an easy-to-handle, high-level language that can be automatically converted to C/C++ code for later prototype building. The algorithm was developed using pre-recorded tc-dEMG input data from (premature) infants.

3.1.1 Description of dataset

The available input data of the algorithm originated from a completed study within the NICU in the Amsterdam UMC, where the potential of diaphragm activity as a predictor of extubation failure was investigated in infants and children. In this study, patients in the NICU and paediatric intensive care unit (PICU) were included if they received invasive MV for longer than 24 hours, had a GA above 26 weeks and were deemed eligible for extubation. In total, the data of 147 subjects was analysed. The dEMG data was recorded using the Porti signal amplifier (TMSi, Oldenzaal, The Netherlands), at a sampling frequency of 1024 Hz through a Polybench (Applied Biosignals, Weener, Germany) software application. A bilateral configuration was used: two electrodes on the costo-abdominal margin on the midclavicular line, and one reference electrode on the sternum. The recordings were started approximately 15 minutes prior to extubation and stopped 180 minutes after. After extubation, the patients received either no respiratory support or a form of non-invasive respiratory support (LFNC, HFNC, nCPAP or nIPPV) [95].

For the purposes of the current study, which investigates triggering in the neonatal population, only the data obtained from the NICU was used. Due to a limited amount of time, only a small selection of subjects was made. As the GA was expected to be of influence on the quality of triggering (due to typically higher and more irregular RR's of extreme and very premature infants), a selection of the data was made by arbitrarily selecting 4 subjects from 4 age categories, concerning the GA at the time of measurement: (1) 26 till 29 weeks, (2) 29 till 33 weeks, (3) 33 till 37 weeks and (4) from 37 weeks. This led to a total of 16 included subjects. For each subject a 3-minute time epoch was manually selected from the data period after the extubation procedure. The time epoch was selected in a period with the absence of artifactual data (based on visual inspection). The amount of artifacts within the time epoch was observed by processing the signal into a respiratory waveform (computation of the MA). Finally, the raw tc-dEMG data was downsampled from 1024 to 500 Hz. The selected data was used as training set to develop the triggering algorithm.

3.1.2 Development of algorithm

The algorithm comprised of different components, given in an overview in Figure 3.1, which are further described in this section.

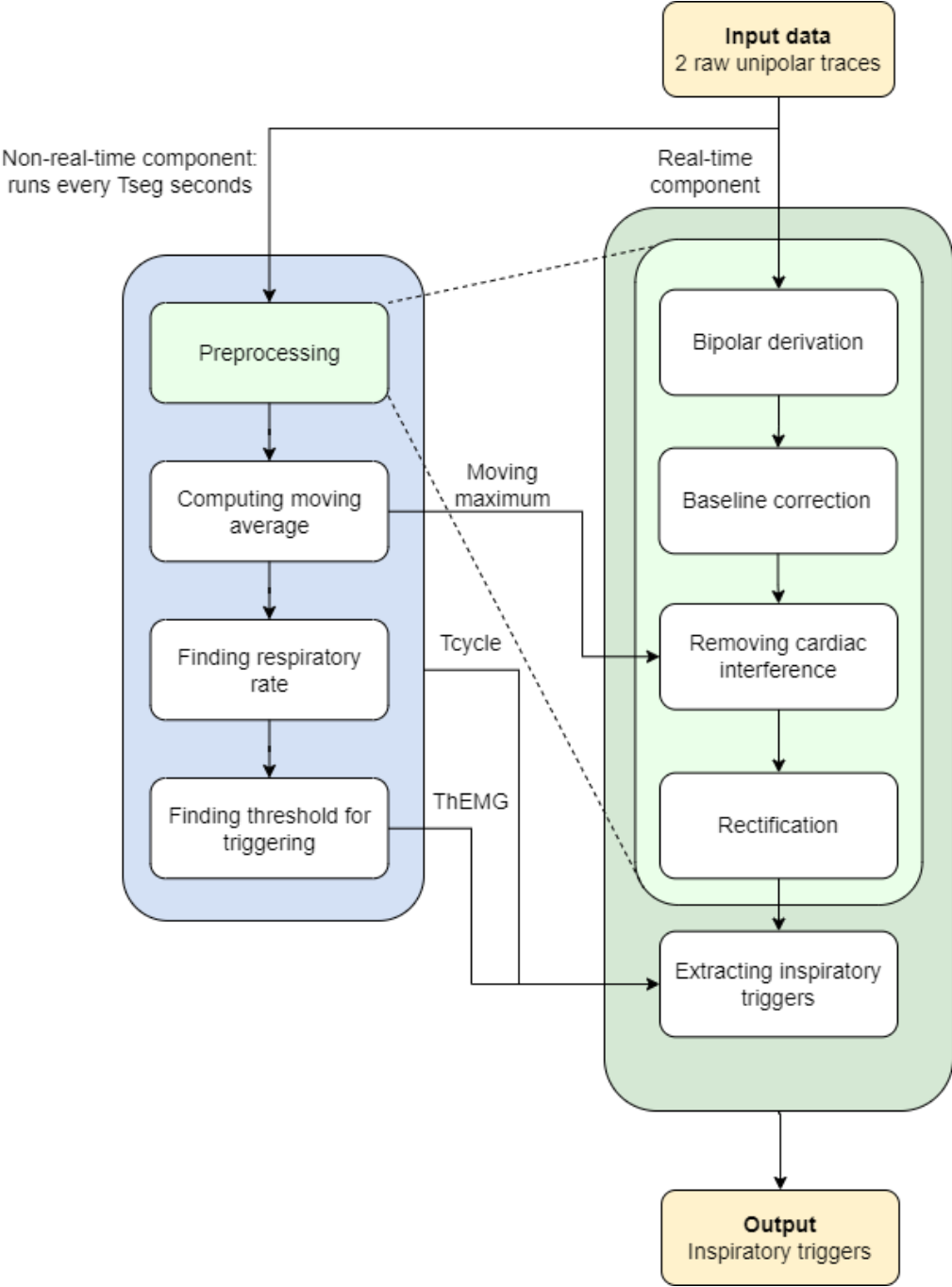


Figure 3.1: Overview of the model components and data flow of the tc-dEMG based triggering algorithm.

Pre-processing of the data

The several processing steps are broken down below.

- *Obtaining bipolar derivation*: the two unipolar tc-dEMG traces, $EMG_{uni,1-2}$ were loaded and subtracted from each other in order to derive the bipolar derivation, see Eq. 3.1.

$$EMG_{bi} = EMG_{uni,1} - EMG_{uni,2} \quad \text{Eq. 3.1}$$

- *Baseline correction*: in order to perform baseline correction, the signal was high-pass filtered using a causal, 2nd-order IIR (Butterworth) filter with a cut-off frequency of 40 Hz. The cut-off frequency was experimentally determined.
- *QRS-gating*: in order to reduce cardiac interference in the signal, the QRS-gating method was applied. First, the R-peaks were detected using a Stateflow function called PeakFollower, specifically designed for this purpose within the department of paediatrics of Medical Spectrum Twente (MST), Enschede. A detailed explanation of the PeakFollower can be found in the accompanying master's thesis [96]. In short, the PeakFollower detects R-peaks by tracing rising segments of the input signal. The moment the input signal converts from rising into descending state, a peak is detected. The PeakFollower will descend at a fixed pace (determined by a time constant) until it encounters the input signal again in rising state and the next peak can be detected. The PeakFollower needs four sources of input:
 1. Input signal;
 2. State of the input signal: rising or descending;
 3. Maximum value: a value at which the PeakFollower starts descending, even though the input signal is still in rising state. This is to prevent the PeakFollower from tracing artifacts, causing delay to the start of the descending state and therefore risk of missing the next R-peak(s);
 4. Time constant: determines the pace of the descending state (set to $2/f_s$).

The output of the PeakFollower is the detected R-peaks, given as a series of pulses. These pulses are prolonged to 100 ms, in order to enclose the QRS-complexes.

- *Reducing P- and T-tops*: the gates will remove the QRS-complexes, but they do not reduce cardiac interference from P- and T-tops. Using separate gates to remove this interference will not only induce more processing delay, it will also result in more removed data and therefore more loss of information. The P- and T-tops often have much less signal power compared to QRS-complexes and therefore can be reduced using additional filtering. A high-pass causal 2nd-order IIR (Butterworth) filter was used. The cut-off frequency was experimentally determined at 100 Hz.
- *Aligning QRS-gates*: the starting point of the QRS-gates will perfectly align with the R-peaks. To enclose the QRS-complexes with the gates, the input signal was delayed half the length of the QRS-gates, L_{gate} . However, since prior to alignment an additional high-pass filter was imposed on the signal to reduce P- and T-tops, the input signal was already partially delayed with the delay of the filter, τ_{HF} . Therefore, the delay to use for proper alignment, τ_{align} , is given in Eq. 3.2. With the described filter settings, the τ_{HF} was 5 ms, which resulted in a τ_{align} of 45 ms.

$$\tau_{align} = \frac{L_{gate}}{2} - \tau_{HF} \quad \text{Eq. 3.2}$$

- *Filling the gates:* the gates are filled using a copy of the previous segment, by replacing each i^{th} sample within the gate, $x_{gate}(i)$ (see Eq. 3.3).

$$x_{gate}(i) = x(i - L_{gate}) \quad \text{Eq. 3.3}$$

- *Rectification of the signal:* the last pre-processing step is to rectify the signal, using full-wave rectification, see Eq. 3.4.

$$x(i) = |x(i)| \quad \text{Eq. 3.4}$$

Extracting inspiratory triggers

In contrast to the pre-existing offline processing algorithm, no MA was computed in order to reduce the processing delay. Therefore, the inspiratory triggers were extracted from the pre-MA signal, in a two-step process:

- *Comparison to the threshold:* a threshold value (Th_{EMG}) was set for the pre-MA signal. If the pre-MA signal was higher than the given threshold, an inspiratory trigger was placed. How the Th_{EMG} was determined is described in the next subsection.
- *Incorporating trigger-block:* in order to prevent triggers being placed too quickly in succession, after each trigger a ‘trigger-block’ period was instituted. No triggers could be placed within this ‘refractory’ period. This was meant to decrease the amount of double triggering and triggering during the expiration period. The trigger-block length is defined based on the RR of the subject, or rather time of a respiratory cycle, T_{cycle} . The T_{cycle} is calculated from the RR, in which the RR is defined as breaths per minute and T_{cycle} is defined as the duration of a single respiratory cycle (given in seconds), see Eq. 3.5. Next, the trigger-block period is calculated using a timing factor, k , see Eq. 3.6. For this algorithm the timing factor was set to 0.6, which means that a consecutive inspiratory effort could not be detected within $0.6 * T_{cycle}$ seconds after the start of the previous effort.

$$T_{cycle} = \frac{60}{RR} \quad \text{Eq. 3.5}$$

$$T_{block} = kT_{cycle} \quad \text{Eq. 3.6}$$

Incorporating adaptivity

Within the developed algorithm there are several system parameters that are dependent on the input signal, e.g. patient-specific and/or environmental dependent. To correct for this, the algorithm must be either manually tuned to the input signal or it must be made adaptive. The latter is preferred, not in the least because patient-specific and environment circumstances can also change within a recording. Making parameters adaptive can be done by saving past input data, on which the parameters are continuously updated. The length of the data segment (T_{seg}) to be saved for this purpose, depends on the parameters to be calculated and on the internal memory of the hardware prototype device. As the parameters are calculated on a segment of past data, the processing does not act in real-time. Instead, the calculations are only executed every T_{seg} seconds.

For the algorithm developed during this thesis, three system parameters were made adaptive, T_{cycle} , Th_{EMG} and the maximum value needed for the PeakFollower. The T_{cycle} is not only very dependent on the subject, it is also known to be highly variable over time, specifically for the neonatal population. Th_{EMG} can depend on the subject, e.g. the level of diaphragm activation, but also on electrode configuration. The last variable, the moving maximum, depends on the signal strength of the cardiac interference (R-peaks in particular) and is therefore also dependent on

the subject and electrode configuration. The remaining system parameters (given in an overview in Appendix C) are also possibly dependent per subject and within a measurement and could benefit from being made adaptive. However, based on the dependencies of the forementioned system parameters, it was hypothesized that these three would benefit most from an adaptive approach and were therefore singled-out in order to reduce the model's complexity in the first phase of algorithm development. This was done using a non-real-time component of the model using the following methods:

- T_{cycle} : for each segment of past data of length T_{seg} , the processing steps were executed as described for the real-time component, with the addition that also the MA was computed, using a window length of 500 ms. From the resultant respiratory waveform, the amount of inspirations (N_{ins}) was calculated by continuous computation of the slope with an experimentally determined time interval of $\Delta t = 0.25s$, and subsequently counting the zero-crossings. After the detection of an individual inspiration, the count was blocked for a certain period, to reduce double-detected inspirations. This detection-block period was set to $t = 0.75 s$, such that the maximal RR to detect was 80/min, which can be considered as a sufficient upper bound. Finally, T_{cycle} was calculated using Eq. 3.7.

$$T_{cycle} = \frac{T_{seg}}{N_{ins}} \quad \text{Eq. 3.7}$$

In case of an apnea, N_{res} decreases which causes the T_{cycle} to continuously increase. To prevent this, a maximum T_{cycle} value of 2 seconds was instituted.

- Th_{EMG} : the Th_{EMG} was calculated through a MATLAB-function within Simulink. It used the pre-MA signal and the amount of detected inspirations, based on the calculation of T_{cycle} described above. Within the MATLAB function, the Th_{EMG} was found using an iterative algorithm called the bisection method. This method used an initial value of Th_{EMG} to calculate the amount of detected inspirations. This amount was then compared to the previously calculated amount of detected inspirations. Based on the performance with the set Th_{EMG} , the algorithm corrected the Th_{EMG} and thus converged towards a value for which the amount of found inspirations corresponded to the prior calculated amount. This is explained in further detail in Appendix D.
- *Maximum value (for PeakFollower)*: the maximum value was calculated by computing the moving average with a window length of 1 second (i.e. likely to minimal contain 1 QRS-complex for the neonatal population), and subsequently taking its mean over T_{seg} .

As the parameters were calculated over a period of T_{seg} seconds, this signified that during the first T_{seg} seconds of input data, the system parameter values were not yet initialized and therefore not available for analysis. A T_{seg} of 60 seconds was used for developing this algorithm.

3.1.3 Data acquisition: Simulink simulations

After development of the algorithm and prior to converting it to a hardware prototype, it was tested through simulations within Simulink. The algorithm was first tested for the primary outcome: whether it was capable of extracting inspiratory triggers from the tc-dEMG signal. Furthermore, as a secondary outcome, the quality of triggering was determined.

Primary outcome: extraction of inspiratory triggers

For each subject, the 3 minute time-epoch was sent as input through the Simulink simulation. First the inspiratory characteristics were determined by creating a positive and negative inspiratory window for each spontaneous inspiration. The inspiratory windows were created based on the respiratory waveform (i.e. MA) of the processed input signal, on which the start

and end of inspiratory efforts were automatically detected. From this, per subject the following inspiratory characteristics were determined: the total amount of inspirations, the RR (total amount of inspirations divided by the amount of minutes in the time-epoch), the median T_i (median length of the positive inspiratory windows) and the median T_{cycle} (median length of the total inspiratory windows).

Furthermore, in order to assess whether the algorithm was capable of extracting inspiratory triggers from the tc-dEMG signal, the triggering characteristic were determined per subject. The inspiratory triggers were categorized into matching and extra triggers. The extra triggers were further divided into double and auto triggers. This distinction is only made in order to provide more intel in the algorithm's performance, as it not clinically relevant. For the categorization of the triggers, first all auto triggers were manually determined, as developing an automated algorithm for this purpose was not considered time-efficient within this thesis. The triggers were superimposed on the processed input signal, i.e. the signal the triggers were determined on using a certain T_{EMG} . An auto trigger was defined as a trigger that was placed due to a distortion of the processed input signal, distinctly unrelated to an inspiratory effort (e.g. a P-top). Next, the triggers were automatically (using MATLAB) further categorized using the defined inspiratory windows. Triggers that were not already categorized as an auto trigger, were considered to be matching if it was the first placed trigger within an inspiratory window, or considered to be a double trigger if it was placed as $\geq 2^{nd}$ trigger in the inspiratory window. Finally, all unsupported inspirations were counted, that is to say, the amount of inspiratory windows in which no trigger was placed.

In order to state that the algorithm was capable of extracting inspiratory triggers, we used three performance indicators: the percentage matching and extra triggers (with respect to the total amount of triggers), and the percentage of unsupported inspirations (with respect to the total amount of inspirations). These percentages were determined per subject. In the reference study, in which these indicators were determined for nPPV, the matching and extra inflations were respectively 86% and 14% of all inflations, and 22% of all inspirations were unsupported. It was stated that ≥ 1 of these performance indicators of the algorithm had to be better compared to the previous study, while none of them performed worse. If that was demonstrated, the algorithms performance was better compared to nPPV from the reference study, and therefore proven capable of extracting inspiratory triggers.

Secondary outcome: Quality of triggering

The quality of triggering was assessed by classifying all triggers that were matched to an inspiration in a synchronous, late or early trigger. The trigger was categorized as synchronous to an inspiration if placed within $\pm 33\%$ of the inspiratory window or categorized as dyssynchronous to an inspiration if placed within -100% till -33% (early trigger), or placed within $+33\%$ till $+100\%$ (late trigger). From this the AI was calculated, see Eq. 3.8. The amount and percentage of auto and double triggers and unsupported inspirations per subject was given separately.

$$AI = \frac{\text{dyssynchronous inspirations}}{\text{total inspirations}} \quad \text{Eq. 3.8}$$

Next, all matching triggers were used to obtain the median detection delay per subject, which was the only delay that could be determined from the Simulink simulations, as the remaining delays were dependent on the hardware integration.

3.1.4 Statistical analysis

The statistical analysis of the baseline characteristics of the study population were performed using MATLAB. Categorical features (sex, respiratory support modality) were described with its number and percentage of occurrence. The discrete features (age and weight at birth and

inclusion) were checked for a Gaussian distribution, i.e. normality. If a Gaussian distribution was confirmed, the feature was described with its mean and standard deviation. Otherwise, the feature was described with its median value and interquartile range.

For the evaluation of the primary research question, it was assessed whether the algorithm performed significantly better than random triggering, based on the amount of matching and extra triggers and amount of unsupported inspirations compared to the previous study using conventional nIPPV. For each subject the percentage of the matching and extra triggers and percentage of the unsupported inspirations was calculated. Subsequently, the one-sample Wilcoxon signed rank test was executed to compare the values with the reference study, assuming a non-normal distribution. A p-value of < 0.05 was considered statistically significant.

3.2 Phase II: Hardware prototype

After the development of the algorithm and the first phase of testing through simulations, the algorithm was converted to a hardware prototype. The prototype was fundamental for creating a bench set-up in which the algorithm could be more extensively tested in relation to the additional hardware components (i.e. ventilator/simulator and test lung).

3.2.1 Description of dataset

The input data used for the bench set-up originated from the same dataset used for the Simulink simulations. The same 3-minute epochs from all 16 subjects were included in the dataset for bench testing.

3.2.2 Development of hardware prototype

For the purposes of developing the hardware prototype, a research collaboration was set up with the TechRes Lab from the Politecnico University. This biomedical engineering Lab is experienced with the development of new techniques in the field of respiratory diagnostics and mechanical ventilation. For the first-phase prototyping of this study, we relied on the experience and available equipment available within this laboratory. For the hardware prototype a nucleo board (NUCLEO-F746ZG, STMicroelectronics, Geneva, Switzerland) was used. This nucleo board contains a general purpose digital signal processor, which is known for its flexibility, high speed, low power consumption/good energy efficiency and low costs [82]. Furthermore, the board was compatible with STM32CubeIDE, the required program to integrate software with hardware. The first step to software-hardware integration was rearranging the Simulink algorithm into a framework from which the code could be converted to C/C++. The framework consisted of a box-structure, where the input and output variable busses were defined outside and the analysing code was placed inside. The contents of the box was subsequently converted to C-code using the embedded coder in MATLAB. To ensure optimal computation speed of the resultant code, the code was generated using the 'maximum execution speed' setting. Next, the code was uploaded into the program STM32CubeIDE, from which it was run onto the nucleo board.

3.2.3 Data acquisition: Bench set-up

The final phase was to test the hardware prototype in a bench set-up. In the bench set-up, the prototype was connected to a custom-made ventilator which administered inflations to a test lung.

Bench set-up design

The bench set-up roughly consisted of the following components (see Figure 3.2):

1. Hardware prototype running the dEMG based triggering algorithm (nucleo board)
2. The custom-made ventilator, called the SAFER (Safe and Effective Respiratory Support) was used, which was designed at the TechRes Lab (Politecnico University, Milan, Italy)

3. A ventilator nucleo board
4. A pressure sensor
5. Two different sized test lungs. For preterm subjects (GA <37 weeks) a test lung with a resistance (R) of 59 cmH₂O/L/s and a compliance (C) of 1 ml/cmH₂O was used. For term subjects (GA ≥37 weeks) the R and C of the test lung were respectively 30 cmH₂O/L/s and 1 ml/cmH₂O.
6. Two laptops with an installed interface to extract the output data from the nucleo boards (both the prototype and ventilator nucleo board).

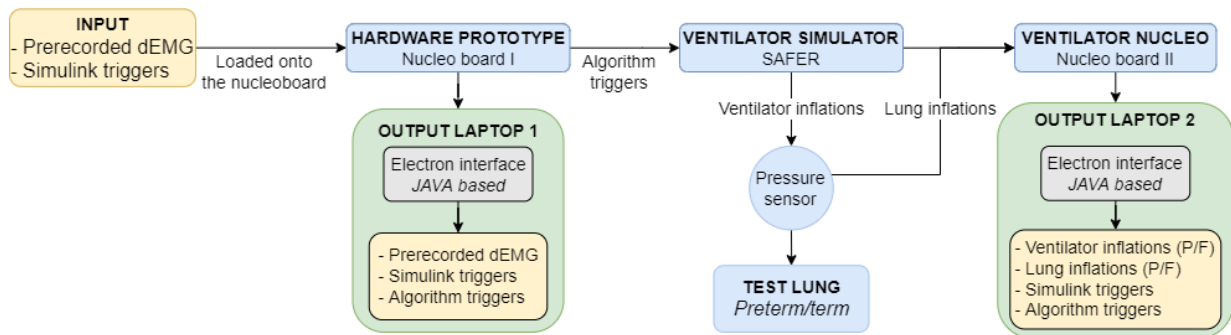


Figure 3.2: Schematic overview of the components and data flow of the bench set-up.

The nucleo board that contains the tc-dEMG based triggering algorithm was connected to a laptop which recorded and saved the output of the prototype. The prototype output (i.e. the inspiratory triggers) was also sent towards the ventilator simulator, which was capable of administering inflations accordingly. These inflations were given to a test lung, depending on the GA of the subject corresponding to the input data. A pressure sensor was placed in front of the test lung, where it measured the lung inflations (at the airway opening). The output of both the ventilator simulator and the pressure sensor was sent to the ventilators nucleo board, that was connected to a second laptop to record and save the outputs.

Primary outcome: extraction of inspiratory triggers

The primary aim of the bench set-up was to evaluate whether the hardware prototype was capable of inducing inflations from the ventilator. In order to do so, for each subject the input data was sent to the prototype and it was assessed whether this resulted in a set of inflations by the SAFER. Additionally to the two raw unipolar channels, also the corresponding time epoch of inspiratory triggers as determined by the Simulink simulations was sent as input to the prototype. These Simulink triggers were sent along in order to evaluate whether the placement of inspiratory triggers corresponded to the real-time placed triggers. This was determined by analysing whether there was a corresponding real-time trigger for each Simulink trigger and if so, whether the time difference between corresponding triggers was fixed or not. If this was both the case, it could be stated that the prototype's behaviour was equal to the Simulink algorithm. It was then assumed that the fixed time shift present between corresponding triggers could be attributed to the computation time of the algorithm. However, if there was no corresponding Simulink trigger for each real-time trigger, this indicated that the prototype behaviour deviated from the Simulink simulations, and the computation time could not be determined.

Secondary outcome: quality of triggering

After evaluating whether the prototype was capable of inducing inflations, and how they were delivered with respect to the triggers generated by the Simulink simulations, the different types of delay were assessed. Whereas for the Simulink simulations only the detection delay could be observed, a bench set-up gives the opportunity to assess all types of delay. In order to

experimentally derive the transmission delay, the input data must be obtained in real-time with a dedicated EMG device, instead of using pre-recorded data. In this phase of the study we only used pre-recorded data and therefore did not experimentally assess this type of delay. The computation delay could be assessed in case of a constant time difference between the Simulink and prototype induced triggers, where the amount of time difference corresponded to the computation delay. In this case, it could also be expected that the detection delay from the bench set-up was equal to the delay found in the Simulink simulations, as the triggers were identical. However, in case of a different pattern of triggering in Simulink compared to prototype induced triggering, both the computation and detection delay can not be obtained from the bench set-up. The ventilation delay was assessed by comparing the trigger placement with the onset of pressure in the ventilator inflations. The mechanical inflation was the duration between onset of ventilator pressure and onset of pressure measured in the (simulated) airway opening. Finally, the trigger delay was evaluated by summation of all delays described above.

3.2.4 Statistical analysis

The baseline characteristics of the study population for the bench set-up were described using the same approach as for the Simulink simulations. No further statistics were performed in phase II.

4. Results

4.1 Description of the datasets

Simulink simulations

For the Simulink simulation testing phase, a total of 16 subjects were selected from the pre-existing database from Van Leuteren et al. (2021) [95]. One subject (from the GA category 26 till 29 weeks) was excluded from the final results, on account of persistently present cardiac interference after processing. Therefore, an amount of 15 subjects was included in the analysis. The baseline characteristics of the study population are given in Table 4.1. In Appendix E the characteristics are given per subject.

Bench set-up

For the bench set-up only 9 out of 16 subjects were used, due to a lack of time. From each age category of the study population for the Simulink simulations, three subjects were included, except for the category of GA 26 till 29 weeks, from which only one subject was included. The baseline characteristics of the study populations for the bench set-up are also given in Table 4.1.

Table 4.1: Baseline characteristics of the study population for the Simulink simulations (n=15) and for the bench set-up (n=9). The data is presented as the amount (percentage) or the median (interquartile range) of all subjects.

Baseline characteristics	Simulation (n = 15)	Bench set-up 2 (n = 9)
Sex		
Male (n, %)	13 (86.7%)	7 (77.8%)
Female (n, %)	2 (13.3%)	2 (22.2%)
GA at birth (weeks)	31.7 (26.1 – 37.0)	33.6 (26.3 – 38.0)
GA at inclusion (weeks)	33.1 (29.6 – 37.6)*	34.1 (31.3 – 38.4)
Weight at birth (g)	1365 (783 – 2679)	1365 (883 – 3184)
Weight at inclusion (g)	1365 (854 – 2730)	1365 (1008 – 3170)
Support after extubation		
No support (n, %)	2 (13.3%)	2 (22.2%)
LFNC (n, %)	1 (6.7%)	1 (11.1%)
HFNC (n, %)	2 (13.3%)	1 (11.1%)
nCPAP (n, %)	7 (46.7%)	5 (55.6%)
nIPPV (n, %)	3 (20.0%)	0 (0.0%)

* 1 subject included with GA at inclusion of 25.9 (outside of inclusion criteria).

GA, gestational age; HFNC, high flow nasal cannula; LFNC, low flow nasal cannula; nCPAP, nasal continuous positive airway pressure; nIPPV, nasal intermittent positive pressure ventilation.

4.2 Development of the algorithm and hardware prototype

Development of the algorithm

A schematic overview of the developed algorithm is given in Figure 4.1. The algorithm was developed based on the pre-recorded dEMG data, and subdivided into an adaptive model and a triggering model. Each model consisted of multiple components, which are described in further detail in Appendix D. The adaptive model ran every T_{seg} seconds which was set to 60 (i.e. 1 minute). The first minute of output data was not relevant for analysis, as no initialization parameters were used during this period. As a result, from each 3 minute time-epoch of input data, only 2 minutes were available for analysis. In the adaptive model the system parameters ‘ T_{EMG} ’, ‘ T_{cycle} ’ and ‘moving maximum’ were updated each T_{seg} and subsequently served as input data to the triggering model. In the triggering model the inspiratory triggers were extracted, which was the main output of the algorithm. In contrary to the adaptive model, the triggering model was meant to run in real-time and as such designed to induce as little processing delay as possible. The only components of the triggering model that were certain to induce a delay were

two high-pass filters (both ~5 ms delay) and the QRS-gating to reduce the cardiac interference (~45 ms), which accounted to a total estimated delay of ~55 ms within the triggering model. In Figure 4.2 the estimation of the processing delay of the triggering model is given per component.

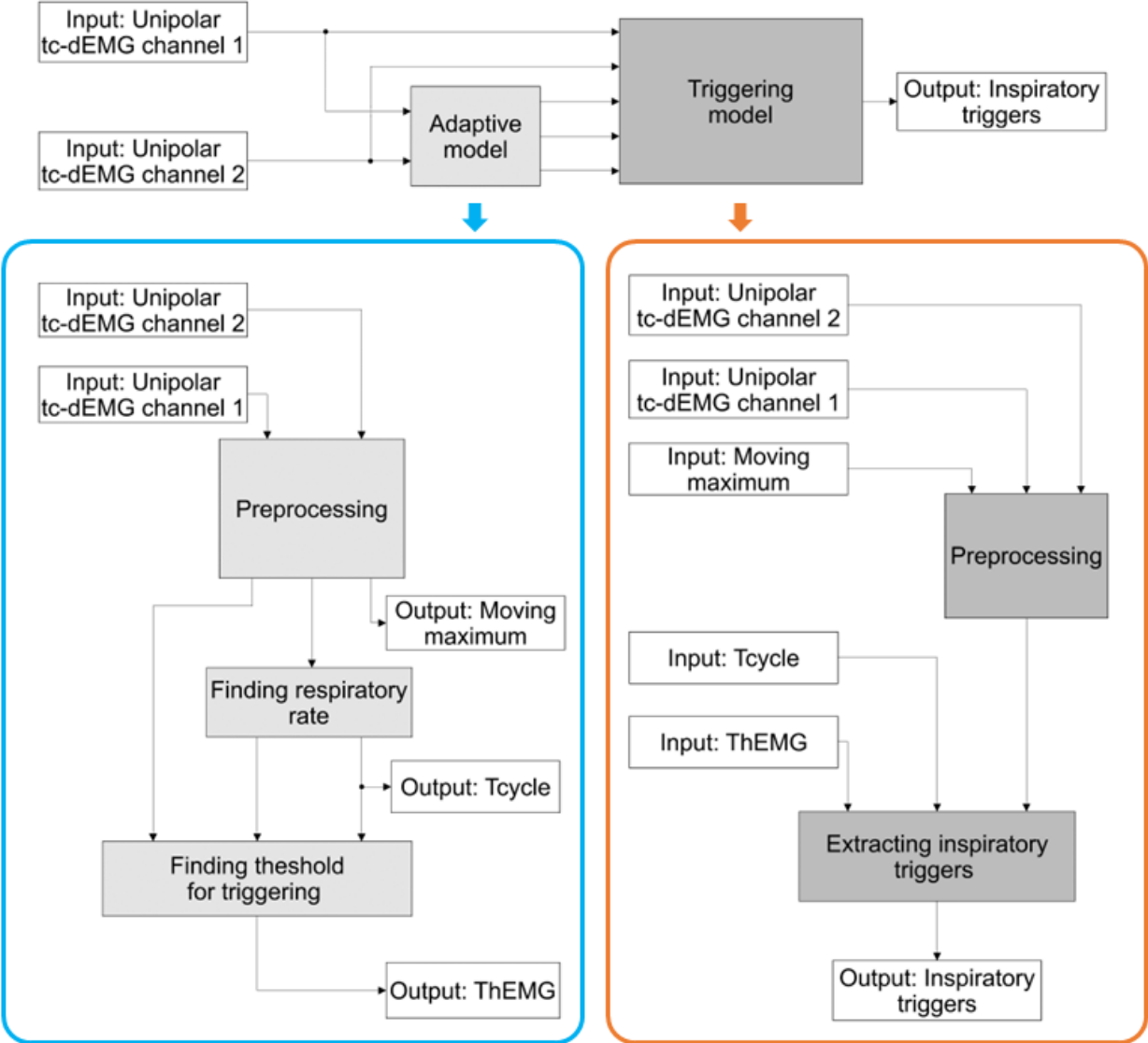


Figure 4.1: The developed Simulink algorithm. Top: overview of the total algorithm. Bottom left (blue): the expanded adaptive model. Bottom right (orange): the expanded triggering model.

ED = Estimated delay

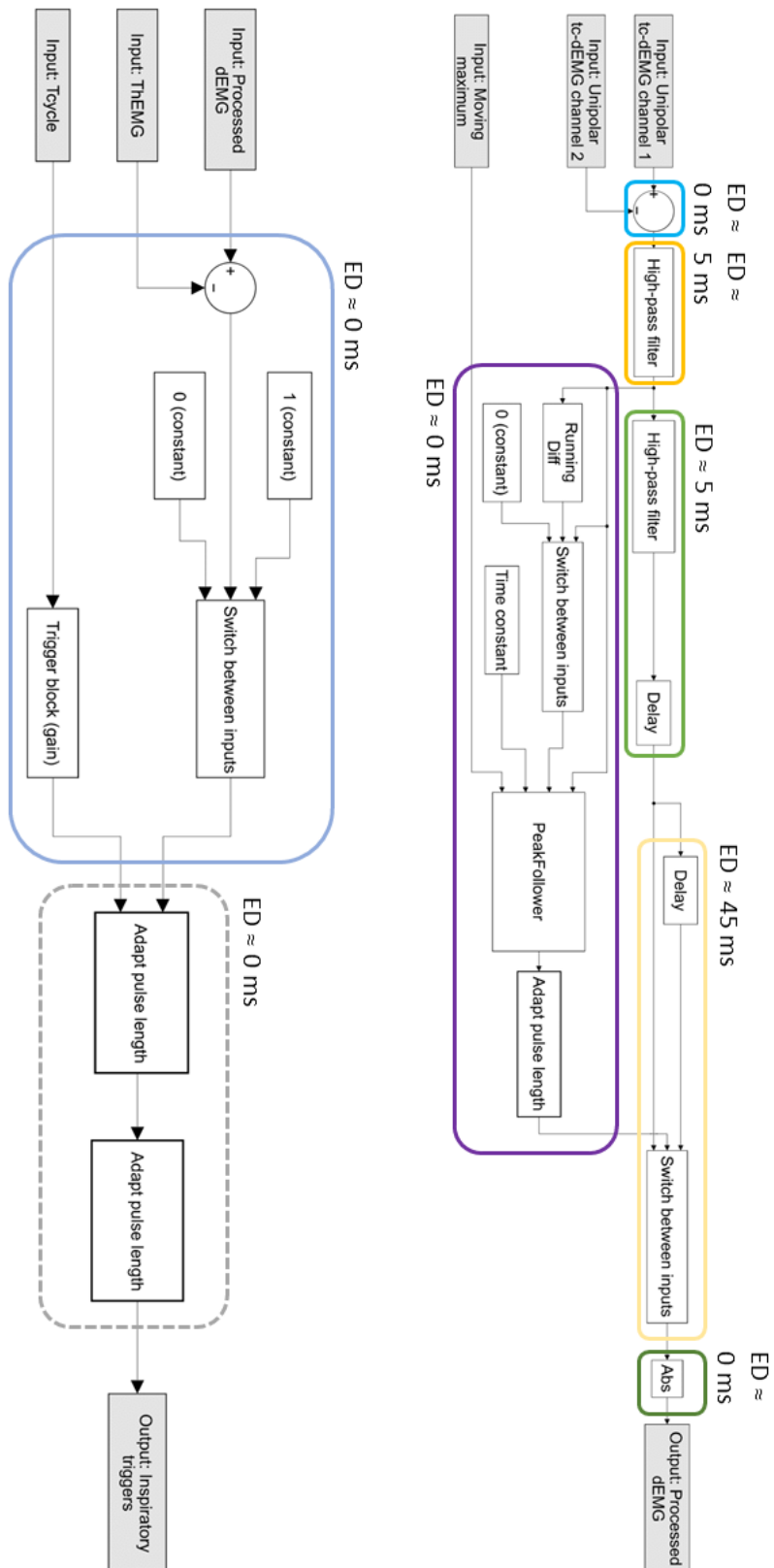


Figure 4.2: Estimated processing delay (ED) of the individual components of the triggering model. Summed ED ≈ 55 ms.

Development of the hardware prototype

During the integration of the, to C-code converted, Simulink algorithm with the hardware prototype, the RAM of the selected nucleo board proved to be insufficient. In order to overcome this issue it was investigated which components of the algorithm could potentially be reduced in amount of RAM it uses. This concerned those functions for which there had to be a built-up of samples in order to compute the output, i.e. high-order filters, window functions and buffers. The most prominent users of the RAM capacity were the buffer functions in the adaptive model, which required more RAM proportional to the length of T_{seg} . It was attempted to reduce the required RAM by reducing the T_{seg} , which led to a maximal T_{seg} of 8 seconds. Under these conditions the algorithm was able to be transitioned to a hardware prototype. During first test measurements it was found that the processing time per sample exceeded the 2 ms, which at a f_s of 500 Hz violated the real-time restriction presented in the technical background (see Eq. 2.3). It was hypothesized that the processing time could be reduced by altering the way the adaptive model was integrated into the algorithm. Within the available time for prototyping, this was not managed. In order to make the transition to a hardware prototype, the adaptive model was removed from the algorithm. The missing variable system parameters were replaced by constant values, that were determined in advance per subject using the Simulink algorithm. The constant values were computed with a T_{seg} of 3 minutes, in order to obtain parameter values that best represented the complete data epoch. Since the obtained triggers from the bench set-up were later compared with the Simulink triggers, the Simulink model was also run with a T_{seg} of 180 seconds for this purpose.

4.3 Data acquisition: Simulink simulations

Primary outcome: extraction of inspiratory triggers

Per subject, the inspiration and triggering characteristics for the Simulink simulations are presented in Table 4.2. The performance indicators (percentage of matching and extra triggers and unsupported inspirations) were compared to the performance of the reference study. All performance indicators were better compared to the reference study, by comparing the median performance indicators among all subjects with the reference value. This was only found to be significant for the percentage of unsupported inspirations (with a $p < 0.05$).

Table 4.2: Primary outcome for the Simulink simulations. The inspiration and triggering characteristics are determined per subject. The data is presented as the median (interquartile range) of all subjects.

Primary outcomes	Simulation (n = 15)
Inspiration characteristics	
Inspirations (n) ¹	106 (81 – 119)
RR (breaths/min)	54 (41 – 60)
T_i (ms)	670 (653 – 913)
T_{cycle} (ms)	1010 (975 – 1413)
Triggering characteristics	
Triggers (n) ²	108 (100 – 123)
Trigger ratio	1.0 (1.0 – 1.2)
Unsupported inspirations (%)	7.1 (2.1 – 9.7)*
Matching triggers (%)	93.4 (71.2 – 96.7)**
Extra triggers (%)	6.6 (3.3 – 28.8)***
Double triggers (%)	6.6 (3.1 – 16.3)
Auto triggers (%)	0.0 (0.0 – 1.4)

¹Total number of inspirations analysed: 1507, ²Total number of triggers analysed: 1620

*Sig. less from 22%, with $p < 0.05$, **Not sig. more from 86%, with $p \geq 0.05$, ***Not sig. less from 14%, with $p \geq 0.05$

RR, respiratory rate; T_{cycle} , time of respiratory cycle; T_i , inspiratory time.

In Figure 4.3 the percentage of unsupported inspirations per subject are visualized with respect to the total amount of inspirations, as a function of the RR. There was no visible relation with the RR. In Figure 4.4 the percentage of categorized triggers are visualized with respect to the total amount of placed triggers, also as a function of the RR. There were relatively more matching triggers and less double triggers for an increasing RR. For 8 out of 15 subjects there were no manually detected auto triggers, which indicated that all triggers were placed due to an inspiratory effort (either as matching or double trigger). For the remainder subjects (n=7), it was found that the auto triggers were all placed due to remaining cardiac activity from P-tops. There was no visible correlation between the amount of auto triggers and the RR.

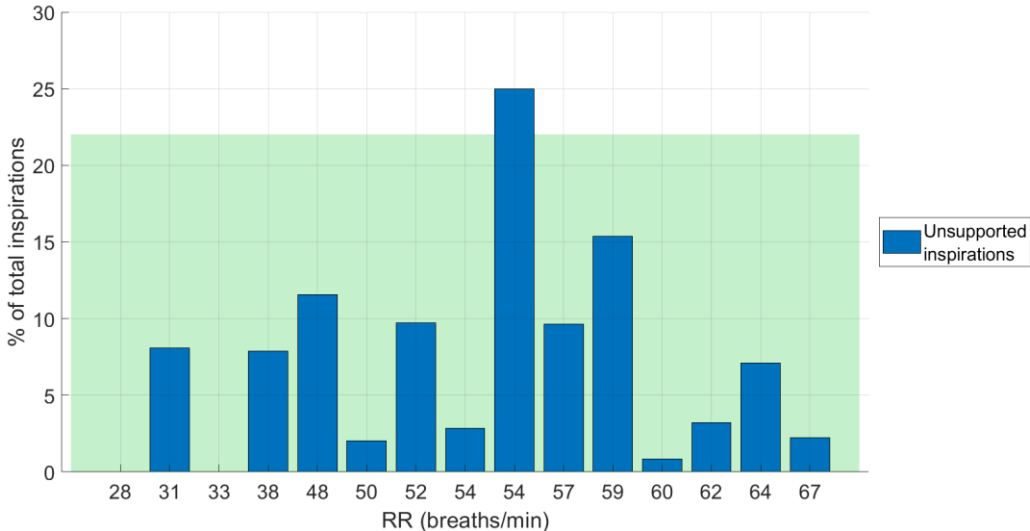


Figure 4.3: Percentage of unsupported inspirations with respect to the total amount of inspirations. Given per subject as a function of the respiratory rate (RR). A reference plane is added at 22% in order to compare the number of unsupported inspirations with the reference study.

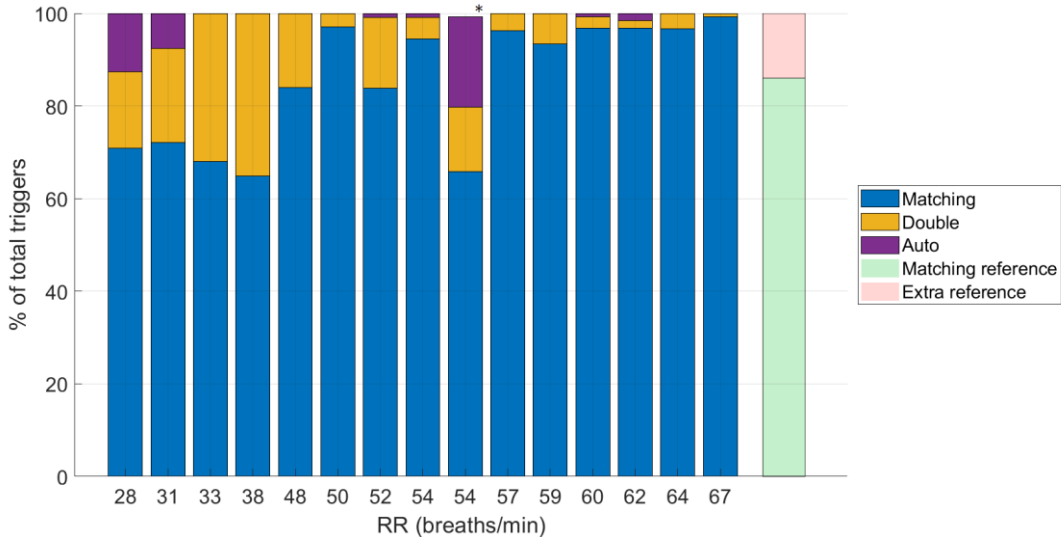


Figure 4.4: The categorization of all triggers in matching, double and auto triggers. Given per subject as a function of the respiratory rate (RR). A reference bar is added divided into 86% +14%, in order to compare the number of matched and extra triggers (double and auto triggers combined) with the reference study.

*1 trigger was not able to be categorized, as it could not be assigned to an inspiratory window.

Secondary outcome: Quality of triggering

Per subject, the triggering categories, the AI and the detection delay are given in Table 4.3. In Figure 4.5 an overview is given of the categorization of all matching triggers into synchronous, early and late triggers, as a function of the RR per subject. For all subjects most matching triggers were categorized as late within the inspiratory window, an effect that increased with a rising RR.

Table 4.3: Secondary outcome of the Simulink simulations. The trigger categories and detection delay are determined per subject. The data is presented as the median (interquartile range) of all subjects.

Secondary outcomes	Simulation (n = 15)
Trigger categories	
Synchronous (%)	12.5 (5.2 - 15.4)
Early (%)	5.1 (1.2 - 13.2)
Late (%)	84.9 (70.5 - 92.8)
AI	0.85 (0.78 - 0.90)
Detection delay	
(ms)	341 (315 - 374)
(% of T_i)	49.6 (43.5 - 55.9)

AI, asynchrony index; T_i , inspiratory time.

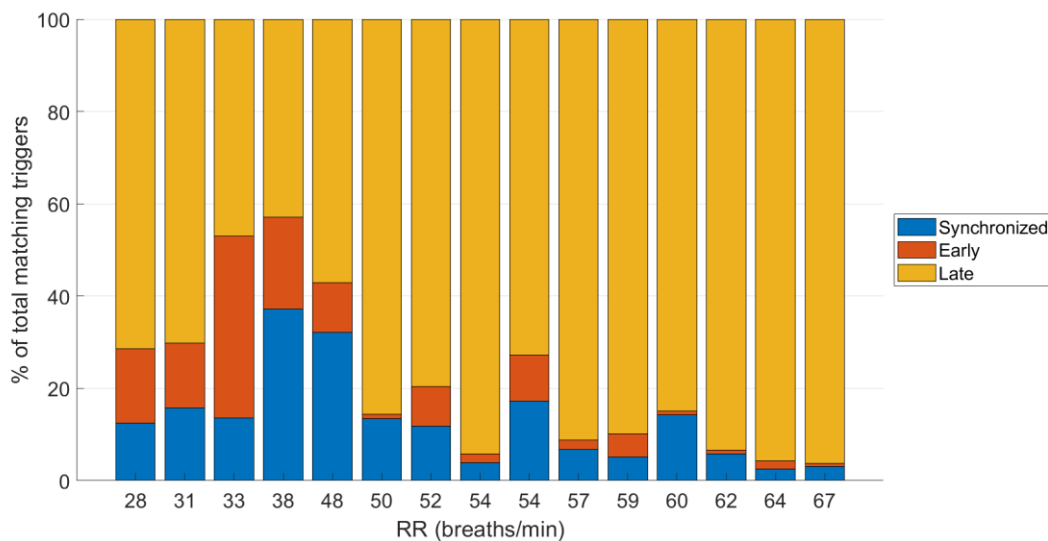


Figure 4.5: The division of all matching triggers into synchronized ($\pm 33\%$ of inspiratory window), early (-100% - -33% of inspiratory window) and late ($+33\%$ - $+100\%$ of inspiratory window). Given per subject as a function of the respiratory rate (RR).

The detection delay was relatively constant for subjects with a different RR. This is visualized in Figure 4.6, per subject as a function of the RR. When determining the detection delay with respect to the T_i , the percentual delay increased with a higher RR, see Figure 4.7. In this figure the subjects are divided into categories based on their GA at inclusion, which shows that the percentual detection delay is generally lower for subjects with a higher GA at inclusion.

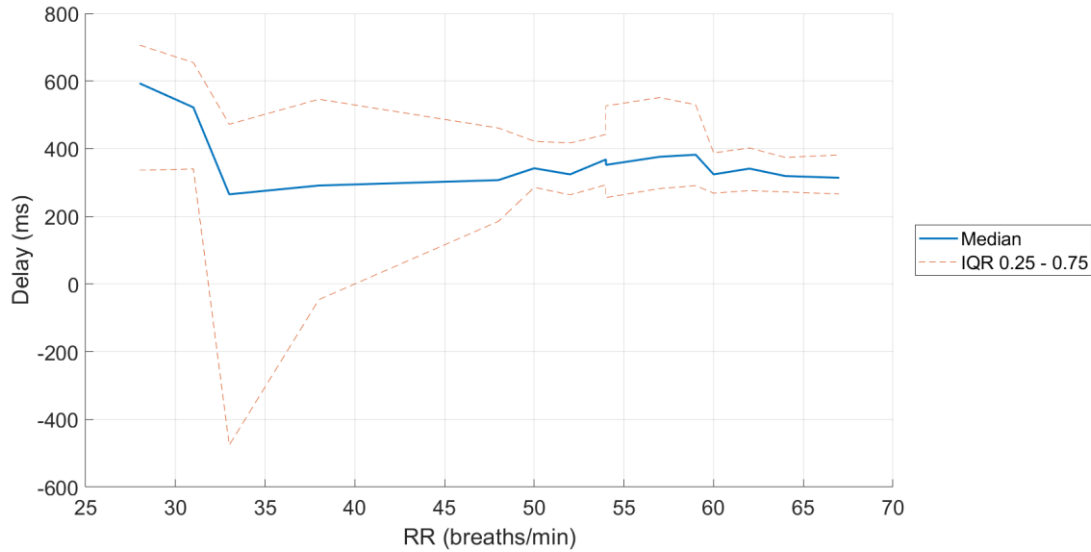


Figure 4.6: The median detection delay (expressed in ms), given per subject as a function of the respiratory rate (RR). Given with the interquartile ranges (IQR).

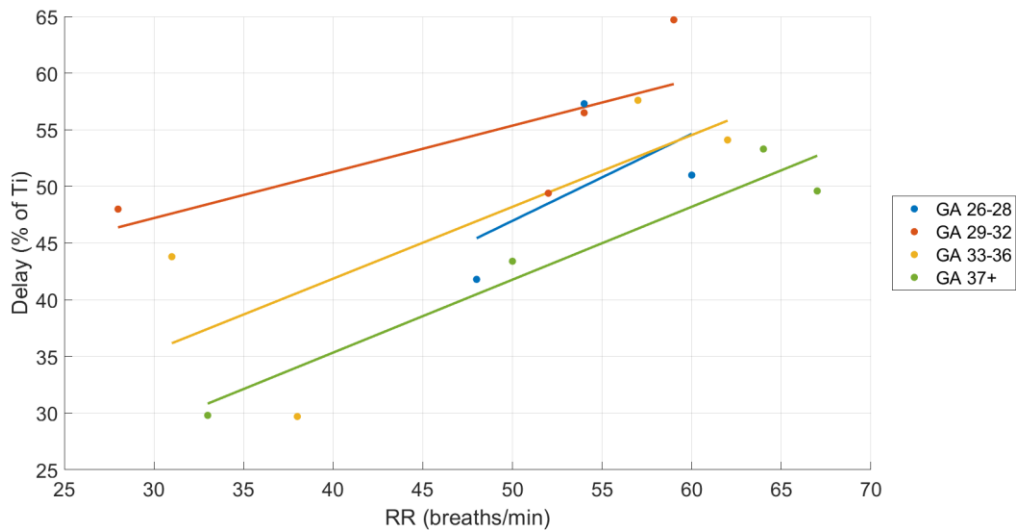


Figure 4.7: The median detection delay (expressed as a percentage of the inspiratory time (T_i)), given per subject as a function of the respiratory rate (RR). Divided into four categories based on the gestational age (GA) at inclusion.

4.4 Data acquisition: Bench set-up

Bench set-up design

The bench set-up was assembled in the TechRes Lab from the Politecnico University in Milan (Italy). The set-up is shown in Figure 4.8, in which the different components are indicated. Both nucleo boards (the hardware prototype and the ventilator nucleo board) were connected to a laptop. On both laptops an electron interface (JAVA based) was installed which was used to record and save the data. In case of the hardware prototype, the laptop was also supposed to serve as the transmitter of the input data. Due to technical difficulties, the transmission speed of the input data from the laptop to the prototype did not match real-time requirements. In order to ensure testing of the prototype in a real-time setting, for each included subject, 1 minute of the time-epoch was loaded onto the prototype. Using this construction, it was possible to process the input data in real-time.

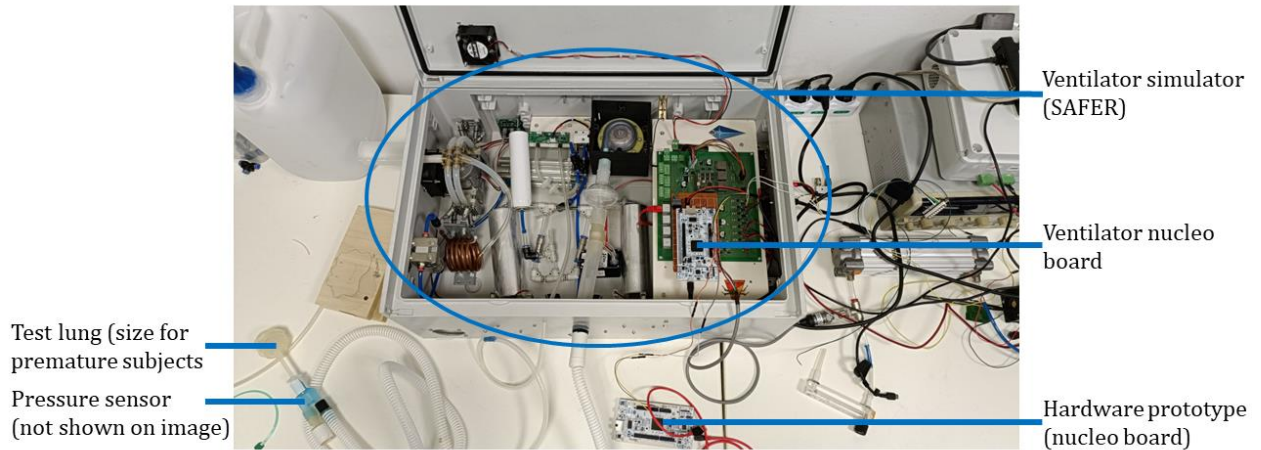


Figure 4.8: A picture taken of the bench set-up as constructed at the TechRes Lab.

Primary outcome: extraction of inspiratory triggers

All test measurements using the bench set-up resulted in a set of inflations given by the SAFER. For each subject the inspiratory triggers resultant from the hardware prototype deviated from the triggers of the Simulink simulations (see Figure 4.9 for an example), as there was no corresponding Simulink trigger for each real-time trigger.

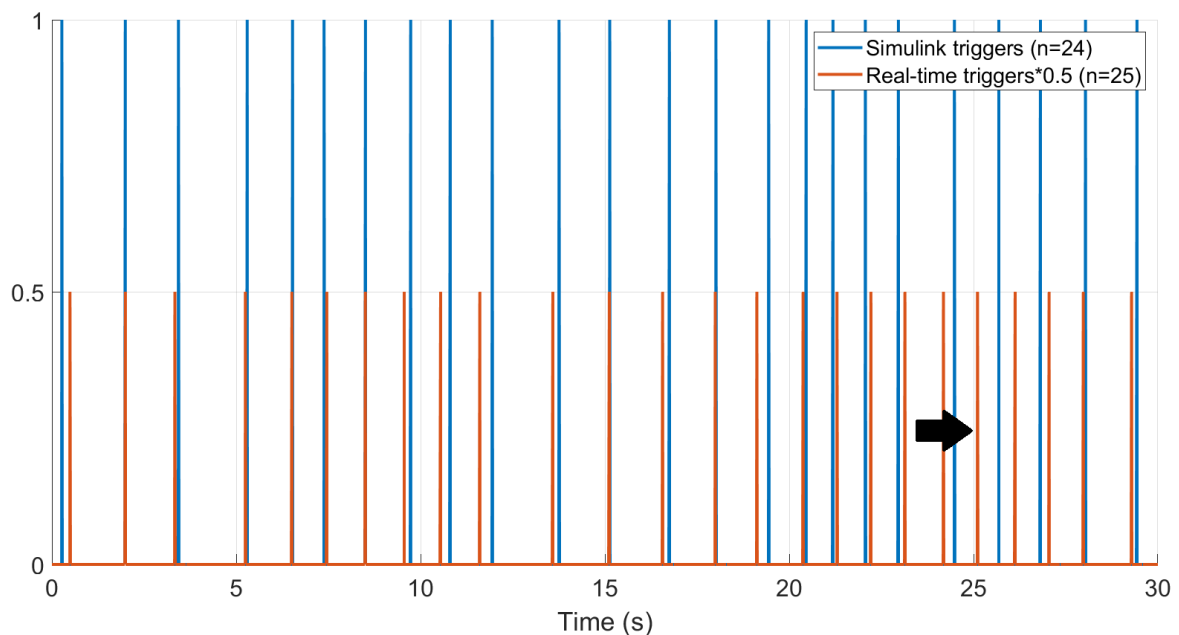


Figure 4.9: Example comparison of inspiratory triggers (length 0.3 sec) from the Simulink algorithm and the hardware prototype. The black arrow indicates a real-time trigger for which there is no corresponding Simulink trigger.

Secondary outcome: quality of triggering

As the triggers resultant from the hardware prototype did not match with those from the Simulink simulations, both the computation and detection delay could not be obtained from the bench set-up. Only the ventilation and mechanical delay were determined in this testing phase. Both delays were constant among all subjects and within the measurements. The ventilation and mechanical delay respectively amounted to approximately 8 and 0 ms. The mechanical delay could therefore be considered negligible. In Figure 4.10 an example is given that visualizes two inspiratory triggers, and the resultant pressure from the ventilator and measured pressure at the airway opening.

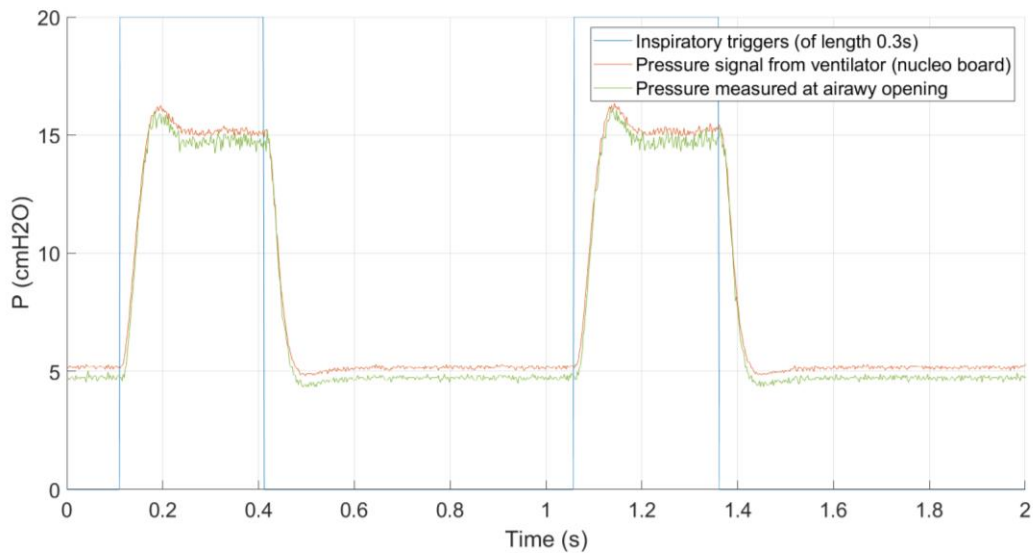


Figure 4.10: Example illustration of placement of inspiratory triggers, pressure signal from the ventilator and the measured pressure at the airway opening.

The trigger delay consisted of the transmission, computation, detection, mechanical and ventilation delay. Since the transmission and computation delay could not be obtained from the Simulink simulations/bench set-up, their values were estimated. The transmission delay is dependent on the properties of the chosen dEMG-device (e.g. wired or wireless connection). It is assumed that the transmission delay of an dEMG-device with a wired connection is negligible, which led to an estimation of the transmission delay at 0 ms. For the computation delay (which consists of the processing time and processing delay), the processing delay was estimated at minimal 55 ms based on the nature of the operations within the triggering model, see Figure 4.2. The processing time could not be estimated. Therefore, the hypothetical minimal trigger delay of the algorithm is estimated at 404 ms, see Figure 4.11.

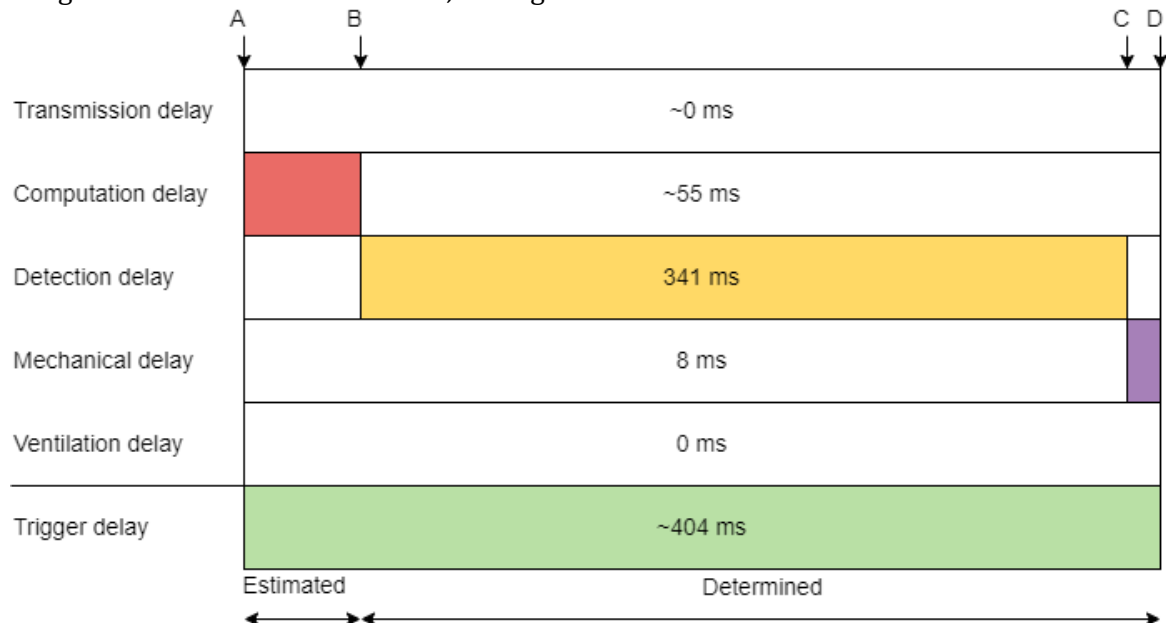


Figure 4.11: Distribution of delays components with respect to the trigger delay. Based on estimated (transmission and computation delay) and determined (detection, mechanical and ventilation delay) values. Timepoints; A: recording of patient data/receiving of patient data by the algorithm; B: processed data; C: detected inspiratory effort (placed trigger); D: receiving of trigger by ventilator/administration of inflation.

5. Discussion

To our knowledge, this is the first study in which the potential of tc-dEMG based inspiratory triggering was investigated by means of algorithm development, prototyping and testing. It was found that the algorithm was capable of extracting inspiratory triggers from the tc-dEMG signal, and subsequently triggering a ventilator. Although capable of triggering, the placed triggers were relatively late with respect to the onset of inspiratory efforts. The trigger delay was estimated at ~404 ms, which mostly consisted of the detection delay (~341 ms).

5.1 Interpretation of results

5.1.1 Primary outcome: extraction of inspiratory triggers

The results from the Simulink simulations showed that the developed triggering model was capable of extracting inspiratory triggers from tc-dEMG data, by comparing it to the reference study which investigated conventional nIPPV [5]. This comparison showed that the algorithm had a significantly lower percentage of unsupported inspirations with respect to the total amount of inspirations and was therefore capable of supporting more inspirations as would be the case for random triggering. This was strengthened in combination with the observation that the algorithm had less extra placed triggers in comparison with the inflations from the reference study, as this excludes the theory that a higher amount of inspirations were supported simply due to an excess of placed triggers. Finally, the algorithm also had a higher percentage of matching triggers compared to the matching inflations from the reference study. Although the latter two comparisons were not found to be significant, these results suggest that the developed algorithm had a better performance compared to random administration of inflations based on the defined criteria in this study. As a result, it was stated that tc-dEMG is capable of extracting inspiratory triggers and is therefore a potentially promising future triggering modality.

The amount of unsupported inspirations, matching and extra triggers were all visualized per subject as a function of the RR, in order to further investigate the algorithm performance for different RR's. There seemed to be no correlation between the percentage of unsupported inspirations and the RR, which indicated that the algorithm was adaptive to subjects with different RR. However, it was shown that subjects with a higher RR had relatively more matched triggers and less double triggers. A possible explanation for this phenomenon is that the subjects with a lower RR had more variation in their T_i compared to the subjects with a higher RR. A more variable RR leads to a less effective use of the trigger-block period in the model, as it is not fitting for respiratory intervals that deviate from the average. Therefore, double triggering can be more prevalent for these subjects, which also inherently decreases the percentage of matching triggers. As irregular breathing patterns are associated with prematurity (due to the immaturity of the brainstem) [97], it was expected that the model performance would deteriorate with decreasing GA. However, this correlation was not found in the current study.

The found presence of remaining P-top activity can be attributed to the limitations imposed on processing in order to minimize the processing delay. The amount of auto triggering in some infants, which was in all cases exclusively caused by P-top activity, indicates that it is relevant to investigate how to further attenuate P-top-activity, while considering its effect on the delay (e.g. by optimizing current filtering settings). Furthermore, it was not surprising that all auto triggers were placed due to cardiac interference and none due to other artifacts, since the data segments were selected based on the absence of artifactual data. However, it is expected that more representative data segments will contain a variety of artifacts (e.g. due to infant movements, clinical procedures, kangaroo care), and will therefore cause more auto triggering or possibly obstruct triggering altogether. In previous studies by Kraaijenga et al (2014), Van Leuteren et al. (2021) and Scholten et al. (2022) it was found that approximately 20-40% of dEMG data cannot be analysed due to presence of artifacts [101]–[103].

From the bench set-up it was confirmed that the hardware prototype was also able to extract triggers from the tc-dEMG signal and could subsequently activate a custom-made ventilator to administer inflations. However, the placement of the real-time obtained triggers was different compared to the triggers derived from Simulink. The cause for the difference in triggering of the hardware prototype can potentially be attributed to the alternative way of data transmission that was used in the bench set-up.

An important sidenote from the Simulink simulations is that the median T_i found in the measurements was found to be remarkable long (with a T_i/T_{cycle} ratio of 0.66), using the set definitions for inspiration and expiration. Generally, the T_i comprises of approximately one third to half of the T_{cycle} for (preterm) infants, when based on flow-measurements [98]. For the purposes of this study, it is highly relevant to consider the flow-based definition of T_i (as opposed to an alternative dEMG-based T_i -definition), as the aim is to administer inflations within the window of spontaneously generated inwards flow by the patient. A possible explanation for the divergent obtained values is that the classification of the positive and negative window used in this study was not suitable for neonatal tc-dEMG data. In literature an alternative method to classify the end of inspiration in neonatal dEMG data was found. Studies by Beck et al. (2011) and Gibu et al. (2017), who both investigated neural breathing in preterm infants, used peak dEMG to define the end of an inspiration, instead of 30% decrease of dEMG amplitude [8], [99], which is potentially more suitable.

5.1.2 Secondary outcome: quality of triggering

As a secondary outcome, the quality of the matched triggers was assessed. It was found that for all subjects most matching triggers were categorized as late within the inspiratory window, an effect that increased with a rising RR. This correlation was expected since subjects with a higher RR generally have a shorter T_i and are therefore more prone to late triggering due to the trigger-block period. The high amount of late triggers resulted in an inspiratory AI with a median of 0.85 among all subjects. This was considerably higher compared to the reference study, in which an inspiratory AI of 0.68 was found [5]. An AI of 0.68 confirms the 'randomness' of triggering for nIPPV (since an inflation was only considered synchronous within 33% of the total inspiratory window), whereas the high AI of this study showed that the triggering was not arbitrary. Instead, it indicates that most triggers were the result of an inspiratory effort, although the detection of these efforts tended to be late.

The observation that the found triggers were late within the inspiratory window was confirmed by the found detection delay, which had a median of 341 ms among all subjects. The detection delay was visualized per subject as a function of the RR, which showed that the delay was relatively constant for different RR's. This was unexpected, as it was hypothesized that the tc-dEMG signal would vary for different RR's, e.g. by a more abrupt onset of inspiratory effort for subjects with higher RR. In order to further investigate what potentially influenced the detection delay, it was evaluated if there was a correlation between the percentual detection delay with respect to the T_i and the GA at inclusion. For each GA category, the percentual detection delay increased with an increasing RR. This was expected, since the T_i decreases with a higher RR, whereas it was found that the absolute value of detection delay remained relatively constant, thus leading to a relatively long detection delay. The other correlation that was found, was that for subjects with a lower GA at inclusion, the percentual detection delay was generally higher. This can potentially be attributed to a more irregular RR for the younger subjects, and therefore less accurate triggering. Another explanation is that the data of the younger subjects contained more noise, causing the triggering threshold to be placed higher, and therefore inspiratory efforts to be detected slower. Important to realize is that the percentual detection delays with respect to the T_i found in this study are subject to change, as it is expected that the T_i was incorrectly determined and therefore consistently overestimated.

The hypothetical minimum trigger delay of the algorithm when using the entire setup was estimated at 404 ms, which consisted in large part of the detection delay. In order to place this found delay in the perspective of clinical feasibility, it must be compared to the T_i of the study population. The median T_i in this study was expected to be inaccurate due to an unlikely high value of 670 ms. The variable T_{cycle} was much less susceptible to incorrect determination, as it was simply defined from onset of one inspiratory effort till the next. Therefore, the found values for T_{cycle} are more reliable and can be used to estimate the T_i of this study population by taking one third or half of this value. This leads to an estimation of a median T_i of approximately 333 to 505 ms. In order to be clinically feasible, the trigger delay should be a maximum of 33% of the T_i , when considering Sinderby's definition of synchronous inflations. This leads to an upper limit of approximately 110 to 165 ms of the trigger delay, which is much less than the estimated trigger delay found in this study. Therefore, it is essential that future studies focus on reduction of the trigger delay.

5.2 Previous studies

As this is the first study into the potential of tc-dEMG as a modality for inspiratory triggering, it cannot be compared to previous studies. However, there are studies that have investigated the trigger delay of (NIV-)NAVA, which is also based on electrical diaphragm activity and is therefore the most suitable triggering modality to use for comparison. Each study defined the trigger delay between the onset of dEMG and the onset of inflation, and it varied between the 35 and 125 ms [8], [21], [100]. Therefore, the delay obtained with NAVA is considerably lower compared to the trigger delay found in this study. This can be explained by the differences in processing mechanism of both techniques. For NAVA a number of seven electrode pairs are placed on a transesophageal tube, from which continuously the closest pair to the center of the electrically active region of the diaphragm is selected (as the diaphragm moves with respect to the electrodes during a respiratory cycle). Next, the electrode pair caudal and cephalad from the closest pair are subtracted from each other, which highly reduces the signal-to-noise ratio [101]. This technique allows for obtaining a dEMG signal that is not only retrieved from an optimised position with respect to the diaphragm, but also a signal that contains a considerably less noise compared to a transcutaneous obtained signal. This eases the establishment of fast triggering. However, when comparing both trigger delays, it is important to consider that tc-dEMG based triggering is yet at a very early stage of development compared to the (NIV-)NAVA technique.

5.3 Study strengths and limitations

This is the first study in which real-time inspiratory triggering based on tc-dEMG was investigated. This was not only investigated through a simulation model that was able to perform real-time simulations, but also a bench set-up was constructed in which the algorithm was able to be tested as a hardware prototype in an actual real-time fashion. This study is therefore fit to serve as a starting point for future research into this field and it provides a reference to which further advancements in tc-dEMG based triggering can be compared. Also, whereas studies on (NIV-)NAVA only documented the overall trigger delay, this study narrowly investigated the separate delay components. This allowed for better understanding of the delay origin and provided concrete leads for further improvements and reduction of the trigger delay.

There are also several limitations that should be taken into consideration when interpreting the results. First, the data epochs used for this study were selected based on the absence of signal artifacts. By excluding artifacts from the analysis, it was not assessed how the algorithm responds to this type of data. It is expected that this would have led to an underestimation of the amount of auto triggers. The auto triggers that were present, were identified manually, as it was not deemed feasible to implement a method of automatic auto trigger classification within the timeframe of this study. However, this made the detection of auto triggers vulnerable to subjectivity. Also, for analysis of the results, the definition of the inspiratory window was not focussed on the neonatal population. Instead, the definition was adopted from Sinderby et al.

(2013) [94]. The resultant values of the T_i , which directly follow from the definition of the positive inspiratory window, were unlikely high, which suggest this definition is unsuitable for neonatal data.

For the bench set-up it was not managed to transmit the pre-recorded input data from the laptop towards the hardware prototype in real-time. Therefore, instead of transmitting the input data via a laptop, the data was loaded onto the nucleo board. This solution was limited, as it required RAM capacity from the nucleo board to load the input data. As a result, per subject only 1 minute of input data could be used for the bench set-up. Also, the alternative approach of data transmission might have impacted the prototype's behaviour, potentially explaining the difference between the prototype and Simulink triggers. More recently, it was managed establish real-time transmission of pre-recorded data to the prototype. However, as this is still ongoing research, it was not incorporated in the results of this study.

Finally, we were not able to assess all components of the trigger delay. We only performed measurements with pre-recorded data and therefore did not determine the transmission delay. Ongoing research is currently focussing on the connection of a wireless (Bluetooth-based) dEMG device from Demcon macawi respiratory systems (Demcon, Enschede, the Netherlands) with the prototype, from which in a later phase the transmission delay can be assessed. However, for this study the transmission delay was estimated based on the assumption that for a wired dEMG device this type of delay is negligible. The computation delay was assessed by theoretically estimating the processing delay of the triggering model (i.e. the real-time component of the algorithm). However, as there is no full intel on how the Simulink operations are executed, it is possible that the true computation delay is longer.

6. Recommendations and future perspectives

After completing the first-ever study into tc-dEMG based triggering, it is relevant to discuss the recommendations and future perspectives for tc-dEMG based triggering.

6.1 Reduction of the trigger delay

The main recommendation and essential for potential future use of dEMG-based triggering is to reduce the trigger delay. For future enhancement of the algorithm, it is recommended to review the used triggering mechanism. In this study a real-time triggering mechanism was used, for which both the capability and the delay were determined. Whereas the algorithm did prove to be capable of extracting inspiratory triggers, the trigger delay was still too high in order to be clinical feasible, with a hypothetical minimal delay of 404 ms. The detection delay made up the largest part of the trigger delay, and is therefore most important to reduce in future studies. Whether this can be accomplished through enhancement of the used triggering method in Simulink, is uncertain. The detection delay can mostly be contributed to the considerable amount of noise that the processed dEMG signal still contains, which hampers the detection of inspiratory efforts close to their onset. Overcoming this problem would either require more intensive and efficient pre-processing or to make the transition of real-time threshold-based triggering to prediction-based triggering.

Reducing the detection delay through implementing more extensive Simulink-based pre-processing methods, is expected to be challenging as this will likely further increase the computation delay. In this study it was found that in order to be clinical feasible, the trigger delay should be limited to approximately 110 to 165 ms. This signifies that the detection delay must be reduced to approximately 50 to 105 ms (considering the remainder delay components at a fixed value of ~60 ms). Whether real-time triggering using Simulink could reduce the detection delay to such a level is uncertain.

Another option to consider is using a different mechanism of triggering, called prediction-based triggering. By using this mechanism, in which the goal is to support the next inspiration instead of the current, it is possible to 'escape' the detection delay. This can be accomplished by predicting the position of the subsequent inspiration(s), based on the prior measured dEMG data. There are multiple ways imaginable to establish prediction-based triggering, e.g. by predicting the start of an inspiratory effort based on the start of the previous inspiratory effort or based on the end of the previous inspiratory effort. The latter method, although possibly better capable of making correct predictions, also provides less time to predict the next inspiration, and therefore might still introduce a small detection delay. The downside of implementing prediction-based triggering in infants, is that it can be challenging to accurately predict the start of inspiratory efforts, as the RR is known to be (highly) variable for this population. However, even with a certain number of inaccurate predictions, prediction-based triggering could potentially still result in lower PVA compared to non-synchronized ventilation. Considering the delay-challenge that is faced using real-time triggering, it is recommended to investigate whether prediction-based triggering can match the capability of real-time triggering and whether it can improve the trigger quality. For this alternative triggering mechanism, it is interesting to consider using machine learning (ML). ML is a type of artificial intelligence, that has the ability to learn from data and to improve its operating mechanism accordingly [102]. Therefore, it is potentially better capable of making correct predictions compared to a Simulink-based approach.

6.2 Further enhancement of the algorithm

The algorithm developed in this study was primarily focussed on the detection of inspiratory efforts. However, in order to establish a triggering mechanism (either real-time or prediction-based) that is feasible for clinical implementation, there are additional triggering functionalities

that should be implemented, such as a back-up rate. A back-up rate is crucial to implement within the algorithm, as it can be used as a safety net when the detection of inspiratory efforts is disrupted. The back-up rate can be activated in situations when there are no detection of inspiratory efforts for a certain amount of time, e.g. during periods of apnea. Also for periods of artifactual data (e.g. movement artifacts or persistent P-top activity) it is relevant to switch over to a back-up rate, as the placed triggers are no longer reliable. A method to assess for these periods of artifactual data, is by continuously evaluating the amount of disruptions in the signal and subsequently define a 'noise level/disruption factor'. The disruption factor can e.g. be defined by analysing the frequency characteristics of the signal. In case the disruption factor rises above a pre-set threshold value, the data is considered artifactual and the back-up rate will be activated. After implementation of the back-up rate and disruption factor into the algorithm, it can be assessed how the algorithm performs on realistic neonatal dEMG input (i.e. data that is not pre-selected on the absence of artifacts).

Another option for algorithm enhancement is to incorporate proportional assist (creating a PIP that corresponds to the neural respiratory drive based on dEMG activity) and synchronization on expiration, as is already implemented for NAVA.

6.3 Optimization of system parameters

The value for T_{seg} of the adaptive model was determined at 60 seconds for this study. The parameters were repeatedly determined over T_{seg} seconds of data and this value was subsequently used for the next T_{seg} seconds of data. This did signify that the currently used parameter values were always slightly outdated as they were determined over the previous minute of data. Therefore, in case of a stand-alone deviation in the data, the currently used system parameters would not account for it, and the currently calculated system parameters will not be accurate for the next segment of data. This would advocate for instituting a longer T_{seg} such that stand-alone deviations will be averaged out. However, with a longer T_{seg} the model will lack flexibility to keep track of short and fast fluctuations in T_{cycle} . Therefore, it is advised to experimentally investigate what the most fitting definition of T_{seg} is. During this assessment, it can also be considered to make T_{seg} dependent per subject, e.g. based on the general trend of variability in the measured data. Also, on a more general note, it is recommended for future studies to investigate which system parameters will benefit from being made adaptive (e.g. by assessing their variability within a measurement).

Also the definition of the trigger-block period is eligible for optimization. In this study it was stated that the trigger-block period was directly proportional to the length of T_{cycle} . However, for subjects with a higher RR the T_i is relatively longer with respect to the T_{cycle} . Therefore, it can be argued that for subjects with a higher RR a relatively longer trigger-block period is required compared to subjects with a lower RR. Also, the irregularity of the RR will influence the effectiveness of the trigger-block period, which should also be taken into account for the definition of the timing factor. Another method to define the trigger-block period is by placing the condition that the dEMG activity must have lowered below a threshold for a certain amount of time after placement of the last trigger before a new trigger can be placed. It is advised to experimentally compare different definitions of the trigger-block period in order to assess what is most effective.

6.4 Future perspectives

The results from this study showed that it is possible to extract inspiratory triggers from a neonatal tc-dEMG signal in real-time. Although the capability of triggering was confirmed, the results also indicated that the quality of triggering was not yet up to standard in order to be clinically feasible. After further improvements of the algorithm, the next steps to be followed in this line of research are described below (see Appendix F for an overview).

After enhancement of the algorithm, the new prototype can be connected to a dedicated dEMG device in order to execute test runs with real-time obtained dEMG data. If the connection is successfully made, this also opens the door to further testing in a setting that more closely resembles the clinical environment. For example, the wireless dEMG device can be used to measure data from a patient admitted to the NICU, while being connected to the prototype which in turn activates a dummy ventilator (that is not yet connected to the patient). By doing so, it is possible to evaluate the performance of the prototype in a real-life setting, and it can be assessed whether tc-dEMG based triggering is clinical feasible by evaluating the trigger accuracy and delay. The only aspect that is not accounted for in this measurement, is the patient-ventilator interaction.

The final step is to perform a clinical trial, in which it can be evaluated whether providing s-nIPPV has clinical value over nIPPV, e.g. by performing a cross-over trial. Both triggering modalities can be compared by assessing the PVA and clinical parameters such as WOB, gas exchange, and frequency and duration of periods of apnea (and accompanied desaturations and bradycardia). Also, the patient-ventilator interaction for s-nIPPV can be assessed, by evaluating whether the respiratory pattern of the infant is influenced by the administration of the inflations. Eventually, the ultimate aim of the clinical trial should be to assess whether tc-dEMG based s-nIPPV positively influences the short- (e.g. incidence of apnea periods or intubation prevention) and long-term (e.g. amount of ventilator days) clinical outcome of the target population.

7. Conclusion

The primary aim of this study was to evaluate whether it is possible to trigger a ventilator during non-invasive ventilation based on tc-dEMG data for the neonatal population. To that end, a tc-dEMG based triggering algorithm was developed and converted to a hardware prototype, which was tested in Simulink simulations and a bench set-up. The results showed that the algorithm was capable of real-time ventilator triggering. However, the triggers were given relatively late, mostly due to the delay introduced by the time needed to detect an inspiratory effort based on a tc-dEMG signal.

In conclusion, our study shows that dEMG-based ventilator triggering is technically feasible and shows potential as a new triggering modality in order to synchronize nIPPV in infants. However, future research is required to further reduce the triggering delay and to test the algorithm in various clinical settings.

References

- [1] A. H. van Kaam *et al.*, “Modes and strategies for providing conventional mechanical ventilation in neonates,” *Pediatric Research 2019*, pp. 1–6, Nov. 2019, doi: 10.1038/s41390-019-0704-1.
- [2] E. Atkinson and A. C. Fenton, “Management of apnoea and bradycardia in neonates,” *Paediatr Child Health*, vol. 19, no. 12, pp. 550–554, Dec. 2009, doi: 10.1016/J.PAED.2009.06.008.
- [3] E. Bancalari and N. Claure, “The evidence for non-invasive ventilation in the preterm infant,” *Arch Dis Child Fetal Neonatal Ed*, vol. 98, no. 2, pp. F98–F102, Mar. 2013, doi: 10.1136/ARCHDISCHILD-2011-301266.
- [4] R. W. van Leuteran, “Electromyography of the diaphragm in infants: Where technique becomes practice,” 2021.
- [5] C. G. de Waal, R. W. van Leuteran, F. H. de Jongh, A. H. van Kaam, and G. J. Hutten, “Patient-ventilator asynchrony in preterm infants on nasal intermittent positive pressure ventilation,” *Arch Dis Child Fetal Neonatal Ed*, vol. 104, no. 3, pp. F280–F284, May 2019, doi: 10.1136/ARCHDISCHILD-2018-315102.
- [6] H.-Y. Chang, N. Claure, C. D’Ugard, J. Torres, P. Nwajei, and E. Bancalari, “Effects of Synchronization During Nasal Ventilation in Clinically Stable Preterm Infants,” *Pediatric Research 2011 69:1*, vol. 69, no. 1, pp. 84–89, Jan. 2011, doi: 10.1203/pdr.0b013e3181ff6770.
- [7] L. Huang, M. R. Mendler, M. Waitz, M. Schmid, M. A. Hassan, and H. D. Hummler, “Effects of Synchronization during Noninvasive Intermittent Mandatory Ventilation in Preterm Infants with Respiratory Distress Syndrome Immediately after Extubation,” *Neonatology*, vol. 108, no. 2, pp. 108–114, Aug. 2015, doi: 10.1159/000431074.
- [8] C. K. Gibu, P. Y. Cheng, R. J. Ward, B. Castro, and G. P. Heldt, “Feasibility and physiological effects of noninvasive neurally adjusted ventilatory assist in preterm infants,” *Pediatric Research 2017 82:4*, vol. 82, no. 4, pp. 650–657, Jul. 2017, doi: 10.1038/pr.2017.100.
- [9] C. Gizzi *et al.*, “Is synchronised NIPPV more effective than NIPPV and NCPAP in treating apnoea of prematurity (AOP)? A randomised cross-over trial,” *Arch Dis Child Fetal Neonatal Ed*, vol. 100, no. 1, pp. F17–F23, Jan. 2015, doi: 10.1136/ARCHDISCHILD-2013-305892.
- [10] C. R. Tabacaru, R. R. Moores, J. Khoury, and H. J. Rozycki, “NAVA—synchronized compared to nonsynchronized noninvasive ventilation for apnea, bradycardia, and desaturation events in VLBW infants,” *Pediatr Pulmonol*, vol. 54, no. 11, pp. 1742–1746, Nov. 2019, doi: 10.1002/PPUL.24464.
- [11] E. Futier *et al.*, “Pressure support ventilation attenuates ventilator-induced protein modifications in the diaphragm,” *Critical Care 2008 12:5*, vol. 12, no. 5, pp. 1–9, Sep. 2008, doi: 10.1186/CC7010.
- [12] C. S. H. Sassoon, E. Zhu, and V. J. Caiozzo, “Assist–Control Mechanical Ventilation Attenuates Ventilator-induced Diaphragmatic Dysfunction,” *Am J Respir Crit Care Med*, vol. 170, no. 6, pp. 626–632, Dec. 2012, doi: 10.1164/RCCM.200401-0420C.
- [13] D. Valverde Montoro, P. García Soler, A. Hernández Yuste, and J. M. Camacho Alonso, “Ultrasound assessment of ventilator-induced diaphragmatic dysfunction in mechanically

- ventilated pediatric patients," *Paediatr Respir Rev*, vol. 40, pp. 58–64, Dec. 2021, doi: 10.1016/J.PRRV.2020.12.002.
- [14] B. Polla, G. D'Antona, R. Bottinelli, and C. Reggiani, "Respiratory muscle fibres: specialisation and plasticity," *Thorax*, vol. 59, no. 9, pp. 808–817, Sep. 2004, doi: 10.1136/THX.2003.009894.
- [15] N. Rittayamai *et al.*, "Effect of inspiratory synchronization during pressure-controlled ventilation on lung distension and inspiratory effort," *Annals of Intensive Care 2017 7:1*, vol. 7, no. 1, pp. 1–10, Oct. 2017, doi: 10.1186/S13613-017-0324-Z.
- [16] R. A. Darnall, "The role of CO₂ and central chemoreception in the control of breathing in the fetus and the neonate," *Respir Physiol Neurobiol*, vol. 173, no. 3, pp. 201–212, Oct. 2010, doi: 10.1016/J.RESP.2010.04.009.
- [17] M. E. Patrinos and R. J. Martin, "Apnea in the term infant," *Semin Fetal Neonatal Med*, vol. 22, no. 4, pp. 240–244, Aug. 2017, doi: 10.1016/J.SINY.2017.04.003.
- [18] R. E. Alvaro and H. Rigatto, "Control of Breathing in Fetal Life and Onset and Control of Breathing in the Neonate," in *Fetal and Neonatal Physiology*, 5th ed., vol. 1, R. A. Polin and S. H. Abman, Eds. Elsevier, 2017, pp. 737–747.
- [19] H. Stein, K. Firestone, and P. C. Rimensberger, "Synchronized mechanical ventilation using electrical activity of the diaphragm in neonates," *Clin Perinatol*, vol. 39, no. 3, pp. 525–542, Sep. 2012, doi: 10.1016/J.CLP.2012.06.004.
- [20] S.-C. Yong, S.-J. Chen, U. Kebangsaan Malaysia, J. Y. Latif, and T. Razak, "Incidence of nasal trauma associated with nasal prong versus nasal mask during continuous positive airway pressure treatment in very low birthweight infants: a randomised control study," *Arch Dis Child Fetal Neonatal Ed*, vol. 90, no. 6, pp. F480–F483, Nov. 2005, doi: 10.1136/ADC.2004.069351.
- [21] J. Lee *et al.*, "Non-invasive neurally adjusted ventilatory assist in preterm infants: a randomised phase II crossover trial," *Arch Dis Child Fetal Neonatal Ed*, vol. 100, no. 6, pp. F507–F513, Nov. 2015, doi: 10.1136/ARCHDISCHILD-2014-308057.
- [22] C. Borràs-Novell, M. G. Causapié, M. Murcia, D. Djian, and Ó. García-Algar, "Development of a 3D Individualized Mask for Neonatal Non-Invasive Ventilation," *Int J Bioprint*, vol. 8, no. 2, pp. 25–30, 2022, doi: 10.18063/IJB.V8I2.516.
- [23] F. Cresi *et al.*, "Short-term effects of synchronized vs. non-synchronized NIPPV in preterm infants: study protocol for an unmasked randomized crossover trial," *Trials 2021 22:1*, vol. 22, no. 1, pp. 1–9, Jun. 2021, doi: 10.1186/S13063-021-05351-0.
- [24] C. Moretti, G. Lista, V. Carnielli, and C. Gizzi, "Flow-synchronized NIPPV with double-inspiratory loop cannula: An in vitro study," *Pediatr Pulmonol*, vol. 56, no. 2, pp. 400–408, Feb. 2021, doi: 10.1002/PPUL.25161.
- [25] V. Dumpa, K. Katz, V. Northrup, and V. Bhandari, "SNIPPV vs NIPPV: does synchronization matter?," *Journal of Perinatology 2012 32:6*, vol. 32, no. 6, pp. 438–442, Nov. 2011, doi: 10.1038/jp.2011.117.
- [26] D. J. Stern, M. D. Weisner, and S. E. Courtney, "Synchronized neonatal non-invasive ventilation-a pilot study: the graseby capsule with bi-level NCPAP," *Pediatr Pulmonol*, vol. 49, no. 7, pp. 659–664, 2014, doi: 10.1002/PPUL.22880.

- [27] C. G. de Waal, J. v. Kraaijenga, G. J. Hutten, F. H. de Jongh, and A. H. van Kaam, "Breath detection by transcutaneous electromyography of the diaphragm and the Graseby capsule in preterm infants," *Pediatr Pulmonol*, vol. 52, no. 12, pp. 1578–1582, Dec. 2017, doi: 10.1002/PPUL.23895.
- [28] E. Charles, K. A. Hunt, G. F. Rafferty, J. L. Peacock, and A. Greenough, "Work of breathing during HHHFNC and synchronised NIPPV following extubation," *European Journal of Pediatrics* 2018 178:1, vol. 178, no. 1, pp. 105–110, Oct. 2018, doi: 10.1007/S00431-018-3254-3.
- [29] J. Kocjan, M. Adamek, B. Gzik-Zroska, D. Czyżewski, and M. Rydel, "Network of breathing. Multifunctional role of the diaphragm: a review," *Adv Respir Med*, vol. 85, no. 4, pp. 224–232, 2017, doi: 10.5603/ARM.2017.0037.
- [30] M. Kallio *et al.*, "NIV NAVA versus Nasal CPAP in Premature Infants: A Randomized Clinical Trial," *Research Briefings Neonatology*, vol. 116, pp. 380–384, 2019, doi: 10.1159/000502341.
- [31] A. C. Yagui, J. Meneses, B. A. Zólio, G. M. G. Brito, R. J. da Silva, and C. M. Rebello, "Nasal continuous positive airway pressure (NCPAP) or noninvasive neurally adjusted ventilatory assist (NIV-NAVA) for preterm infants with respiratory distress after birth: A randomized controlled trial," *Pediatr Pulmonol*, vol. 54, no. 11, pp. 1704–1711, Nov. 2019, doi: 10.1002/PPUL.24466.
- [32] A. Bordessoule, G. Emeriaud, S. Morneau, P. Jouviet, and J. Beck, "Neurally adjusted ventilatory assist improves patient–ventilator interaction in infants as compared with conventional ventilation," *Pediatric Research* 2012 72:2, vol. 72, no. 2, pp. 194–202, May 2012, doi: 10.1038/pr.2012.64.
- [33] C. Breatnach, N. P. Conlon, M. Stack, M. Healy, and B. P. O. Hare, "A prospective crossover comparison of neurally adjusted ventilatory assist and pressure-support ventilation in a pediatric and neonatal intensive care unit population," *Pediatric Critical Care Medicine*, vol. 11, no. 1, pp. 7–11, 2010, doi: 10.1097/PCC.0B013E3181B0630F.
- [34] F. Longhini *et al.*, "Neurally Adjusted Ventilatory Assist in Preterm Neonates with Acute Respiratory Failure," *Neonatology*, vol. 107, no. 1, pp. 60–67, Dec. 2015, doi: 10.1159/000367886.
- [35] H. Stein and K. Firestone, "Application of neurally adjusted ventilatory assist in neonates," *Semin Fetal Neonatal Med*, vol. 19, no. 1, pp. 60–69, Feb. 2014, doi: 10.1016/J.SINY.2013.09.005.
- [36] G. J. Hutten, L. A. van Eykern, P. Latzin, M. Kyburz, W. M. van Aalderen, and U. Frey, "Relative impact of respiratory muscle activity on tidal flow and end expiratory volume in healthy neonates," *Pediatr Pulmonol*, vol. 43, no. 9, pp. 882–891, Sep. 2008, doi: 10.1002/PPUL.20874.
- [37] G. C. Schoenwolf, S. B. Bleyl, P. R. Brauer, and P. H. Francis-West, "Development of the Respiratory System and Body Cavities," in *Larsen's Human Embryology*, 5th ed., Elsevier, 2015, pp. 251–266.
- [38] C. M. Chao, E. el Agha, C. Tiozzo, P. Minoo, and S. Bellusci, "A breath of fresh air on the mesenchyme: Impact of impaired mesenchymal development on the pathogenesis of bronchopulmonary dysplasia," *Front Med (Lausanne)*, vol. 2, no. APR, p. 27, 2015, doi: 10.3389/FMED.2015.00027/BIBTEX.

- [39] R. P. Davis and G. B. Mychaliska, "Neonatal pulmonary physiology," *Semin Pediatr Surg*, vol. 22, no. 4, pp. 179–184, Nov. 2013, doi: 10.1053/J.SEMPEDSURG.2013.10.005.
- [40] C. B. Mantilla, M. A. Fahim, J. E. Brandenburg, and G. C. Sieck, "Functional Development of Respiratory Muscles," in *Fetal and Neonatal Physiology*, 5th ed., vol. 1, R. A. Polin and S. H. Abman, Eds. Elsevier, 2017, pp. 627–641.
- [41] D. G. Nichols, "Medical Progress: Respiratory muscle performance in infants and children," *J Pediatr*, vol. 118, no. 4, 1991, doi: 10.1016/S0022-3476(05)83368-2.
- [42] T. H. Shaffer, D. Alapati, J. S. Greenspan, and M. R. Wolfson, "Neonatal non-invasive respiratory support: Physiological implications," *Pediatr Pulmonol*, vol. 47, no. 9, pp. 837–847, Sep. 2012, doi: 10.1002/PPUL.22610.
- [43] C. C. W. Hsia, D. M. Hyde, and E. R. Weibel, "Lung Structure and the Intrinsic Challenges of Gas Exchange," *Compr Physiol*, vol. 6, no. 2, p. 827, Apr. 2016, doi: 10.1002/CPHY.C150028.
- [44] J. P. Brandt and P. Mandiga, "Histology, Alveolar Cells," *StatPearls*, Jun. 2020.
- [45] V. K. Weinheimer *et al.*, "Influenza A Viruses Target Type II Pneumocytes in the Human Lung," *J Infect Dis*, vol. 206, no. 11, pp. 1685–1694, Dec. 2012, doi: 10.1093/INFDIS/JIS455.
- [46] C. Z. Zhao, X. C. Fang, D. Wang, F. di Tang, and X. D. Wang, "Involvement of type II pneumocytes in the pathogenesis of chronic obstructive pulmonary disease," *Respir Med*, vol. 104, no. 10, pp. 1391–1395, Oct. 2010, doi: 10.1016/J.RMED.2010.06.018.
- [47] J. A. Whitsett, S. E. Wert, and T. E. Weaver, "Alveolar Surfactant Homeostasis and the Pathogenesis of Pulmonary Disease," *Annu Rev Med*, vol. 61, p. 105, Feb. 2010, doi: 10.1146/ANNUREV.MED.60.041807.123500.
- [48] X. Lin, Y. Y. Zuo, and N. Gu, "Shape affects the interactions of nanoparticles with pulmonary surfactant," vol. 58, no. 1, 2015, doi: 10.1007/s40843-014-0018-5.
- [49] G. Enhorning, "Surfactant in Airway Disease," *Chest*, vol. 133, no. 4, pp. 975–980, Apr. 2008, doi: 10.1378/CHEST.07-2404.
- [50] G. B. Richerson and W. F. Boron, "Control of ventilation," in *Medical Physiology: A Cellular and Molecular Approach*, 2nd ed., 2012, pp. 725–745.
- [51] D. F. McCool, J. Hilbert, L. F. Wolfe, and J. O. Benditt, "The Respiratory System and Neuromuscular Diseases," in *Murray & Nadel's Textbook of Respiratory Medicine*, 7th ed., Elsevier Health Sciences, 2022, pp. 1812–1828.
- [52] G. Emeriaud, J. Beck, M. Tucci, J. Lacroix, and C. Sinderby, "Diaphragm Electrical Activity During Expiration in Mechanically Ventilated Infants," *Pediatric Research* 2006 59:5, vol. 59, no. 5, pp. 705–710, May 2006, doi: 10.1203/01.pdr.0000214986.82862.57.
- [53] C. Gaultier, "Respiratory muscle function in infants," *European Respiratory Journal*, vol. 8, pp. 150–153, 1995, doi: 10.1183/09031936.95.08010150.
- [54] A. H. Numa and C. J. L. Newth, "Anatomic dead space in infants and children," *J. Appl. Physiol*, vol. 80, no. 5, p. 14851489, 1996, doi: 10.1152/jappl.1996.80.5.1485.

- [55] M. di Cicco, A. Kantar, B. Masini, G. Nuzzi, V. Ragazzo, and D. Peroni, "Structural and functional development in airways throughout childhood: Children are not small adults," *Pediatr Pulmonol*, vol. 56, no. 1, pp. 240–251, Jan. 2021, doi: 10.1002/PPUL.25169.
- [56] A. A. Hutchison, "The Respiratory System," in *Pediatric and Neonatal Mechanical Ventilation*, P. C. Rimensberger, Ed. Springer-Verlag Berlin and Heidelberg GmbH & Co. KG, 2015, pp. 55–100.
- [57] R. P. Neumann and B. S. von Ungern-Sternberg, "The neonatal lung - Physiology and ventilation," *Paediatr Anaesth*, vol. 24, no. 1, pp. 10–21, Jan. 2014, doi: 10.1111/PAN.12280.
- [58] A. B. te Pas, P. G. Davis, S. B. Hooper, and C. J. Morley, "From Liquid to Air: Breathing after Birth," *J Pediatr*, vol. 152, no. 5, pp. 607–611, May 2008, doi: 10.1016/J.JPEDI.2007.10.041.
- [59] C. McPherson and J. A. Wambach, "Prevention and Treatment of Respiratory Distress Syndrome in Preterm Neonates," *Neonatal Network*, vol. 37, no. 3, pp. 169–177, May 2018, doi: 10.1891/0730-0832.37.3.169.
- [60] C. C.-H. Ma and S. Ma, "The Role of Surfactant in Respiratory Distress Syndrome," *Open Respir Med J*, vol. 6, no. 1, p. 44, Jul. 2012, doi: 10.2174/1874306401206010044.
- [61] J. J. Coalson, "Pathology of new bronchopulmonary dysplasia," *Seminars in Neonatology*, vol. 8, no. 1, pp. 73–81, Feb. 2003, doi: 10.1016/S1084-2756(02)00193-8.
- [62] N. N. Finer, R. Higgins, J. Kattwinkel, and R. J. Martin, "Summary Proceedings From the Apnea-of-Prematurity Group," *Pediatrics*, vol. 117, no. Supplement_1, pp. S47–S51, Mar. 2006, doi: 10.1542/PEDS.2005-0620H.
- [63] J. M. di Fiore, C. F. Poets, E. Gauda, R. J. Martin, and P. MacFarlane, "Cardiorespiratory events in preterm infants: interventions and consequences," *Journal of Perinatology* 2016 36:4, vol. 36, no. 4, pp. 251–258, Nov. 2015, doi: 10.1038/jp.2015.165.
- [64] R. J. Martin, K. Wang, Ö. Köroğlu, J. di Fiore, and P. Kc, "Intermittent Hypoxic Episodes in Preterm Infants: Do They Matter?," *Neonatology*, vol. 100, no. 3, pp. 303–310, Sep. 2011, doi: 10.1159/000329922.
- [65] J. J. Greer, G. D. Funk, and K. Ballanyi, "Preparing for the first breath: prenatal maturation of respiratory neural control," *J Physiol*, vol. 570, no. 3, pp. 437–444, Feb. 2006, doi: 10.1113/JPHYSIOL.2005.097238.
- [66] C. P. Travers, S. H. Abman, and W. A. Carlo, "Control of breathing in preterm infants: Neonatal ICU and beyond," *Am J Respir Crit Care Med*, vol. 197, no. 12, pp. 1518–1520, Jun. 2018, doi: 10.1164/RCCM.201801-0137ED/SUPPL_FILE/DISCLOSURES.PDF.
- [67] L. A. Stokowski, "A primer on apnea of prematurity," *Advances in Neonatal Care*, vol. 5, no. 3, pp. 155–174, Jun. 2005, doi: 10.1016/J.ADNC.2005.02.010.
- [68] J. Zhao, F. Gonzalez, and D. Mu, "Apnea of prematurity: from cause to treatment," *European Journal of Pediatrics* 2011 170:9, vol. 170, no. 9, pp. 1097–1105, Feb. 2011, doi: 10.1007/S00431-011-1409-6.
- [69] B. A. Edwards, S. A. Sands, and P. J. Berger, "Postnatal maturation of breathing stability and loop gain: The role of carotid chemoreceptor development," *Respir Physiol Neurobiol*, vol. 185, no. 1, pp. 144–155, Jan. 2013, doi: 10.1016/J.RESP.2012.06.003.

- [70] A. Khan, M. Qurashi, K. Kwiatkowski, D. Cates, and H. Rigatto, "Measurement of the CO₂ apneic threshold in newborn infants: Possible relevance for periodic breathing and apnea," *J Appl Physiol*, vol. 98, no. 4, pp. 1171–1176, Apr. 2005, doi: 10.1152/JAPPLPHYSIOL.00574.2003.
- [71] J. W. Kwon, "High-flow nasal cannula oxygen therapy in children: a clinical review," *Clin Exp Pediatr*, vol. 63, no. 1, p. 3, Jan. 2020, doi: 10.3345/KJP.2019.00626.
- [72] E. Kepreotes *et al.*, "High-flow warm humidified oxygen versus standard low-flow nasal cannula oxygen for moderate bronchiolitis (HFWHO RCT): an open, phase 4, randomised controlled trial," *The Lancet*, vol. 389, no. 10072, pp. 930–939, Mar. 2017, doi: 10.1016/S0140-6736(17)30061-2.
- [73] X. Durrmeyer and C. Danan, "Neonatal Intubation (Specific Considerations)," in *Pediatric and Neonatal Mechanical Ventilation*, P. C. Rimensberger, Ed. Springer, 2015, pp. 115–121.
- [74] M. K. Brown and R. M. DiBlasi, "Mechanical Ventilation of the Premature Neonate," *Respir Care*, 2011, doi: 10.4187/respcare.01429.
- [75] S. M. Donn and S. K. Sinha, "Mechanical Ventilation," in *Pediatric and Neonatal Mechanical Ventilation*, P. C. Rimensberger, Ed. Springer, 2015, pp. 149–262.
- [76] R. A. Mahmoud, C. C. Roehr, and G. Schmalisch, "Current methods of non-invasive ventilatory support for neonates," *Paediatr Respir Rev*, vol. 12, no. 3, pp. 196–205, Sep. 2011, doi: 10.1016/J.PRRV.2010.12.001.
- [77] G. Bernstein *et al.*, "Randomized multicenter trial comparing synchronized and conventional intermittent mandatory ventilation in neonates," *J Pediatr*, vol. 128, no. 4, pp. 453–463, Apr. 1996, doi: 10.1016/S0022-3476(96)70354-2.
- [78] N. McCallion, R. Lau, C. J. Morley, and P. A. Dargaville, "Neonatal volume guarantee ventilation: effects of spontaneous breathing, triggered and untriggered inflations," *Arch Dis Child Fetal Neonatal Ed*, vol. 93, no. 1, pp. F36–F39, Jan. 2008, doi: 10.1136/ADC.2007.126284.
- [79] V. Chan and A. Greenough, "Randomised controlled trial of weaning by patient triggered ventilation or conventional ventilatton," *European Journal of Pediatrics* 1993 152:1, vol. 152, no. 1, pp. 51–54, Jan. 1993, doi: 10.1007/BF02072516.
- [80] J. Y. Chen, U. P. Ling, and J. H. Chen, "Comparison of synchronized and conventional intermittent mandatory ventilation in neonates," *Pediatrics International*, vol. 39, no. 5, pp. 578–583, 1997, doi: 10.1111/J.1442-200X.1997.TB03644.X.
- [81] J. P. Cleary, G. Bernstein, F. L. Mannino, and G. P. Heldt, "Improved oxygenation during synchronized intermittent mandatory ventilation in neonates with respiratory distress syndrome: A randomized, crossover study," *J Pediatr*, vol. 126, no. 3, pp. 407–411, Mar. 1995, doi: 10.1016/S0022-3476(95)70460-4.
- [82] S. M. Kuo, B. H. Lee, and Wenshun. Tian, *Real-time digital signal processing : fundamentals, implementations and applications*, 3rd ed. Wiley, 2013.
- [83] J. v. Kraaijenga, G. J. Hutten, F. H. de Jongh, and A. H. van Kaam, "Transcutaneous electromyography of the diaphragm: A cardio-respiratory monitor for preterm infants," *Pediatr Pulmonol*, vol. 50, no. 9, pp. 889–895, Sep. 2015, doi: 10.1002/PPUL.23116.

- [84] E. Peri *et al.*, "Singular Value Decomposition for Removal of Cardiac Interference from Trunk Electromyogram," *Sensors 2021, Vol. 21, Page 573*, vol. 21, no. 2, p. 573, Jan. 2021, doi: 10.3390/S21020573.
- [85] K. S. Frahm, M. B. Jensen, D. Farina, and O. K. Andersen, "Surface EMG crosstalk during phasic involuntary muscle activation in the nociceptive withdrawal reflex," *Muscle Nerve*, vol. 46, no. 2, pp. 228–236, Aug. 2012, doi: 10.1002/MUS.23303.
- [86] R. W. van Leuteren, G. J. Hutten, C. G. de Waal, P. Dixon, A. H. van Kaam, and F. H. de Jongh, "Processing transcutaneous electromyography measurements of respiratory muscles, a review of analysis techniques," *Journal of electromyography and kinesiology*, vol. 48, pp. 176–186, Oct. 2019, doi: 10.1016/J.JELEKIN.2019.07.014.
- [87] K. M. Lynch, N. Marchuk, and M. L. Elwin, "Digital Signal Processing," in *Embedded Computing and Mechatronics with the PIC32 Microcontroller*, Elsevier Inc., 2015, pp. 341–374.
- [88] L. Xu, E. Peri, R. Vullings, C. Rabotti, J. P. van Dijk, and M. Mischi, "Comparative Review of the Algorithms for Removal of Electrocardiographic Interference from Trunk Electromyography," *Sensors 2020, Vol. 20, Page 4890*, vol. 20, no. 17, p. 4890, Aug. 2020, doi: 10.3390/S20174890.
- [89] J. Barrios-Muriel, F. Romero, F. J. Alonso, and K. Gianikellis, "A simple SSA-based denoising technique to remove ECG interference in EMG signals," *Biomed Signal Process Control*, vol. 30, pp. 117–126, Sep. 2016, doi: 10.1016/J.BSPC.2016.06.001.
- [90] E. J. W. Maarsingh, L. A. van Eykern, A. B. Sprikkelman, M. O. Hoekstra, and W. M. C. van Aalderen, "Respiratory muscle activity measured with a noninvasive EMG technique: Technical aspects and reproducibility," *J Appl Physiol*, vol. 88, no. 6, pp. 1955–1961, 2000, doi: 10.1152/JAPPL.2000.88.6.1955/ASSET/IMAGES/LARGE/JAPP05613003X.JPEG.
- [91] A. Bartolo, R. R. Dzwonczyk, C. Roberts, and E. Goldman, "Description and validation of a technique for the removal of ECG contamination from diaphragmatic EMG signal," *Med Biol Eng Comput*, vol. 34, no. 1, pp. 76–81, 1996, doi: 10.1007/BF02637025.
- [92] A. Bartolo, C. Roberts, R. R. Dzwonczyk, and E. Goldman, "Analysis of diaphragm EMG signals: comparison of gating vs. subtraction for removal of ECG contamination," <https://doi-org.ezproxy2.utwente.nl/10.1152/jappl.1996.80.6.1898>, vol. 80, no. 6, pp. 1898–1902, 1996, doi: 10.1152/JAPPL.1996.80.6.1898.
- [93] M. S. Redfern, R. E. Hughes, and D. B. Chaffin, "High-pass filtering to remove electrocardiographic interference from torso EMG recordings," *Clin Biomech (Bristol, Avon)*, vol. 8, no. 1, pp. 44–48, 1993, doi: 10.1016/S0268-0033(05)80009-9.
- [94] C. Sinderby *et al.*, "An automated and standardized neural index to quantify patient-ventilator interaction," *Critical Care 2013 17:5*, vol. 17, no. 5, pp. 1–9, Oct. 2013, doi: 10.1186/CC13063.
- [95] R. W. van Leuteren, C. G. de Waal, F. H. de Jongh, R. A. Bem, A. H. van Kaam, and G. Hutten, "Diaphragm Activity Pre and Post Extubation in Ventilated Critically Ill Infants and Children Measured With Transcutaneous Electromyography," *Pediatr Crit Care Med*, vol. 22, no. 11, pp. 950–959, Nov. 2021, doi: 10.1097/PCC.0000000000002828.

- [96] L. Zaremba, "Evaluation of Electromyography for assessing Bronchodilator treatment in Paediatrics with a novel algorithm for Respiratory waveform obtainment," Master's thesis, University of Twente, Enschede, 2020.
- [97] P. Indic, D. Paydarfar, and R. Barbieri, "Point Process Modeling of Interbreath Interval: A New Approach for the Assessment of Instability of Breathing in Neonates," *IEEE Trans Biomed Eng*, vol. 60, no. 10, p. 2858, 2013, doi: 10.1109/TBME.2013.2264162.
- [98] T. Dassios, A. Vervenioti, S. Tzifas, S. Fouzas, and G. Dimitriou, "Validation of a non-invasive pressure-time index of the inspiratory muscles in spontaneously breathing newborn infants," *J Clin Monit Comput*, pp. 1–6, Jun. 2022, doi: 10.1007/S10877-022-00882-6/FIGURES/4.
- [99] J. Beck *et al.*, "Characterization of Neural Breathing Pattern in Spontaneously Breathing Preterm Infants," *Pediatric Research 2011 70:6*, vol. 70, no. 6, pp. 607–613, Dec. 2011, doi: 10.1203/pdr.0b013e318232100e.
- [100] J. Beck *et al.*, "Patient-Ventilator Interaction During Neurally Adjusted Ventilatory Assist in Low Birth Weight Infants," *Pediatric Research 2009 65:6*, vol. 65, no. 6, pp. 663–668, Jun. 2009, doi: 10.1203/pdr.0b013e31819e72ab.
- [101] C. A. Sinderby, J. C. Beck, L. H. Lindström, and A. E. Grassino, "Enhancement of signal quality in esophageal recordings of diaphragm EMG," *J Appl Physiol*, vol. 82, no. 4, pp. 1370–1377, 1997, doi: 10.1152/JAPPL.1997.82.4.1370/ASSET/IMAGES/LARGE/JAPP0541205.JPEG.
- [102] C. Janiesch, P. Zschech, and K. Heinrich, "Machine learning and deep learning," *Electronic Markets*, vol. 31, no. 3, pp. 685–695, Sep. 2021, doi: 10.1007/S12525-021-00475-2/TABLES/2.

Appendix

A. Flowchart pre-existing offline dEMG processing algorithm

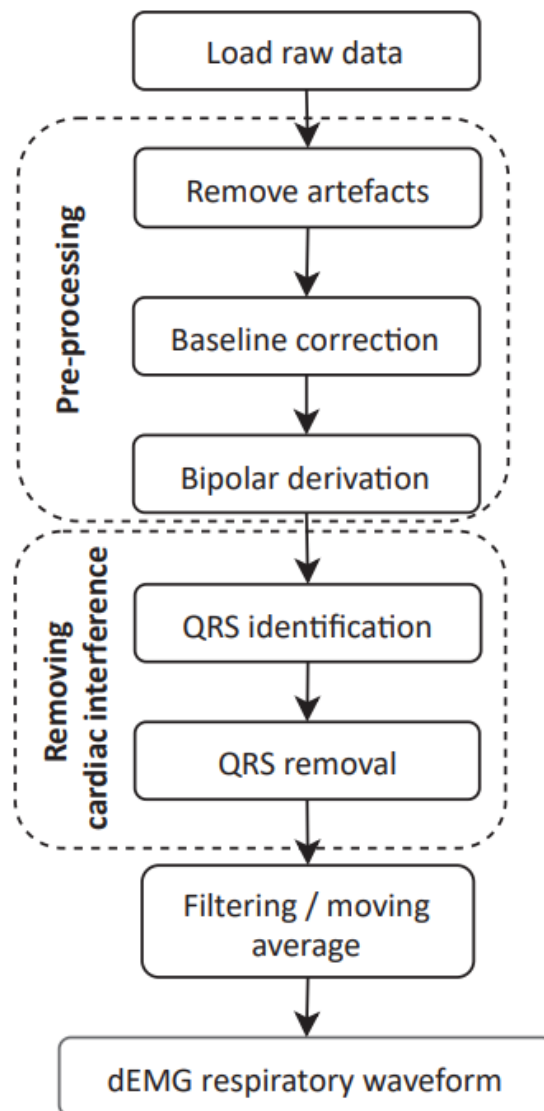


Figure A.1: Flowchart of processing steps from the pre-existing tc-dEMG based algorithm. From Van Leuteren et al. (2021) [4].

B. DSP design applied to tc-dEMG based triggering algorithm

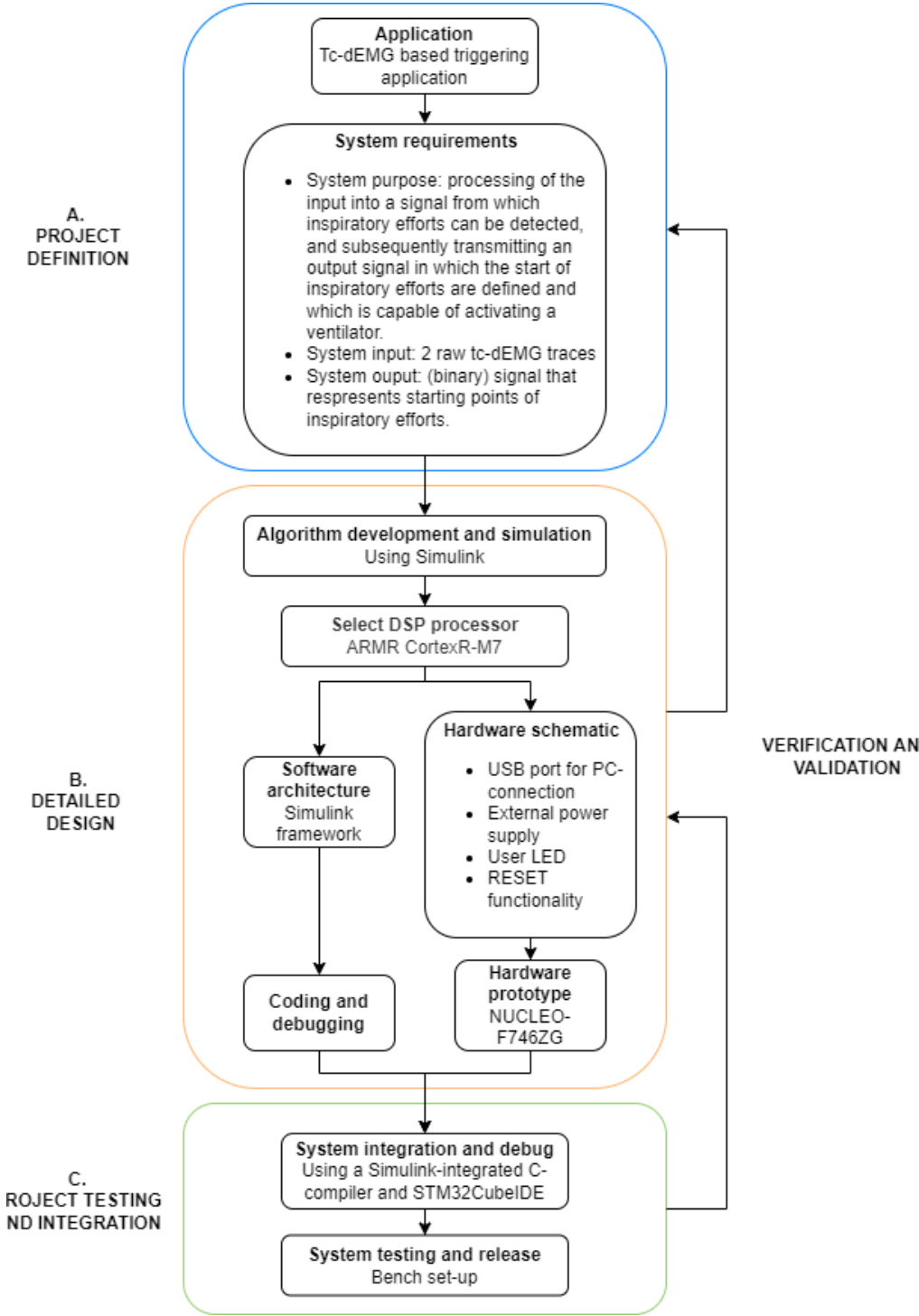


Figure B.1: Simplified DSP design flow applied to the tc-dEMG based triggering algorithm.

C. System parameter values

In the table below an overview is given of all used system parameter values in the algorithm, and how they were determined. For more information on each parameter value, see the corresponding component in Appendix D.

Table C.1: System parameter values used in this thesis.

System parameters per component	Value/setting	Determined how
Pre-processing		
Baseline correction		
High-pass filter (Hz)	40 (2 nd order)	Experimental
Creating pulse train		
Time constant (ms)	2	Experimental
Moving maximum (adaptive model)		
Window length (s)	2	Reasoning
Moving maximum (triggering model)	Adaptive	Dependent per subject (/within measurement)
Pulse length (ms)	100	Literature [90]
Aligning pulse train		
High-pass filter (P- and T-tops) (Hz)	100 (2 nd order)	Experimental
Delay (ms)	5	Determined
Filling gates		
Delay (ms)	45	Reasoning
Creating respiratory waveform		
Window length (ms)	500	Based on pre-existing offline tc-dEMG algorithm
Finding respiratory rate		
Breath detection using respiratory waveform		
Delay (ms)	250	Experimental
Hit-crossing	Only rising crossings	N.A.
Pulse length (1) (ms)	750	Max. RR to detect = 80
Pulse length (2) (samples)	1	N.A.
Calculating Tcycle		
Tseg (s)	60	Reasoning
Maximum Tcycle (s)	2	Reasoning
Extracting inspiratory triggers		
Tcycle	Adaptive	Dependent per subject/within measurement
ThEMG	Adaptive	Dependent per subject (/within measurement)
Constant (1)	1	N.A.
Constant (2)	0	N.A.
Trigger block factor	0.6	Reasoning
Single trigger		
Pulse length (1)	N.A.	N.A.
Pulse length (2) (samples)	1	N.A.

D. Detailed description of Simulink algorithm

Overview

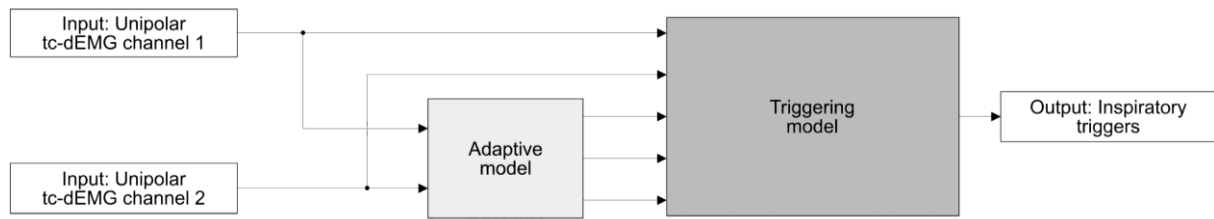


Figure D.1: Overview of Simulink algorithm, consisting of two models: the adaptive model and the triggering model.

Input: Raw dEMG channels 1 and 2.

Adaptive model: Model that buffers data over T_{seg} seconds and determines three variables from the data (ThEMG, Tcycle and moving maximum). These variables are sent to the triggering model where they are used for real-time triggering. Since these variables are calculated over the past T_{seg} seconds, they are always slightly outdated. However, under the assumption that these variables are relatively constant over short periods of time, it is expected that this will not be a large issue.

Triggering model: This is the real-time triggering model, in which triggers are extracted from the processed dEMG signal. It has as input the raw input and the variables from the adaptive model.

Output: The derived inspiratory triggers, processed in a binary signal and therefore suitable to activate a ventilator.

Adaptive model

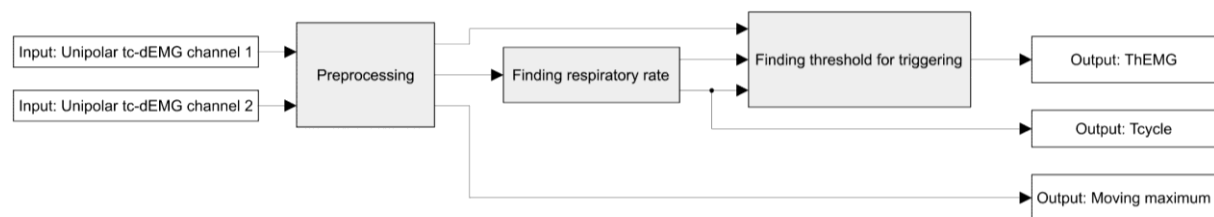


Figure D.2: The expanded adaptive model, consisting of three components: pre-processing, finding respiratory rate, and finding threshold for triggering.

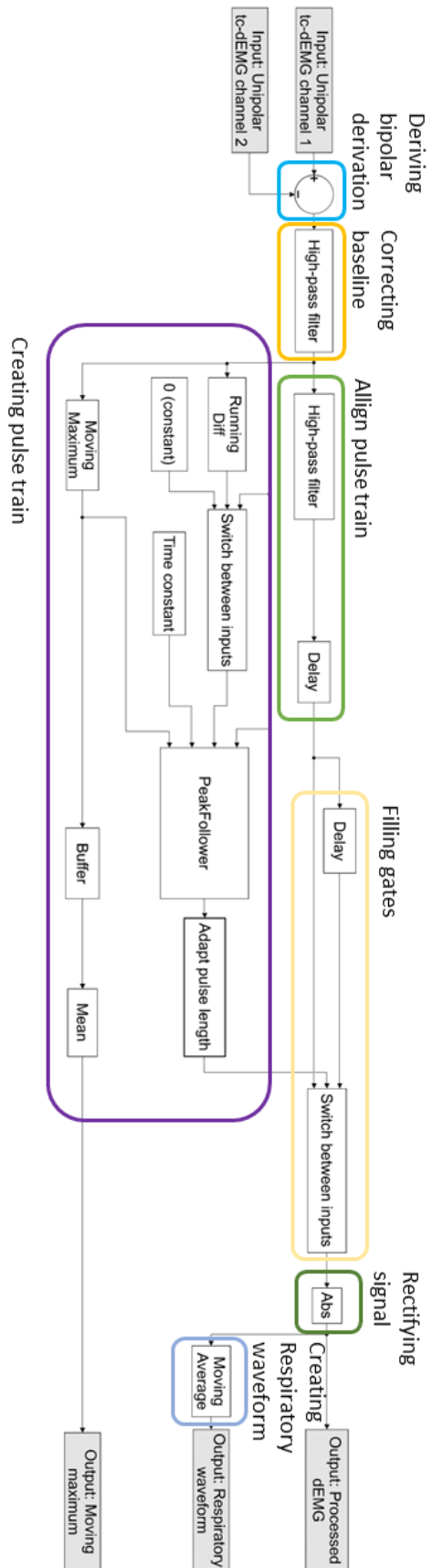


Figure D.3: Expanded subcomponent pre-processing (from the adaptive model).

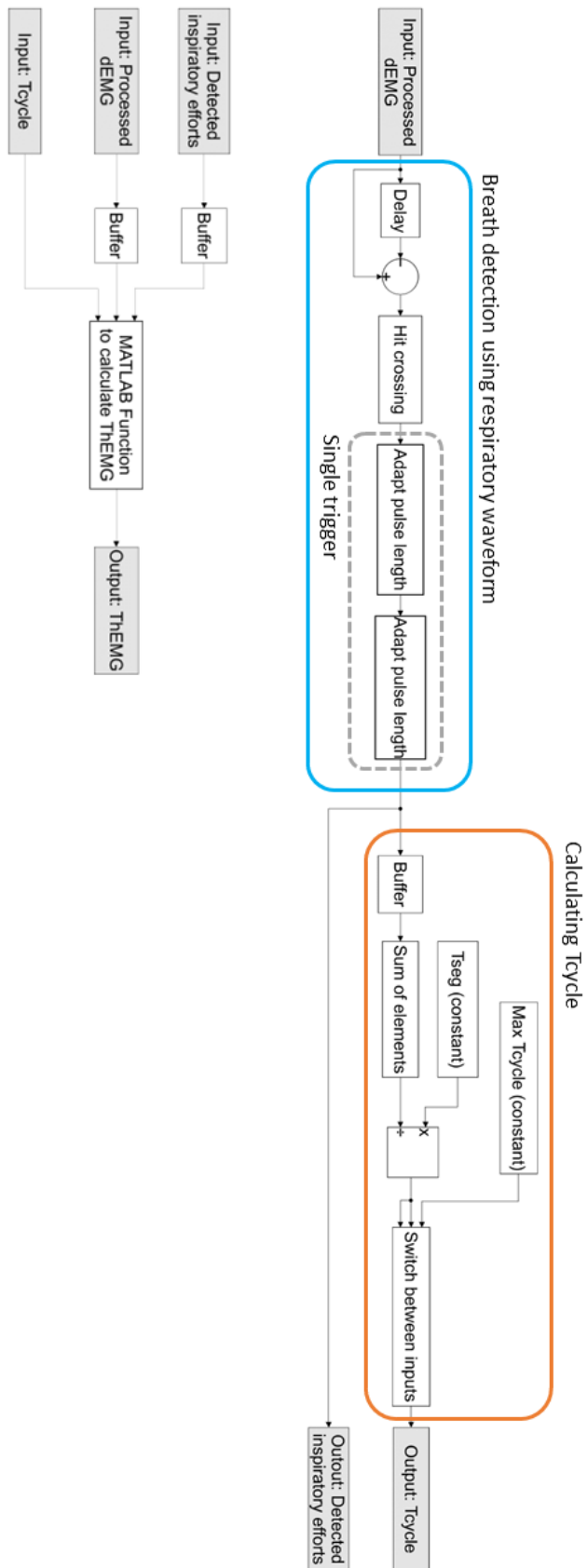


Figure D.4: Expanded components finding respiratory rate and finding threshold for triggering (from the adaptive model).

MATLAB function to calculate ThEMG

```
function trigger_threshold = fcn(detBreaths, rect_EMG, Ttot)

nr_detBreaths = sum(detBreaths); %number of detected breaths in resp. waveform
(for comparison)

%Initialize variables
a = 0;
b = max(rect_EMG);
tol = 0;
nr_triggers_rect = 0;
diff = nr_detBreaths - nr_triggers_rect;
th = 0; %initializing th
it = 0;
k_block = 0.6; %trigger block factor

%Bisection method
while abs(diff) > tol
th = (a+b)/2; %calculate new threshold to try on data
it = it+1; %count iterations
%get triggers with set threshold
trigger_array = zeros(length(rect_EMG),1);
rect_EMG_use = rect_EMG;
for i = 1:length(rect_EMG_use)
%give pulse if rect_EMG is higher than threshold. Assign all
%consecutive rect_EMG samples within Tcycle*k_block to zero so there will
%be no additional trigger within Tcycle*k_block
if rect_EMG_use(i) > th && i <=length(rect_EMG_use)-(round(Ttot*k_block))
trigger_array(i) = 1;
rect_EMG_use(i:i+(round(Ttot*k_block))) = 0; %block new pulses for Tcycle*k_block
ms
%same as before. Only this describes the case at the end of the
%rect_EMG signal.
elseif rect_EMG_use(i) > th && i > length(rect_EMG_use)-(round(Ttot*k_block))
trigger_array(i) = 1;
rect_EMG_use(i:end) = 0;
else
trigger_array(i) = 0;
end
end
nr_triggers_rect = sum(trigger_array);
diff = nr_detBreaths - nr_triggers_rect; %calculate difference between nr. of
found
%triggers and nr. of detected breaths through Simulink

if sign(diff) == 1 %if nr_detBreaths > nr_triggers_rect
b = th;
else %if nr_detBreaths < nr_triggers_rect
a = th;
end

if it == 20 %stop after 20 iterations
```

```

        break
    end
end

%Minimalize threshold further (on the condition that the amount of triggers does
not
%increase
condition = nr_triggers_rect;
nr_triggers_rect2 = condition;
th2 = 0;

while nr_triggers_rect2 == condition
    th2 = th - 0.01; %keep trying to decrease threshold with 0.01

    %get triggers

```

Pre-processing

Goal: to derive the respiratory waveform from which the adaptable system parameters can be determined, that will subsequently serve as input for the triggering model.

Loading data

Subtraction of the raw dEMG channels, to obtain the bipolar derivation of the dEMG signal.

Filtering

The baseline was corrected using a 2nd-order high-pass filter, which is of the lowest possible order and therefore induces as little delay as possible. The accompanied cut-off frequency (40 Hz) was experimentally determined, based on this filter order.

Creating pulse train

This subblock is all about detecting the QRS-pulses. For this we used the peakfollower (stateflow chart). How this Stateflow chart detects QRS-pulses, is explained in detail in the accompanying master's thesis [96]. The PeakFollower needs 4 inputs:

- dEMG signal:
 - o The so-far processed dEMG signal.
- Increase detection:
 - o This input equals the dEMG signal when it increases, and it equals zero when the dEMG signal decreases. This is accomplished by continuously calculating the running difference. If the running difference is positive (and therefore the signal is rising), the dEMG signal is passed. If the running difference is negative, zeros are passed through.
- Max value:
 - o The maximum value (for which the PeakFollower starts descending, even though the dEMG signal is still in rising state) is obtained by calculation of the moving maximum. The moving maximum is obtained over 2 seconds (as it will contain at least >1 QRS-peaks). The aim is to find the average amplitude of the QRS-peaks. In order to do so, a large window is applied to average out the effect of artefacts. As a large window is used (and therefore imposes a large delay), it is inconvenient to calculate the moving maximum in the triggering model (which is supposed to run in real-time). Therefore, the moving average is computed in the adaptive model and the mean is taken over T_{seg} seconds (advice is to take the median for future use, but this was not yet implemented in this thesis).

- Time constant:
 - The time constant determines the rate at which the PeakFollower descends and was experimentally determined at 2 ms using the training set.

The PeakFollower has 1 output:

- Gating:
 - This is an array of pulses, in which for each detected QRS-complex a pulse is given. These pulses are prolonged to the length of the QRS-gates, which is set to 100 ms, based on described QRS-gates in literature.

Align pulse train

The so-far processed dEMG signal must be aligned to the QRS-gates (as these start at the R-peak). In order to align the R-peaks to the middle of the QRS-gates, the dEMG signal should be delayed half the gate length, so 50 ms. First a high-pass filter is applied, in order to attenuate P- and T-tops. This filter also inherently induces a delay, which was minimized by using a 2nd-order filter, with an experimentally determined cut-off frequency of 100 Hz. The delay of this filter was determined at 5 ms (by computation of the cross-correlation between the pre- and post-filtered signal). Therefore, the dEMG signal only has to be delayed an additional 45 ms.

Sidenote: As the dEMG signal has to be delayed with 50 ms anyway, it is possible to further advance filtering of P- and T-tops, as the filter delay can be up to 50 ms without this affecting the trigger delay.

Filling gates

All data within the QRS-gates is removed by replacing it with the data segment prior to the QRS-gate. This is accomplished by replacing all samples within the QRS-gate with the sample 100 ms earlier.

Rectify signal

As dEMG activity cannot be negative, the absolute value is taken (full-wave rectification).

Create respiratory waveform

The respiratory waveform is obtained by calculating the moving average. The window length was 500 ms (adopted from the pre-existing offline tc-dEMG algorithm), and therefore the imposed delay was 250 ms. However, as the adaptive model does not run in real-time, this was not an issue.

Finding respiratory rate

Goal: to find the average time of a respiratory cycle (inspiration + expiration), T_{cycle} . Also, the number of inspirations per T_{seg} seconds was computed.

Breath detection using respiratory waveform

The slope of the respiratory waveform is calculated by subtracting from each sample, the sample 250 ms ($f_s/4$) earlier. This value of 250 ms was experimentally determined based on the available training data. It was found long enough to further smoothen the respiratory waveform and to align it around a baseline of zero, yet not so long that inspiratory efforts would be overlooked. Next, the signal is passed through the 'hit-crossing'-block. This block detects all positive zero-crossings, and therefore aims to detect (or count) all inspirations. For each positive zero-crossing a pulse is given. Often it is the case, especially for noisier signals, that there are multiple zero-crossings belonging to a single inspiration. In order to cope with this, the subblock 'single trigger' is implemented.

Single trigger

In order to prevent pulses given quick in succession, a detection-block period is implemented by first prolonged the pulses to 750 ms. If there are multiple pulses within 750 ms, all ≥ 2 pulses

within this period will be absorbed into the first pulse. Next, all prolonged pulses are shortened to 1 single sample. The absorbed pulses are not recovered in the process, resulting in only the first pulses within 750 ms to remain. The detection-block period was fixated on a value of 750 ms, as this meant that the maximum RR to be detected was 80/minute, which was deemed sufficient for this population.

Calculating Tcycle

The value for T_{seg} determines over which period the adaptive parameters are determined. In this study a value of 60 seconds was chosen, assuming that this period would be sufficient to reliably determine the parameter values. However, it was not experimentally backed-up whether this was indeed the case and whether this segment length allowed for enough adaptivity within the model. All pulses are buffered for T_{seg} seconds and subsequently summed. The summation will equal the amount of detected breaths within T_{seg} seconds. Now, the Tcycle can be computed, by dividing T_{seg} by the amount of breaths. In case of apnea, no breaths are detected and the resultant Tcycle will be very large. In order to prevent this, a maximum value for Tcycle is set, at 2 seconds (assuming a minimal RR of 30, and therefore at least once every 2 seconds an inflation must be administered). The obtained Tcycle is first passed through the 'switch'-block. If it is longer than 2 seconds, Tcycle is set at 2 seconds.

Finding dEMG threshold for triggering

Goal: to calculate the optimal dEMG threshold to detect breaths in the final processed dEMG (pre-MA) signal.

In order to do so, the final processed dEMG signal and the detected inspirations are buffered for T_{seg} seconds. Next, the ThEMG is calculated by using these buffered single and the computed Tcycle (which is a single value and therefore has no use in buffering).

MATLAB threshold function

The goal is to find the minimum threshold for which the amount of given triggers on the processed dEMG signal equals the amount of detected breaths using the respiratory waveform. For this, we use the bisection method, here broken down into steps:

1. The threshold is calculated through the following formula:

$$Th = \frac{a + b}{2}$$

For the initial value a is the minimum value (0) and b is the maximum value of the dEMG signal.

2. The amount of triggers using this threshold is calculated and compared to the detected inspirations using the respiratory waveform.
3. If (compared to these detected inspirations) too few triggers were given, the current threshold is too high. In the threshold formula b is replaced with the current threshold value and you return to step 1.
4. If too many triggers were given, the current threshold is too low. In the threshold formula a is replaced with the current threshold value and you return to step 1.
5. If the amount of triggers equal the detected breaths, you exit the loop with the current threshold.

In order to make sure the obtained threshold value is the minimum value for which the amount of triggers equal the detected breaths, an additional loop is created to minimize the threshold. In each iteration the threshold is lowered by 0.01 and the amount of triggers is recalculated. As long as the amount of triggers does not increase, the loop is repeated until the lowest possible threshold (with 0.01 accuracy) is found. The output of the function is the ThEMG.

Triggering model

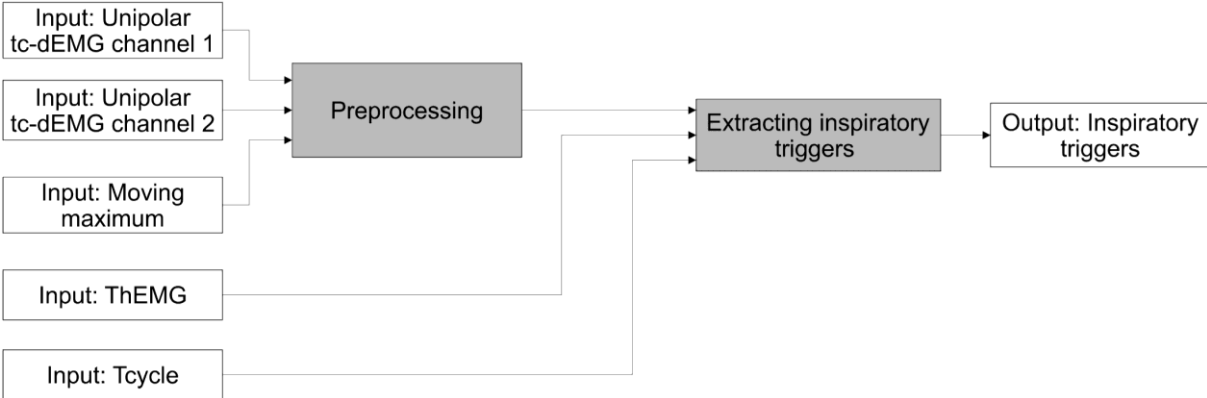


Figure D.5: Expanded triggering model, consisting of two components pre-processing and extracting inspiratory triggers.

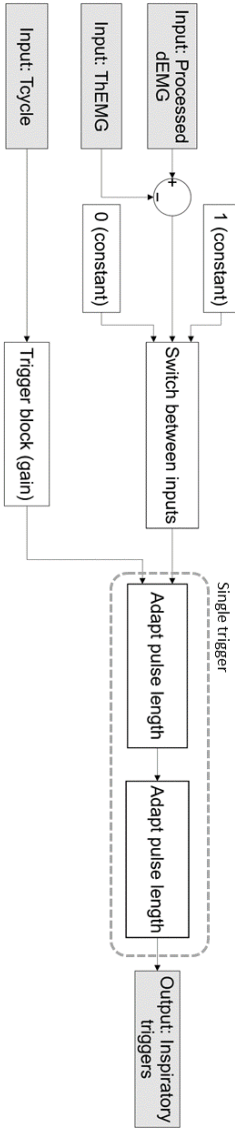


Figure D.6: Expanded subcomponent extracting inspiratory triggers (from the triggering model).

Pre-processing

Goal: to process the raw dEMG signal such that it is fit for triggering of inspirations, with as little delay as possible. In general the pre-processing in the triggering model equals the pre-processing from the adaptive model. The only two differences are that the moving maximum is not calculated, but extracted from the adaptive model (in order to save time) and that the respiratory waveform is not computed.

Extracting inspiratory triggers

Goal: to extract the inspiratory triggers from the processed dEMG signal, using a threshold value.

The inspiratory triggers are given when the processed dEMG signal is higher compared to the given ThEMG.

Single trigger

To prevent a multitude of pulses for a single inspiration, the 'Single trigger' method is used again, explained in Adaptive model/Finding respiratory rate /Breath detection using respiratory waveform. However, now the pulses are first prolonged for $0.6 \cdot T_{\text{cycle}}$. This is the amount of time new pulses are 'blocked'. With a value of 0.6 it was clinically reasoned that if the subject would switch from a RR of 30-40 to a RR of 50-60, it would be possible to detect the subsequent inspirations without any induced delay due to the trigger-block period.

E. Description of dataset per subject

Table E.1: Baseline characteristics for study population of Simulink simulations. Sorted on GA at inclusion.

Subject number	Sex	GA at birth	GA at inclusion	Weight at birth	Weight at inclusion	Support after extubation
GA 26 - 28						
1	F	25+1	25+6	775	660	nIPPV 6/8, RR 40, FiO ₂ 0.34
2	M	26+1	28+0	600	665	CPAP PEEP 8, FiO ₂ 1
3	M	27+3	28+3	805	805	CPAP PEEP 8, FiO ₂ 0.5
4*	M	26+0	28+6	850	900	CPAP PEEP 8, FiO ₂ 0.3
GA 29-32						
5	M	26+1	29+3	960	1000	CPAP PEEP 6, FiO ₂ 0.3
6	M	26+2	30+1	970	1235	CPAP PEEP 10, FiO ₂ 0.5
7	M	24+6	31+4	650	1010	CPAP PEEP 10, FiO ₂ 0.5
8	M	30+6	32+1	1790	1695	HFNC 6 L/min, FiO ₂ 0.21
GA 33-36						
9	M	31+5	33+1	2050	2050	nIPPV** 6/-, FiO ₂ 0.41
10	M	31+5	33+3	550	526	CPAP PEEP 5, FiO ₂ 0.44
11	M	33+4	34+1	1365	1365	HFNC 6 L/min, FiO ₂ 0.21
12	M	35+1	35+4	2293	2293	No support
GA 37+						
13	F	37+5	38+1	3470	3470	LFNC 2 L/min, FiO ₂ 0.21
14	M	38+4	39+1	3088	3070	No support
15	M	40+3	41+1	2808	2875	nIPPV** 6/-, FiO ₂ 0.4
16	M	41+3	42+5	5200	5490	CPAP PEEP 6, FiO ₂ 0.43

*Categorized as an outlier

**RR and PIP unknown

F. Steps to follow for future research into tc-dEMG based triggering

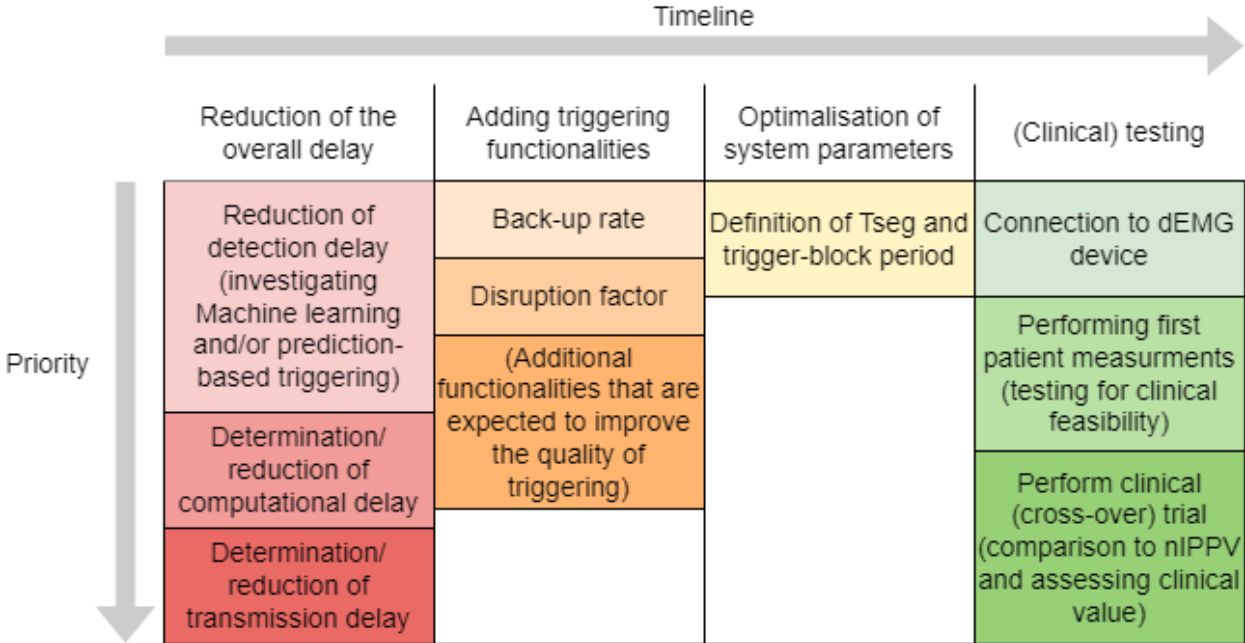


Figure F.1: Recommended timeline of steps to follow for future research.



October 2022